

**FUNCTIONAL CHARACTERIZATION OF SEX HORMONE-BINDING
GLOBULIN GENETIC POLYMORPHISM**

by

TSUNG-SHENG WU

B.Sc., National Cheng Kung University, 2003

M.Sc., National Taiwan University, 2005

A DISSERTATION SUBMITTED IN PARTIAL FULFILLMENT OF
THE REQUIREMENTS FOR THE DEGREE OF

DOCTOR OF PHILOSOPHY

in

THE FACULTY OF GRADUATE AND POSTDOCTORAL STUDIES
(Reproductive and Developmental Sciences)

THE UNIVERSITY OF BRITISH COLUMBIA
(Vancouver)

June 2015

© Tsung-Sheng Wu, 2015

Abstract

Human plasma SHBG is produced by the liver, and it transports biologically active sex steroids and determines their availability to target tissues. The 4.3 kb human *SHBG* transcriptional unit encoding a signal polypeptide for secretion followed by two laminin G (LG)-like domains is utilized by hepatocytes. The N-terminal LG domain of SHBG contains a region responsible for homodimer formation, and a steroid ligand-binding site that accommodates androgens and estrogens in opposite orientations. Among over 250 genetic polymorphisms identified in human *SHBG*, few are functionally characterized. In this research, I have performed a comprehensive analysis of functionally relevant *SHBG* single nucleotide polymorphisms (SNPs). Nine out of nineteen non-synonymous SNPs within the coding region of SHBG N-terminal LG domain were shown to encode SHBG mutants with abnormal properties in steroid ligand binding, calcium coordination, fibulin-2 interaction, glycosylation or secretion. In particular, SHBG R123H (encoded by rs143269613) has a general reduction in affinity for steroid ligands, whereas SHBG E176K (encoded by rs372114420) has a higher affinity specifically for estradiol. Crystallography revealed that instead of losing the structural integrity of the steroid-binding site, reduced flexibility of the loop region that covers the steroid-binding site, and conformational changes at the opening rim of a putative estradiol

entrance, likely account for the abnormal steroid-binding affinities of SHBG R123H and SHBG E176K, respectively. Among eight SNPs within *SHBG* regulatory sequences selected for analysis, only rs138097069 increases *SHBG* promoter activity. *In silico* prediction revealed that rs138097069 is located within a putative FXR binding site, while rs6257, which is linked to low plasma SHBG concentrations, is located within a putative FOXA2 binding element. In HepG2 cells, GW4064-activated FXR and overexpressed FOXA2 both suppress *SHBG* expression by direct binding to their corresponding binding elements in an HNF4 α -independent manner. By contrast, knock-down of FXR reduces, while knock-down of FOXA2 induces, *HNF4 α* expression and SHBG production. Characterization of functional *SHBG* SNPs has provided molecular explanations of how genetic differences contribute to SHBG production and function, and has identified possible roles for two novel regulators, FXR and FOXA2, in a more complex regulatory network that determines *SHBG* expression.

Preface

Portions of the text in Chapter 1 and Figure 1.2 are used with permission from a published review article of which I am an author. Hammond, G.L., **Wu, T.-S.**, and Simard, M. 2012. Evolving utility of sex hormone-binding globulin measurements in clinical medicine. *Curr Opin Endocrinol Diabetes Obes* 19:183-189. Dr. Hammond was the lead investigator, responsible for concept formation and manuscript composition. Dr. Simard and I were involved in figures and tables formation and manuscript composition.

Experiments and descriptions in Section 2.3.1 were conducted by myself under Dr. Hammond's guidance and were included in a published article of which I am one of the authors. Ohlsson, C. et al. 2011. Genetic determinants of serum testosterone concentrations in men. *PLoS Genet* 7:e1002313. A version of the rest Chapter 2 has been published in "Molecular Endocrinology". **Wu, T.-S.**, and Hammond, G.L. 2014. Naturally occurring mutants inform SHBG structure and function. *Mol Endocrinol* 28:1026-1038. The experiments were designed and conducted by myself under Dr. Hammond's supervision. The manuscript was prepared by myself and revised by Dr. Hammond.

Experiments in Chapter 3 were designed by myself under Dr. Hammond's supervision. Most of the work were conducted by myself with exceptions that Dr. Das did the X-ray data collection and structure refinement. Dr. Van Petegem provided valuable suggestions in crystallographic experiment troubleshooting and data interpretation.

Experiments in Chapter 4 were designed and conducted by myself under Dr. Hammond's supervision.

The secondary use of human serum samples, as described in Chapter 2, was approved by the University of British Columbia Clinical Research Ethics Board under the project title "SHBG: Beyond Plasma Transport" and certificate number H12-02373.

Table of Contents

Abstract.....	ii
Preface	iv
Table of Contents	vi
List of Tables	xi
List of Figures.....	xii
List of Abbreviations	xiv
Acknowledgements.....	xviii
Chapter 1 : Introduction.....	1
1.1 Sex steroid hormones.....	1
1.2 Physiological roles of sex hormone-binding globulin.....	3
1.2.1 Plasma transport of sex steroids and regulation of their bioavailability.....	3
1.2.2 SHBG within tissues or cells	5
1.2.3 SHBG levels and roles during the life cycle.....	6
1.3 Molecular properties of sex hormone-binding globulin	8
1.3.1 <i>SHBG</i> gene structure	8
1.3.2 Biochemical properties of SHBG	9
1.3.3 Crystal structure of SHBG.....	12
1.3.3.1 Steroid-binding site.....	13
1.3.3.2 Dimer interface	15
1.3.3.3 Flexible loop region.....	16
1.3.3.4 Zinc effects on SHBG.....	17
1.4 Regulation of SHBG production in the liver	18

1.4.1	Body composition.....	18
1.4.2	Dietary and nutritional factors.....	18
1.4.3	Thyroid hormone and peroxisome proliferator-activated receptor- γ	19
1.4.4	Sex steroid hormones.....	20
1.4.5	Growth hormone.....	21
1.4.6	Other transcription factors predicted to regulate hepatic <i>SHBG</i> expression ..	22
1.5	The clinical utility of serum SHBG measurements	27
1.6	Naturally occurring genetic polymorphism of human <i>SHBG</i> gene	28
1.7	Objectives	29
Chapter 2 : Naturally occurring mutants inform SHBG structure and function.....		34
2.1	Introduction.....	34
2.2	Material and methods	36
2.2.1	Antibodies and reagents.....	36
2.2.2	Cell culture.....	37
2.2.3	Production of human SHBG mutants	37
2.2.4	Immuno-fluorometric assay (IFA).....	38
2.2.5	Steroid-binding capacity measurements	39
2.2.6	Steroid-binding kinetics.....	39
2.2.7	Western blotting.....	40
2.2.8	SHBG dimerization assay.....	41
2.2.9	GST pull-down assays	41
2.2.10	Statistical analysis.....	42
2.3	Results	42
2.3.1	The rs6258 polymorphism affects SHBG binding affinity for testosterone ...	42

2.3.2 Comparison between immuno-reactivity and DHT-binding activity of SHBG versus the selected non-synonymous SHBG mutants	43
2.3.3 Steroid-binding properties of SHBG and previously uncharacterized non- synonymous SHBG mutants.....	44
2.3.4 Mutations that influence steroid-binding through abnormal calcium binding or dimerization.....	45
2.3.5 SHBG mutations that influence interaction with fibulin-2.....	46
2.3.6 Flux of steroids into and out of the SHBG steroid-binding site	48
2.3.7 Characterization of SHBG glycosylation variants.....	49
2.4 Discussion.....	51
Chapter 3 : Crystal structure analysis of the SHBG R123H and SHBG E176K mutant N- terminal LG domains	74
3.1 Introduction.....	74
3.2 Material and methods	76
3.2.1 Recombinant protein overproduction	76
3.2.2 Protein purification	77
3.2.3 Crystallization.....	78
3.2.4 Crystallographic analysis.....	79
3.3 Results	80
3.3.1 Characteristics of the SHBG R123H and SHBG E176K N-terminal LG domain crystals	80
3.3.2 The steroid-binding pocket and dimerization domain of SHBG R123H are structurally similar to those of SHBG	81
3.3.3 The Arg135 of SHBG R123H replaces the space occupied by Lys134 in	

SHBG.....	81
3.3.4 Substitution of Glu176 with lysine caused a local conformational change at the SHBG N-terminal LG domain surface	82
3.4 Discussion.....	82
Chapter 4 : Functional characterization of naturally occurring genetic polymorphism in <i>SHBG</i> regulatory sequences	94
4.1 Introduction.....	94
4.2 Material and methods	96
4.2.1 Antibodies and reagents.....	96
4.2.2 Cell culture and transient transfection	96
4.2.3 Expression plasmids and luciferase reporter gene constructs.....	97
4.2.4 Luciferase reporter gene assay.....	97
4.2.5 Immuno-fluorometric assay (IFA).....	98
4.2.6 Western blotting.....	99
4.2.7 RNA isolation and quantitative reverse transcription polymerase chain reaction (RT-PCR)	99
4.2.8 Chromatin Immunoprecipitation (ChIP) assays	100
4.2.9 Statistical analysis.....	101
4.3 Results	101
4.3.1 Effects of the SNPs within the <i>SHBG</i> proximal promoter regulatory region on transcriptional activity	101
4.3.2 SNP rs138097069 is located within a putative FXR binding element	102
4.3.3 FXR agonist GW4064 reduces SHBG production independent of HNF4 α	103
4.3.4 Knockdown of FXR reduces <i>HNF4α</i> and <i>SHBG</i> expression.....	104

4.3.5 GW4064-activated FXR binds the FXRE within the <i>SHBG</i> promoter	104
4.3.6 Overexpression of FOXA2 suppresses SHBG production in an HNF4 α - independent manner	105
4.3.7 Knockdown of FOXA2 induces HNF4 α and SHBG production	106
4.3.8 FOXA2 directly binds to <i>SHBG</i> intron1	106
4.4 Discussion	107
Chapter 5 : Conclusion	126
5.1 Non-synonymous <i>SHBG</i> genetic polymorphism encoding SHBG variants with altered molecular properties	128
5.2 Factors independent of structural integrity of the steroid-binding pocket contribute to normal SHBG ligand-binding properties	129
5.3 FXR and FOXA2 both regulate <i>SHBG</i> expression in HNF4 α dependent and independent manners	130
References	132

List of Tables

Table 1.1 Structural formula of cholesterol and sex steroids that bind SHBG with high affinities	31
Table 2.1 Oligonucleotide sequences for site-directed mutagenesis to produce SHBG mutants with specific amino acid substitutions	60
Table 2.2 Non-synonymous single nucleotide polymorphisms (SNPs) within human <i>SHBG</i> are identified by their corresponding rs numbers	61
Table 2.3 Steroid-binding affinities and specificities of SHBG and SHBG mutants.....	62
Table 2.4 Summary of the abnormal properties associated with SHBG mutants	63
Table 3.1 X-ray diffraction data and refinement statistics for SHBG R123H and SHBG E176K versus SHBG (WT) N-terminal LG domain crystals	87
Table 4.1 Properties of SNPs selected within the <i>SHBG</i> promoter and intron1 region	111
Table 4.2 Oligonucleotide sequences (5' to 3') for molecular cloning, site-directed mutagenesis, quantitative RT-PCR, or ChIP assay	112

List of Figures

Figure 1.1 Sex steroid hormone synthesis, transport, and actions	32
Figure 1.2 The levels and occupancy of human plasma SHBG throughout the life	33
Figure 2.1 Affinities of serum or recombinant SHBG and SHBG mutant for testosterone	64
Figure 2.2 Sequence alignment of the N-terminal LG domains of human SHBG and its orthologues in other mammals showing the positions of amino acid substitutions associated with the non-synonymous SNPs studied	65
Figure 2.3 Comparison of DHT-binding capacity assay and immuno-fluorometric assay (IFA) values of recombinant SHBG and SHBG mutants	66
Figure 2.4 Kinetics of DHT binding to SHBG (WT) and SHBG mutants with a suspected abnormally low DHT-binding affinity (SHBG T48I, SHBG R123H, and SHBG G195E)	67
Figure 2.5 Influence of calcium supplementation on SHBG mutants with abnormally low DHT-binding affinity	68
Figure 2.6 Identification of SHBG mutants with abnormal interactions with fibulin-2	70
Figure 2.7 Effects of S1B5 antibody binding to SHBG on steroid-binding kinetics	71
Figure 2.8 Glycosylation status of SHBG T7N and SHBG G195E	72
Figure 2.9 Crystal structure of the N-terminal LG domain of human SHBG in complex with estradiol (PDB code: 1LHU, estradiol shown in cyan) showing the residues where amino acid substitutions were found to alter the functional properties of SHBG .	73
Figure 3.1 Purification of the N-terminal LG domain of SHBG	88
Figure 3.2 Crystals of the N-terminal LG domain of SHBG R123H and SHBG E176K	89
Figure 3.3 Molecular properties of DHT-bound SHBG and SHBG R123H revealed by the	

crystal structures of their N-terminal LG domains	90
Figure 3.4 The flexible loop region above the steroid-binding pocket of SHBG and SHBG R123H	91
Figure 3.5 Estradiol-binding properties of the SHBG E176 N-terminal LG domain	92
Figure 3.6 Lys176 pushed Lys173 outward from the “hollow tube” of SHBG E176K.....	93
Figure 4.1 Diagrams of <i>SHBG</i> luciferase reporter gene constructs	113
Figure 4.2 Orthologous sequence alignment of the <i>SHBG</i> proximal promoter	116
Figure 4.3 Location of SNP rs138097069 within a putative FXR binding element (FXRE) and luciferase reporter gene activities for mutants within FXRE	117
Figure 4.4 FXR agonist GW4064 reduces SHBG production in an HNF4 α -independent manner	118
Figure 4.5 Effects of FXR agonist GW4064 on <i>SHBG</i> promoter activity	119
Figure 4.6 Effects of knock-down of FXR on <i>SHBG</i> and <i>HNF4α</i> expression	120
Figure 4.7 GW4064 activated FXR directly binds to the <i>SHBG</i> promoter.....	121
Figure 4.8 Overexpression of FOXA2 or FOXA2-T156A represses <i>SHBG</i> expression in an HNF4a-independent manner	123
Figure 4.9 Knock-down of FOXA2 induces <i>HNF4α</i> and <i>SHBG</i> expression	124
Figure 4.10 Endogenous and overexpressed FOXA2 directly binds to <i>SHBG</i> intron 1	125

List of Abbreviations

ABP	Androgen binding protein
APO	Apolipoprotein
Bp	Base pair
cDNA	Complementary deoxyribonucleic acid
ChIP	Chromatin immunoprecipitation
CHO	Chinese hamster ovary
ChREBP	Carbohydrate response element binding protein
COUP-TF	Chicken ovalbumin upstream promoter transcription factor
CRISPR	Clustered regularly interspaced short palindromic repeats
CYP	Cytochrome P450
DCC	Dextran-coated charcoal
DHT	5 α -dihydrotestosterone
DNA	Deoxyribonucleic acid
DR-1	Direct repeat-1
E.coli	Escherichia coli
EDTA	Ethylenediaminetetraacetic acid
EGTA	Ethylene glycol tetraacetic acid
FABP1	Fatty acid binding protein 1
FBS	Fetal bovine serum
FOXA2	Forkhead box A2
FP	DNaseI footprinting region
FPLC	Fast protein liquid chromatography

FSH	Follicular-stimulating hormone
FXR	Farnesoid X receptor
FXRE	FXR binding element
G6Pase	Glucose-6-phosphatase
GAPDH	Glyceraldehyde-3-phosphate dehydrogenase
GAS6	Growth arrest-specific protein 6
GH	Growth hormone
GnRH	Gonadotropin releasing hormone
GST	Glutathione S-transferase
HDL	High density lipoprotein
HEPES	Hydroxyethyl piperazineethanesulfonic acid
HepG2	Human hepatoblastoma
HNF4 α	Hepatocytes nuclear factor 4 α
IFA	Immuno-fluorometric assay
IGF-1	Insulin-like growth factor-type 1
Kd	Dissociation constant
kDa	Kilo dalton
Kir6.2	Inward rectifier potassium channel member 6.2
KLK	Kallikrein-related peptidase
LDL	Low-density lipoprotein
LG	Laminin globular-like
LH	Luteinizing hormone
L-PK	Liver-type pyruvate kinase

LRH-1	Liver receptor homolog 1
MCH	Melanin-concentrating hormone
2-MeOE2	2-methoxyestradiol
mRNA	Messenger ribonucleic acid
NCBI	National Center for Biotechnology Information
PAGE	Polyacrylamide gel electrophoresis
PBS	Phosphate-buffered saline
PCR	Polymerase chain reaction
PDB	Protein data bank
PDX1	Pancreatic and duodenal homeobox 1
PEPCK	Phosphoenolpyruvate carboxykinase
PEG	Polyethylene glycol
PMSF	Phenylmethylsulfonyl fluoride
PPAR	Peroxisome proliferator-activated receptor
PVDF	Polyvinylidene fluoride
RT-PCR	Reverse transcription polymerase chain reaction
RXR	Retinoid X receptor
SD	Standard deviation
SDS	Sodium dodecyl sulfate
SHBG	Sex hormone-binding globulin
SHP	Small heterodimer partner
SMRT	silencing mediator of retinoic acid and thyroid hormone receptor
SNP	Single nucleotide polymorphism

SREBP	Sterol regulatory element-binding protein
STAT5B	Signal transducer and activator of transcription 5B
Sur1	Sulfonylurea receptor 1
USF	Upstream stimulatory factor
VLDL	Very low-density lipoprotein
WT	Wild Type (used to signify the common allele variant)

Acknowledgements

“If there are too many persons to thank, thank God.” said a famous Chinese writer.

Rather than being that succinct, I prefer to express my gratitude to all those who have helped or supported me throughout these years in a more comprehensive way with this opportunity.

First, I shall thank my supervisor, Dr. Geoffrey Hammond. His guidance has equipped me with skills and knowledge to complete my research and has inspired me in appreciation of fundamental sciences. His passion and willingness to educate and support young researchers are what I admire and hope to emulate in the future.

I thank Dr. Wendy Robinson, Dr. Angela Develin, Dr. Peter CK Leung, and Dr. Anthony Chung for serving on my graduate committee. Especially, Wendy and Angela gave me helpful directions in preparing my comprehensive examination, and provided useful comments to improve the quality of my dissertation.

I would also like to thank Dr. Filip Van Petegem and members in his lab for providing resources and technical supports to my crystal structure studies.

My lab members have always inspired and motivated me with intelligent discussions and great ideas. Thank you all for creating such a joyful working environment.

It's friend that make my life in Canada easier and more colorful. Thank those who have helped me, shared experiences to me, explored and had fun with me. Our friendship never ends.

My love and gratitude to my beloved families go far beyond words. Thank my grand mom and my parents for your understanding and endless supports, which have always strengthened me when I pursue my goal.

Chapter 1 : Introduction

1.1 Sex steroid hormones

The natural steroid hormones are derived from cholesterol and can be grouped by their different physiological roles exerted through activation of their specific intracellular receptors into five classes: glucocorticoids, mineralocorticoids, androgens, estrogens, and progestogens. Sex steroid hormones, including androgens, estrogens and progestogens, are responsible for the differentiation and development of genital systems, and establishment of secondary sexual characteristics. In addition, they are involved in the regulation of metabolism, bone structure, as well as the cardiovascular and central nervous systems. While two major biologically active sex steroid hormones, testosterone and estradiol, are produced mainly in gonads (**Figure 1.1A**), adrenals and peripheral tissues are also indirectly responsible for the biosynthesis or conversion of steroid precursors into active androgens and estrogens respectively. In the testis, testosterone is produced by Leydig cells and diffuses locally into seminiferous tubules for sustaining spermatogenesis (1). Testosterone produced by Leydig cells is also secreted into the blood and accounts for about 95% of circulating testosterone. In the ovary, estradiol synthesis involves two different cell types: the theca cells convert cholesterol to androstenedione, which diffuses to the granulosa cells as a major precursor for estradiol production (2).

Gonadal steroidogenesis is regulated by hypothalamic and pituitary hormones (**Figure 1.1A**) (3). The hypothalamus synthesizes gonadotropin releasing hormone (GnRH) and secretes it in a pulsatile manner to regulate synthesis or release of gonadotropins, luteinizing hormone (LH) and follicular-stimulating hormone (FSH), in the anterior pituitary. Gonadotropins induce steroidogenesis *via* their receptors, which are distributed in a cell-dependent manner. In males for example, LH stimulates testosterone production in Leydig cells, whereas FSH stimulates Sertoli cells and enhances their production of androgen binding protein (ABP), which is secreted to seminiferous tubules and binds testosterone to maintain its high local concentrations required for spermatogenesis. It should be noted that in primates, instead of being produced in Sertoli cells, the ABP ortholog, sex steroid binding globulin (SHBG), is produced in germ cells (4). In females, LH stimulates androgen production in the theca cells, whereas FSH enhances estrogen production in granulosa cells by inducing aromatase expression. Sex steroid hormone production and secretion is controlled by feedback mechanisms in a highly regulated manner within this hypothalamus-pituitary-gonadal axis. For example, production of androgens and estrogens in gonads can exert negative feedback on GnRH and gonadotropins secretion (**Figure 1.1A**).

Sex steroid hormones exert their biological actions on target cells through genomic and/or non-genomic effects (**Figure 1.1C**). The genomic effects are mediated by intracellular

nuclear receptors (5). Upon binding to their respective sex steroid ligands, these nuclear receptors dissociate from the heat shock proteins and translocate to nucleus. After binding to their response elements within regulatory sequences, nuclear receptors recruit co-activator or co-repressor to activate or repress target gene expressions, respectively (6). In contrast to the genomic effects, the non-genomic effects of sex steroid hormones are mediated by receptors at plasma membrane of target cells and are rapid due to induction of secondary messengers, such as cAMP and Ca^{2+} (7).

1.2 Physiological roles of sex hormone-binding globulin

1.2.1 Plasma transport of sex steroids and regulation of their bioavailability

Following production by steroidogenic cells, sex steroids either act locally or are transported in the bloodstream to their target tissues. In the blood, these hydrophobic steroids are bound and transported by steroid-binding proteins (**Figure 1.1B**) (8). Albumin, the most abundant protein in plasma, binds all classes of steroids non-specifically with relatively low ($\sim\mu\text{M}$) affinity. By contrast, a glycoprotein, known as sex hormone-binding globulin (SHBG), specifically binds 5α -dihydrotestosterone (DHT), testosterone, and 17β -estradiol with 3-4 orders of magnitude higher affinity than albumin. It also binds an androgen precursor, 5-androstene- $3\beta,17\beta$ diol, and a major metabolite of DHT, 5α -androstane- $3\alpha,17\beta$ diol, with high affinity similar to testosterone (9).

The concentrations and binding parameters of all endogenous steroids for different plasma steroid-binding proteins have been used to computationally estimate the occupancy of SHBG with different steroid ligands, as well as the distribution of each steroid ligand between un-bound, albumin bound, or SHBG-bound fractions (9). This revealed that the occupancy of SHBG by steroid ligands is markedly different in men when compared to non-pregnant or pregnant women. For example, testosterone is the major SHBG ligand in men and it occupies 36% of SHBG binding site. About 20% of the binding sites are occupied by androgen metabolites or estradiol, leaving 44% of SHBG steroid-binding sites unoccupied in men. By contrast, most (82%) of the steroid-binding sites of SHBG in non-pregnant women are unoccupied. In pregnant women, circulating SHBG concentrations increase by about 5-10 times, but the high levels of estradiol in late pregnancy only occupy 12% of SHBG steroid-binding sites and 66% of which remain unoccupied. It should also be noted that more than 99% of the albumin steroid-binding sites remain unoccupied in all physiological situations, and this tremendous capacity can be attributed to the very high plasma concentrations of albumin. Importantly, physiological changes in SHBG levels within the nano-molar range significantly alter the plasma distribution of testosterone. Therefore, SHBG is the primary determinant of the plasma distribution of sex steroid hormones between the SHBG-bound, albumin-bound and unbound (free) fractions. Accordingly, plasma SHBG levels determine the

access or bioavailability of sex steroid hormones to their target cells in line with the free hormone hypothesis, which states that only free steroids that are not bound by plasma proteins passively diffuse into tissues and cells (10).

1.2.2 SHBG within tissues or cells

Besides the liver, which is the major source of plasma SHBG in mammals, *SHBG* transcripts are expressed as alternatively spliced forms in other tissues, such as testis, prostate, kidney, uterus, and brain (11-16). In testis, the rat *Shbg* ortholog encodes the androgen-binding protein which is produced and secreted into the seminiferous tubules by Sertoli cells, while expression of human *SHBG* in the testis only occurs in germ cells in a highly regulated spermatogenic cycle-dependent manner (4). In male germ cells, human *SHBG* alternative transcripts lack the coding sequence for a secretion signal polypeptide, and encode an N-terminally truncated SHBG isoform that accumulates in the acrosome of sperm (17). This difference in the testicular cell-specific expression pattern between species has been attributed to a *cis*-acting element within the human *SHBG* proximal promoter that is absent in rodent *Shbg* promoters, and which recruits upstream stimulatory factors (USFs) that repress human *SHBG* transcription in Sertoli cells (18).

Studies of human *SHBG* transgene expression in mice have also shown that *SHBG* is expressed in epithelial cells lining the renal proximal convoluted tubules of the kidney (19).

Further studies using an immortalized mouse proximal convoluted tubule epithelial cell line, PKSV-PCT cells, indicated that an incompletely glycosylated form of SHBG accumulates inside the cells and increases androgen receptor-mediated androgen actions (20).

In addition to SHBG's intracellular accumulation, the stromal compartments of some sex steroid-sensitive tissues, such as endometrium, may sequester human SHBG from the plasma, as shown in a "humanized" transgenic mouse model (21). The sequestration of human SHBG by the endometrial stroma of these mice is enhanced during proestrus, when estradiol concentrations are at their highest during the estrus cycle. This extravascular sequestration involves a highly specific interaction of SHBG with two extracellular matrix-associated proteins, fibulin-1D and fibulin-2, and it occurs in a sex steroid ligand dependent manner, with estradiol being the most effective ligand that promotes their interaction. This may be important because this fluctuated sequestration of SHBG into extravascular compartments may actively enhance the access of sex steroids to their target cells under certain physiological conditions.

1.2.3 SHBG levels and roles during the life cycle

Human SHBG is present in fetal blood at mid-gestation (22), and in the amniotic fluid where its concentrations correlate with those of testosterone (23). During fetal life, SHBG probably controls the exposure of tissues to androgens or estrogens and may thereby influence sexual dimorphism at several levels. On the maternal side, plasma SHBG levels increase as

much as 10-fold during mid-to-late pregnancy (9), but the physiological significance of this is still unknown. However, an isolated report of a rare and severe SHBG deficiency in a profoundly, and transiently androgenized pregnant woman, has indicated that the maternal increase in plasma SHBG may help protect mother against exposure to androgens from fetal origin (24).

The levels and occupancy of human plasma SHBG throughout life are depicted in **Figure 1.2**. Plasma SHBG levels are low (~ 6 nM) in both sexes at birth and rise rapidly within 3 months to about 100 nM until onset of puberty (25, 26), and the postnatal increase most likely occurs in response to the postnatal maturation of thyroid hormone action (27). During puberty, SHBG levels decrease to ~50 nM in girls (28) and by a greater extent to ~30 nM in boys (29). The sexual dimorphism of plasma SHBG levels is maintained throughout adult life until around 50 years of age. Postmenopausal women have slightly lower SHBG levels than during their reproductive years (30), while, plasma SHBG increases gradually in men over 60 years old to levels that are comparable to those in postmenopausal women (31).

Sex differences and fluctuations in plasma SHBG concentrations during the normal life cycle occur together with marked changes in sex steroid levels (9), and this influences the occupancy of SHBG steroid-binding sites (**Figure 1.2**). In particular, high levels of SHBG during childhood circulate in a predominantly unoccupied form. This effectively limits free

androgen and estrogen levels and likely protects children from precocious puberty. By contrast, during puberty elevated sex steroid levels in concert with substantial reductions in plasma SHBG levels results in a progressive increase in both free androgen and estrogen levels, which most likely helps to promote the onset of puberty. Furthermore, the occupancy of plasma SHBG by steroids differs between sexes with the number of unoccupied steroid-binding sites in women being much higher than in men (9). This suggests a fundamental sex difference in the way that SHBG acts to transport or regulate the biological activities of sex steroids. For instance, the relatively high proportion of unoccupied SHBG steroid-binding sites in women may serve to more effectively restrict androgen access to cells or remove active androgen metabolites such as DHT from target tissues in women, and thereby effectively protect them from excess androgen exposures.

1.3 Molecular properties of sex hormone-binding globulin

1.3.1 *SHBG* gene structure

The human *SHBG* gene is located in the p12-p13 region of chromosome 17 (32). Two major *SHBG* transcription units have been clearly defined. The 4.3 kb unit, which includes a ~800 bp proximal promoter and eight exons, is utilized by hepatocytes to produce SHBG for secretion into the bloodstream (11, 33). A conventional TATA box is absent in this proximal promoter; instead, a TA-rich HNF4 α /COUP-TF binding site adjacent to the transcriptional

start site acts as an on/off switch in responsible for *SHBG* expression (34). The AUG translation start codon is located in exon1 of this 4.3 kb transcription unit, and it encodes the signal polypeptide for SHBG secretion, while exons 2-8 encode two laminin G (LG)-like domains. The 8 kb human *SHBG* transcript unit contains an alternative promoter and an alternative exon1 that are located about 1.9 kb upstream of the 4.3 kb transcription unit. Expression of this transcription unit in germ cells produces an SHBG isoform that accumulates in acrosome, as demonstrated in *SHBG* transgenic mice studies (4, 17-19).

1.3.2 Biochemical properties of SHBG

The primary structure of human SHBG was deduced by a cDNA clone screened from a human liver cDNA library (33), and obtained directly by amino acid sequence analysis (35). These pioneering studies, followed by the cloning and sequencing of the human *SHBG* gene (11), indicated that the human SHBG precursor polypeptide is comprised of a signal peptide for secretion that is removed co-translationally to yield a mature polypeptide of 373 residues. In addition, one O-linked glycosylation site at Thr7 and two N-linked sites at Asn351 and Asn367 were identified biochemically (36) and from the SHBG primary structure (33), respectively. By comparison with several sequence-related proteins, such as growth arrest-specific protein 6 (GAS6), vitamin K-dependent protein S, and the alpha chain of laminin, it became apparent that SHBG consists of a tandem repeat of LG domains (37).

The molecular weight of the native form of SHBG, when assessed by ultracentrifugation (38) or gel-filtration chromatography (36), was found to be about 90 kDa in early studies. However, under denaturing conditions, the apparent molecular sizes of SHBG assessed by SDS-PAGE analysis were reduced to 52 kDa and 49 kDa in an approximate ratio of 10:1 by intensity (36, 39). This provided the first information that human SHBG circulates as a homodimer in blood (8), and that each monomer may vary in terms of molecular weight.

Removal of oligosaccharides by deglycosylation (40) or mutating the glycosylation sites of SHBG (41) demonstrated that the electrophoretic heterogeneity of SHBG monomers is due to differences in their glycosylation. More importantly, removal of either or both N-linked oligosaccharides at Asn351 and Asn367 increased the plasma half-life of SHBG, which indicates that they play a role in regulating the plasma clearance of SHBG (42). By contrast, an *SHBG* genetic polymorphism (rs6259) encoding an amino acid substitution (Asp to Asn) at residue 327 introduces an extra N-linked oligosaccharide (43), and this extra carbohydrate chain protects SHBG from metabolic clearance (44). In all of these cases, removal or addition of carbohydrates chain had no effect on the steroid-binding properties of SHBG (42, 44).

Studies of the binding parameters of natural or synthetic steroids to SHBG demonstrated that the planarity, i.e. the plane angles between the A and B, C, D rings of the steroid molecule, is an important determinant of SHBG steroid-binding affinity (8, 9). Also, a 17 β -hydroxy

group is present in all steroid ligands that bind SHBG with high binding affinity. In these steroids, an oxygen at C3 appeared to be more important than a hydroxyl group at this site for optimum binding, and this was interpreted as an explanation for SHBG's higher binding affinity for DHT and testosterone than for estradiol, which were all assumed to compete for a single steroid-binding pocket.

Studies of human and rabbit serum SHBG with a luminescent probe, Terbium, revealed that each dimer of SHBG contains four metal-binding sites (45). The removal of cations from SHBG destabilizes it, and this explained why serum SHBG is very unstable if blood samples are collected in the presence of EDTA (46). It is also known that EDTA treatment disrupts SHBG dimer formation, and that calcium and zinc supplementation reverses this (47). Therefore, it was concluded that SHBG binds calcium and zinc, and that calcium is especially important for protecting SHBG from losing its steroid-binding activity and dimer formation (48).

While the C-terminal LG domain of SHBG contains sites for N-linked glycosylation, only the N-terminal LG domain is required for steroid binding and dimer formation (49). Therefore, solving the structure of SHBG N-terminal LG domain was considered to be an important priority for understanding how steroid ligands are coordinated within the steroid-binding site, and how dimer forms and may affect the stability of SHBG. The bacterium, *E.coli*,

was chosen as the preferred host for recombinant human SHBG production because it does not glycosylate proteins and this mitigates problems associated with micro-heterogeneity in crystal formation. It was also noted that the yields of full length SHBG were much lower than those obtained for just the N-terminal LG domain when expressed as a GST-fusion protein in *E.coli*. In addition, the recombinant SHBG N-terminal LG domain produced in this way bound steroids with appropriate affinities and could be easily purified after release from its GST fusion partner (118).

1.3.3 Crystal structure of SHBG

The first crystal structure of the N-terminal LG domain of human SHBG was solved using an *E. coli* expressed recombinant protein comprising residues 1-205 of the mature polypeptide in complex with DHT (50). It revealed that this domain is spherical in shape and consists of two sets of antiparallel β -sheets packed on top of each other. In addition, this structure provided direct evidence for several of the observed biochemical properties of SHBG. The dimer interface was located within the N-terminal LG domain and found to be positioned far from the steroid-binding sites in the SHBG monomers of each dimer. In addition, a calcium ion was observed in the structure, and its binding site was positioned far from the steroid-binding site and dimer interface. This suggested that the effect of calcium on SHBG stabilization and dimerization occurs indirectly through affecting the overall structure of

SHBG. In addition, this original structure revealed that two other metal ions might exist; these were later identified as zinc ions, one of which was located immediately above the steroid-binding site (51). Based on this crystal structure, the site-direct mutagenesis of key residues for steroid binding and dimer formation, and other structural analyses for SHBG in complex with other steroid ligands were performed as described below (for a more extensive review, see (52))

1.3.3.1 Steroid-binding site

Steroids are buried deeply within the core of the SHBG N-terminal LG domain and are held in place by hydrophobic interactions with several residues and by hydrophilic anchoring involving hydrogen bonds between functional groups at the C3 and C17 atoms of the steroid rings A and D, respectively (50). In the case of DHT, the oxygen atom attached at C3 forms a hydrogen bond with the side chain of a phylogenetically conserved residue, Ser42 in human SHBG, while its hydroxyl group at C17 forms two additional hydrogen bonds with Asp65 and Asn82 (50). By contrast, studies of the crystal structure of SHBG in complex with estradiol (53) revealed that while the overall volume and position occupied by estradiol is almost identical to that of DHT, the orientation is opposite (53). The hydroxyl at C3 was anchored at Asp65, Asn82 and Lys134, while the β -hydroxyl at C17 was anchored at Ser42 and Val105 by hydrogen bonds. The structural analysis of the SHBG steroid binding pocket is in agreement

with the results of previous mutagenesis (54) and photoaffinity labeling (55) experiments. For example, mutation of Ser42 to leucine completely abolished steroid binding of SHBG, and Met139 identified by photoaffinity labeling with $\Delta 6$ -testosterone is located only 4.5 Å from C6 of the steroid ring B. In addition, mutation of Asp65 to alanine remarkably inhibits estradiol binding, but it has no effect on DHT or testosterone binding of SHBG (53). Therefore, the interaction between SHBG Asp65 and steroids appears to be particularly important for estradiol binding.

The steroid-binding pocket of SHBG accommodates a wide range of natural and synthetic steroids with about a 20-fold difference of their binding affinity. For example, a synthetic progestin, levonorgestrel, is accommodated in the same orientation as DHT in the steroid-binding pocket (53). In addition, the biologically active estrogen metabolite, 2-methoxyestradiol, binds to SHBG in the same orientation as estradiol, but binds more effectively due to a better accommodation of its methoxy group at C2 with Asn82 (56). However, the adaptability has limits. The ethinyl group of C17 of ethinylestradiol, or the bowing angle between planes of A and B ring of 5β -DHT likely generate steric clashes with the steroid-binding pocket, and this probably accounts for their poor binding affinities to SHBG (8).

To date the conformation of SHBG without ligands (apo form) remains unknown.

However, the dissociation rate of SHBG for steroid ligands is far more rapid than that of the sex steroid receptors for their cognate ligands. Therefore, it is unlikely that a large ligand-induced conformational change of SHBG steroid-binding pocket occurs as is typical of the nuclear steroid hormone receptors, in which the helix 12 of the ligand-binding domain moves to firmly trap the ligand in the binding site (57).

1.3.3.2 Dimer interface

The crystal structure of SHBG revealed that dimerization occurs at the edge of a β -sheet sandwich of each N-terminal LG domain in a head to head manner (50). The β -strand 7 of one monomer is adjacent to the β -strand 10 of the other monomer and *vice versa*. The hydrophobic nature of the dimer interface is mediated by several phylogenetically conserved residues (58). Among these residues, substitution of Val89 or Leu122 with glutamic acid creates steric clashes at the dimer interface and these SHBG mutants therefore exist as a monomer (58). Importantly, the steroid binding affinity and specificity of the dimerization-deficient SHBG mutants are indistinguishable from those of SHBG. Therefore, the prevailing model is that each monomer in SHBG homodimer has a similar binding affinity for steroids irrespective of the occupancy of steroid-binding site of the adjacent monomer. However, a recent study indicated that binding of testosterone to the SHBG dimer may involve a multi-step dynamic process (59). In that study, the binding of testosterone to one SHBG monomer was suggested

to trigger an allosteric rearrangement of the other monomer, with at least two interconverting microstates being proposed for unliganded SHBG. Further studies are required to determine whether this model is correct and can be used to improve the mathematical algorithms used to calculate free testosterone levels (59).

1.3.3.3 Flexible loop region

A disordered region (residues 130-135) in the first crystal structure of SHBG in complex with DHT (50) was not visible until the crystal structures of SHBG were obtained in complex with estradiol (53) or in the absence of zinc (60). These studies indicated that this region is more flexible when SHBG is in complex with DHT, and that binding of estradiol or removal of zinc stabilizes it. Previous photoaffinity-labeling studies demonstrated that Lys134 is closely approximate to steroid ligands (61, 62), but mutagenesis experiments demonstrated that it is not essential for SHBG steroid-binding activity (53, 60). By contrast, the side chain of a phylogenetically conserved residue, Leu131, may protrude into the steroid-binding pocket, and mutation of this residue to glycine caused a remarkable reduction of steroid-binding affinity (53), indicating that Leu131 is critical for stabilizing the hydrophobic steroid-binding pocket of SHBG. This flexible loop region is positioned above the steroid-binding pocket, and there is now credible evidence that its flexibility has a great impact on SHBG binding

specificity for steroid ligands, and its effects are influenced by the occupancy of a zinc-binding site in this location (51).

1.3.3.4 Zinc effects on SHBG

By soaking SHBG crystals with $ZnCl_2$, two zinc binding sites within the N-terminal LG domain of SHBG were revealed in a crystal structure (51). The one located above the steroid-binding pocket is coordinated with the side chains of His83 and His136 and the carboxylate group of Asp65. While the binding-affinity for DHT is not affected by the presence or absence of zinc, zinc specifically reduces SHBG binding affinity for estradiol by two mechanisms (51). First, zinc diverts the side chain of Asp65 away from the steroid-binding site. As mentioned above, the hydrogen bond formation between the side chain of Asp65 and the hydroxyl at C3 of estradiol is critical for binding of SHBG to estradiol, but not DHT or testosterone (53). Second, zinc reorients the side chain of His136 inward to the zinc binding site, and this levers and destabilizes the flexible loop region (51, 60), which apparently affects the way that estradiol binds to SHBG. The effects of zinc on the steroid-binding specificity of SHBG may not be significant in the blood circulation because most of the zinc is bound to albumin. However, this effect of zinc on the affinity of human SHBG for estradiol may be important in tissues with high free zinc concentrations, such as prostate and male reproductive tract, and the preference of SHBG for androgens over estrogens may either promote androgenic actions

in male reproductive system and influence sperm development (63, 64), or enhance the local actions of estradiol in tissues like the prostate stroma (65)

1.4 Regulation of SHBG production in the liver

1.4.1 Body composition

The production of SHBG by hepatocytes is controlled by metabolic as well as endocrine factors (66). Body composition, and the fat to lean ratio in particular, is a major determinant of circulating SHBG levels (67, 68). This effect is determined primarily by alterations in the hepatic levels of two related nuclear receptor family members, HNF4 α and COUP-TF1, which compete for the same DNA-binding site close to the human *SHBG* transcription start site (34). The binding of HNF4 α to this *cis*-acting element increases *SHBG* promoter activity, whereas the binding of COUP-TF1 represses it. Hepatic HNF4 α production is induced by exercise (69), and this induction likely explains the effect of exercise on increasing plasma SHBG levels (70). By contrast, in obese individuals and patients with steatosis in particular, plasma SHBG levels are very low (71). There is evidence that monosaccharide-induced lipogenesis causes a decrease in HNF4 α levels, so that COUP-TF1 can replace it and reduce SHBG production in HepG2 cells (72). This likely explains low plasma SHBG levels observed in obese individuals.

1.4.2 Dietary and nutritional factors

It is widely believed that insulin is an important regulator for *SHBG* expression since

numerous studies indicated that low plasma SHBG levels are associated with high insulin levels (73, 74). However, hyper-insulinemic individuals often suffer from hyperglycemia, which more likely accounts for the reduced SHBG levels (75). Two early *in vitro* studies showed that treatment of insulin decreased SHBG production in HepG2 cells (76, 77), but generalized reductions in protein secretion by insulin were not considered (78). While there is no evidence that insulin directly suppresses *SHBG* expression, it is clear that monosaccharide-induced lipogenesis down-regulates human *SHBG* expression in transgenic mice or in HepG2 cells by suppressing hepatic HNF4 α levels, and that an increase in palmitate levels within hepatocytes likely accounts for this (72).

1.4.3 Thyroid hormone and peroxisome proliferator-activated receptor- γ

Thyroid hormone increases the production of plasma SHBG indirectly by increasing HNF4 α levels in the liver (79), and this explains why SHBG levels are generally low in hypothyroid patients and high in those with hyperthyroidism (80). When a patient's thyroid status is difficult to assess, failure of thyroid hormone treatment to elicit a rapid and robust increase in SHBG levels identifies those individuals with peripheral resistance to thyroid hormone.

By contrast, peroxisome proliferator-activated receptor- γ 2 (PPAR- γ 2) reduces hepatic *SHBG* expression *in vitro* likely through a DR-1 nuclear hormone-response element, a second

potential HNF4 α binding site in the *SHBG* promoter (81). In addition, a genetic variant, PPAR- γ P12A (82), that was characterized with a reduced transcriptional activity (82) is associated with higher plasma SHBG levels (83). This and the observation that PPAR- γ P12A has a milder effect on *SHBG* promoter activity (81) further support the inhibitory role of PPAR- γ 2 on *SHBG* expression.

1.4.4 Sex steroid hormones

Increases in estrogen exposures have been associated with increased plasma SHBG levels. For example, the very high levels of plasma estrogens in pregnant women are associated with 5-10 fold higher plasma SHBG than in non-pregnant women (84), and administration of synthetic estrogens as contraceptives or for hormone replacement increases plasma SHBG levels (85-87). By contrast, androgen levels are negatively associated with plasma SHBG levels based on several clinical observations, such as the rapid decline of SHBG levels in boys during puberty as testosterone levels increase (29), and the lower testosterone and higher SHBG levels in old men (31), as well as reduced SHBG levels in athletes treated with high doses of testosterone (88).

However, there is no evidence that sex steroid hormones directly regulate *SHBG* expression, and changes in plasma SHBG levels in other clinical or physiological situations suggest that the effects of sex steroid on modulating plasma SHBG levels may be modest. For

instance, plasma SHBG and sex steroids levels are not correlated in girls during puberty, and actually decrease in spite the rise of estrogen levels. There are also no clear fluctuations in plasma SHBG during the menstrual cycle (84), nor is there a substantial decrease of plasma SHBG levels concomitant with the marked reduction of estradiol levels during the menopause (89). In addition, orchiectomy in prostate cancer patients very effectively decreases plasma testosterone but has no influence on plasma SHBG levels (90), and in certain pathological conditions, such as prepubertal hyperandrogenism, plasma SHBG levels are slightly but not significantly lower than in reference groups (91). It is therefore also possible that sex steroids act indirectly by changing other endocrine mediators or by inducing sexually dimorphic differences in liver metabolic state that alter SHBG production.

1.4.5 Growth hormone

Growth hormone (GH) levels increase during puberty (92) and decline with age after the second decade of life (93). In addition, GH secretion is sexually dimorphic: men have a higher nocturnal amplitude and lower frequency of growth hormone secretion, whereas the opposite occurs in women (94). In the liver, GH rapidly induces the expression of insulin-like growth factor-type 1 (*IGF-1*) by phosphorylating and activating STAT5B (95, 96). Some studies have shown that GH is negatively correlated with plasma SHBG levels (97, 98), and IGF-1 inhibits SHBG production (99). Therefore, different patterns of growth hormone secretion between

male and female may contribute to sexually dimorphic SHBG levels after puberty through effects on hepatic IGF-1 production.

1.4.6 Other transcription factors predicted to regulate hepatic *SHBG* expression

Based on a bioinformatic analysis of potential transcription factors that might bind to *cis*-acting elements containing the rs138097069 and rs6257 SNPs within the human *SHBG* sequence, I have explored the possibility that FXR and FOXA2 interact with their binding sites in these regions, respectively, and regulate *SHBG* expression.

The transcription factor, FXR, was first identified as a heterodimeric partner of RXR in rat liver and named because of its weak activation under supra-physiological concentrations of farnesol (100). Shortly after, bile acids, including chenodeoxycholic, deoxycholic, cholic, and lithocholic acid, were identified as its endogenous ligands (101-103). In *Fxr* deficient mice, elevated serum bile acid levels, but reduced fecal bile acid excretion, were observed (104). In addition, serum and hepatic levels of cholesterol, triglycerides, as well as very low-density and low-density lipoprotein (VLDL and LDL respectively) were increased (104). These results indicated that FXR is an intracellular bile acid sensor that is critically involved in the regulation of bile acid and lipid homeostasis. The molecular basis of FXR's action as a bile acid sensor and a regulator of bile acid homeostasis is well established (105-107). In hepatocytes, FXR binds to excess bile acids and transactivates small heterodimer partner (*SHP*) expression (108,

109). SHP is an atypical member of the nuclear receptor family that has no DNA-binding domain (110). SHP heterodimerizes with liver receptor homolog 1 (LRH-1) and inactivates it. This results in suppression of *CYP7A1*, which encodes cholesterol 7 α -hydroxylase, the rate-limiting enzyme of the bile acid synthesis pathway (111).

In addition to maintaining bile acid homeostasis, FXR plays significant roles in triglyceride, cholesterol, and glucose metabolism (106, 112). Hyper-triglyceridaemia was observed in *Fxr*-deficient mice (104), and this phenotype can be attributed to the ability of FXR to up-regulate apolipoprotein C-II (*APOC2*), but down-regulate apolipoprotein C-III (*APOC3*) expression (113, 114). In addition, activated FXR induces expression of a nuclear receptor gene, *PPAR α* (115), whereas the expression of sterol regulatory element-binding protein 1c (*SREBP-1c*) is reduced *via* SHP (116). Therefore, FXR regulates triglyceride levels via multiple pathways, including suppression of lipogenesis and stimulation of catabolism and clearance of lipids.

The anti-atherosclerotic effect of FXR has been demonstrated in studies of apolipoprotein E (*ApoE*^{-/-}) or LDL receptor (*LDLR*^{-/-}) deficient mice (117, 118). For instance, activation of FXR blocks Western diet-induced elevation of plasma triglyceride and non-HDL cholesterol levels in *ApoE* or *LDLR* deficient mice (117). Furthermore, activated FXR also attenuates bacterial lipopolysaccharide-stimulated pro-inflammatory cytokines production and

cholesterol uptake in human macrophages (118). In addition to the anti-atherosclerotic effect, FXR also regulates glucose metabolism. In FXR-null mice, elevated blood glucose levels, impaired glucose tolerance, and reduced insulin sensitivity were observed (119, 120). By contrast, administration of bile acids or overexpression of constitutively active FXR in wild-type or diabetic db/db mice significantly decreased serum glucose levels, partially due to up-regulating hepatic glycogen synthesis and suppressing key enzymes involved in gluconeogenesis, such as phosphoenolpyruvate carboxykinase (PEPCK) and glucose-6-phosphatase (G6Pase) (119, 120). Taken together, FXR is an intriguing pharmaceutical target for treatment of cholestasis, atherosclerosis, metabolic syndrome, and diabetes.

The *forkhead box (fox)* gene family was named after the discovery that mutations in these genes resulted in a spiked head appearance during the head involution in *Drosophila* (121). In vertebrates, the *Foxa* subfamily, which is comprised of *Foxa1*, *Foxa2* and *Foxa3*, is most closely related to the *Drosophila fox* genes. FOXA proteins are highly homologous and contain a conserved helix-turn-helix DNA binding domain, as well as N- and C-terminal transactivation domains (122). Besides direct binding to the consensus sequence on the target genes (123), FOXA proteins also regulate gene expression as “pioneer factors”, which open the compacted chromatin by binding to the core histones H3 and H4, and by replacing the linker histone H1 of the target nucleosomes (124, 125).

The role of FOXA proteins as pioneer factors has been demonstrated to be critical during development (126, 127). Among *Foxa* genes, *Foxa2* is the first one expressed during mouse gastrulation at the primitive streak and node on embryonic day 6.5 (E6.5) (128, 129). The expression of *Foxa2* is also required for neural tube, notochord, and gut tube formation, as indicated by the observation that mouse embryos lacking *Foxa2* died by E10-11 (130, 131). The *Foxa* family also plays crucial roles in organogenesis (126, 127). For instance, FOXA2 coordinates with FOXA1 to establish the competence of foregut endoderm (132). After which, loci co-occupancy of FOXA2 with other transcriptional factors, such as PDX1 or HNF4 α , drives expression of pancreatic islet- or liver-specific genes for organ specification (133). Moreover, co-overexpression of *Hnf4 α* with *Foxa1*, *Foxa2*, or *Foxa3* can even convert non-hepatic lineage cells into hepatocyte-like cells (134).

Conditional deletion of *Foxa2* in differentiated mouse hepatocytes resulted in blunted activation of gluconeogenesis genes during fasting, or under glucagon or glucocorticoid stimulations (135). This implies that FOXA2 is essential for executing the hepatic gluconeogenic program to maintain blood glucose levels during food deprivation. The ability of FOXA2 to function as a survival adaptor of starvation has also been demonstrated in other contexts. In the brain, the hypothalamic FOXA2 stimulates the production of orexin and melanin-concentrating hormone (MCH), both function as “feeding signals” to initiate and

promote food intake (136, 137). In the pancreas, FOXA2 is required for α -cell differentiation and is involved in glucagon biosynthesis and secretion, especially under low glucose conditions (138, 139). Moreover, mice specifically lacking *Foxa2* in pancreatic β cells exhibited severe hyperinsulinemic hypoglycaemia because FOXA2 regulates insulin secretion, but not biosynthesis, through maintaining steady-state expression of two ATP-sensitive K^+ channel subunits, sulfonylurea receptor 1 (*Sur1*) and inward rectifier potassium channel member 6.2 (*Kir6.2*), in β cells (140, 141).

In addition to glucose homeostasis, hepatic FOXA2 regulates lipid metabolism by activation of genes involved in triglyceride metabolism, fatty acid β -oxidation, and ketogenesis during fasting or diabetic, but not postprandial states (142-144). The ability of FOXA2 to regulate these target genes is controlled by insulin and glucagon. The insulin/PI3K/Akt signal cascade phosphorylates FOXA2 at a conserved threonine (Thr156) residue and excludes FOXA2 from the nucleus to the cytosol (145), whereas glucagon induces acetylation of FOXA2, which facilitates its nuclear localization (146) and protein stability (147) of FOXA2. Overall, while insulin-stimulated nuclear exclusion of FOXA2 is still under debate (135), the ability of several constitutively active forms of FOXA2 to normalize the elevated hepatic triglycerides and plasma glucose and insulin levels, as well as to improve hepatic insulin

sensitivity in diabetic mice renders FOXA2 a potential pharmacological target for treatment of diabetes (142, 146).

1.5 The clinical utility of serum SHBG measurements

Blood SHBG levels are associated with body composition, insulin sensitivity, thyroid hormone and sex steroids levels, and therefore have been used as a biomarker for metabolic or endocrine related diseases (148). In premenopausal women, low SHBG levels are linked with increased free testosterone levels and its clinical manifestations, such as hirsutism. In polycystic ovarian syndrome (PCOS) women, low SHBG levels, which reflects underlying metabolic disorder, may also contribute to the imbalance of free sex steroids levels and abnormal gonadotropin production (149). Abnormally high SHBG levels reflecting the chronically fasted state in anorexia nervosa patients may cause low free estrogen and androgen levels and likely contribute to amenorrhea in women. Serum SHBG levels decrease significantly after refeeding or weight gain and are therefore a potential diagnostic and follow-up biomarker for nutritional status in these patients (150). In addition, SHBG measurements are frequently used to determine free testosterone levels in men with symptoms of hypogonadism or androgen insufficiency in elderly men.

1.6 Naturally occurring genetic polymorphism of human *SHBG* gene

Several genetic polymorphisms have been associated with plasma SHBG levels and linked to metabolic or reproductive diseases (for review, see (151)). However, little is known about the causative mechanisms underlying these associations, especially for those polymorphisms in strong linkage disequilibrium with others (152). While mutagenesis studies based on biochemical or structural results informed the biological properties of SHBG, identification and investigation of naturally occurring genetic polymorphisms that affect SHBG production or function will help understand the physiological significance of SHBG. For example, the rs6259 in exon8 of *SHBG* causes an N-linked glycosylation site being introduced at residue 327 within the C-terminal LG domain of SHBG, and the additional carbohydrate chain on this site (43) reduces its metabolic clearance rate and hence increases its plasma levels in carriers (153). The rs6259 is commonly distributed in a broad range of frequency across ethnic groups, with lowest frequency in Africa-Americans (~2%) and significantly higher frequency in Caucasians (~7.5-12%) (153-155). This is in line with an inverse correlation between SHBG levels and risk of prostate cancer (156) and may in part explain why Africa-American men have higher risk of prostate cancer than Caucasians (157).

Next-generation sequencing platforms with massively parallel sequencing technology (158) allow high-throughput screening of genetic polymorphism in the general population. To

date, more than 250 genetic polymorphisms have been identified in the human *SHBG*. Among these, non-synonymous polymorphisms are relatively easy to study because of well-established biochemical approaches, e.g. mutagenesis, recombinant protein expression and purification, and X-ray crystallography. By contrast, studies of the molecular properties and physiological significance of genetic polymorphism within regulatory sequences are more challenging due to limitations of promoter activity assays and the complexity and limited throughput of emerging methods for genome editing (159).

1.7 Objectives

There is increasing evidence that differences in plasma SHBG levels are an inherited trait (160). As outlined in the following chapters, several genetic variants are not only associated with SHBG levels, but are also related to reproductive or metabolic diseases (148). A causative role for SHBG in the etiology of these diseases has been suggested (161), but this is not yet been established (162). In addition, many novel SNPs have been discovered recently due to human whole genome or exome sequencing projects. My studies therefore set out to define the functional consequences of SNPs in *SHBG* regulatory and coding sequences, in anticipation that new information obtained in this way will improve the interpretation of Mendelian randomization tests of the causality of SHBG levels/activity on diseases. In addition, the identification of SNPs that alter the molecular properties of SHBG, such as steroid-binding

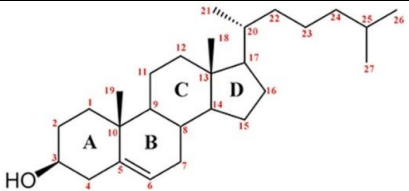
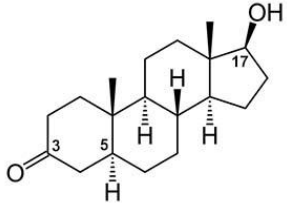
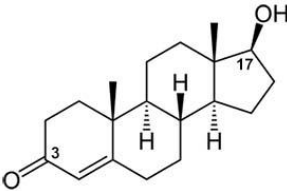
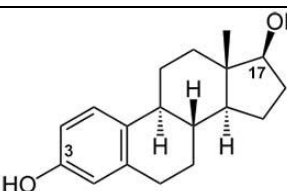
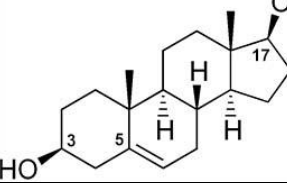
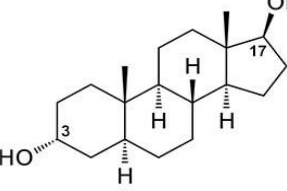
affinity or immuno-reactivity to antibodies used for clinical measurements, are expected to improve current models for estimating free sex steroid levels.

In my research, I undertook a comprehensive interrogation of the existing single nucleotide polymorphism (SNP) databases. SNPs that alter phylogenetically conserved residues and/or functionally relevant residues based on our knowledge of SHBG structure were prioritized for characterization. In **Chapter 2**, SHBG mutants encoded by *SHBG* non-synonymous SNPs were studied biochemically in terms of their steroid ligand-binding properties, dimerization, glycosylation, and ability to interact with fibulin-2.

In a follow-up study (**Chapter 3**), a mutant that is deficient in steroid binding (SHBG R123H), and a mutant that specifically binds estradiol with higher affinity were crystalized and analyzed structurally. In **Chapter 4**, SNPs within potential *SHBG* regulatory sequences were examined for their effects on *SHBG* expression.

Table 1.1 Structural formula of cholesterol and sex steroids that bind SHBG with high affinities

Carbon atoms of cholesterol are labelled with red numbers, and three 6-carbon and one 5-carbon rings are labelled with A, B, C, and D, respectively. The carbon atoms with functional groups of other sex steroids were labelled with black numbers. RBA: relative binding affinity (fold) to testosterone

Cholesterol	
Dihydrotestosterone (DHT) (RBA=2.20)	
Testosterone (RBA=1.00)	
17β-Estradiol (E2) (RBA=0.49)	
5-androstene-3β,17βdiol (RBA=0.97)	
5α-androstane-3α,17βdiol (RBA=0.82)	

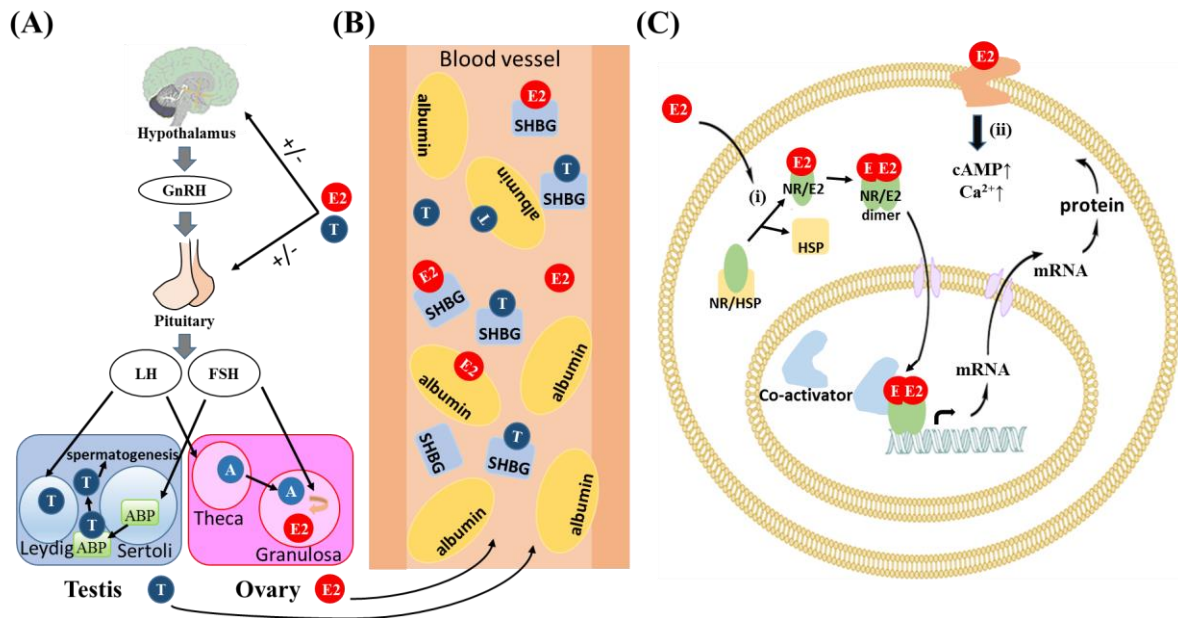


Figure 1.1 Sex steroid hormone synthesis, transport, and actions

(A) Sex steroid hormone synthesis in gonads is regulated by GnRH stimulated LH and FSH. In the testis, LH stimulates testosterone synthesis in Leydig cells, whereas FSH stimulates ABP expression in Sertoli cells to bind and increase local testosterone concentrations for spermatogenesis. In the ovary, LH stimulates androgen synthesis in the theca cells, whereas FSH promotes estradiol synthesis in the granulosa cells using androgens diffused from the theca cells as precursors. The sex steroid hormones can regulate the secretion of GnRH and gonadotropins by positive and/or negative feedback mechanisms. (B) In the circulation, sex steroid hormones are transported by albumin. In higher primates, circulating SHBG transports and determines the access or bioavailability of sex steroid hormones to their target cells. (C) Genomic actions of sex steroid hormones (i) involve nuclear receptor activation in the cytosol, followed by nuclear translocation and activation of target gene expression. Non-genomic actions of sex steroid hormones (ii) are mediated by receptors at the plasma membrane and rapid induction of secondary messengers, such as cAMP and Ca²⁺. GnRH, gonadotropin releasing hormone; LH, luteinizing hormone; FSH, follicular-stimulating hormone; ABP, androgen binding protein; T, testosterone; E2, estradiol; A, androstenedione; SHBG, sex hormone-binding globulin; NR, nuclear receptor; HSP, heat shock protein.

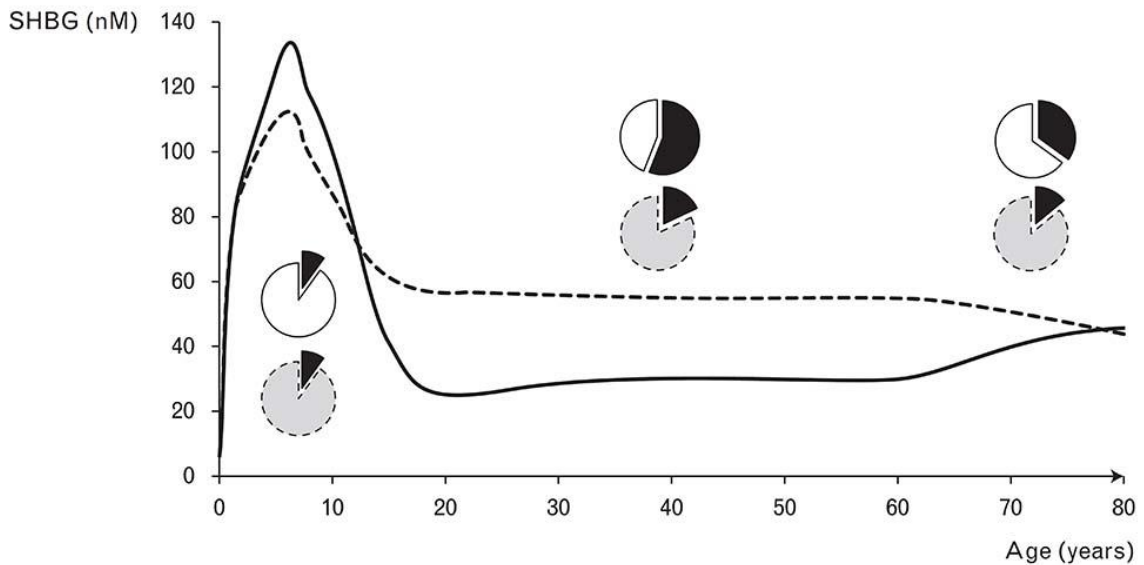


Figure 1.2 The levels and occupancy of human plasma SHBG throughout the life

Human plasma SHBG levels in males (solid line) and females (dashed line) from birth to old age, together with pie charts showing the proportions of occupied (filled black) vs. unoccupied SHBG-binding sites in males (white) and females (grey) at different stages of life are illustrated based on published values of plasma SHBG levels (25, 26, 28-31) and calculation of SHBG steroid-binding site occupancy (9).

Chapter 2 : Naturally occurring mutants inform SHBG structure and function

2.1 Introduction

Plasma sex hormone-binding globulin (SHBG) is secreted by the liver as a homodimeric glycoprotein with nanomolar affinities for sex steroids (66). With 3-4 orders of magnitude greater affinity for androgens and estrogens than albumin, SHBG is the primary determinant of the plasma distribution and access of these sex steroids to their target tissues (148, 163).

A crystal structure of the human SHBG N-terminal LG domain in complex with its preferred ligand, 5 α -dihydrotestosterone (DHT), revealed the topography of the hydrophobic steroid-binding pocket (50). It also revealed a calcium-binding site previously suspected of being an important determinant of the structural integrity of SHBG (45, 50). Additional crystal structures of this domain together with the biochemical characterization of strategically targeted mutants further demonstrated how androgens and estrogens are preferentially accommodated in opposite orientations within the single steroid-binding site of the SHBG monomer (53). They also provided evidence that human SHBG is a zinc-binding protein (51), and localized amino acids that participate in homodimer formation (36, 58). Further studies have demonstrated that SHBG interacts with other extracellular proteins, including members

of the fibulin family of extracellular matrix-associated proteins (164), as well as Kallikrein-related peptidase 4 that specifically cleaves human SHBG between its two LG domains (165). Less is known about the structural and functional importance of the C-terminal LG domain, but it contains two sites for N-glycosylation, the utilization of which affects the plasma clearance of SHBG (42) without influencing its steroid-binding properties (41).

Two non-synonymous, single nucleotide polymorphisms (SNPs) in the *SHBG* coding region have been identified and characterized. A common SNP (rs6259) located within exon 8 of the *SHBG* gene results in the substitution of Asp327 to Asn (D327N) in the mature SHBG polypeptide sequence (43). This substitution introduces an extra N-linked glycosylation site, the utilization of which retards the plasma clearance of SHBG (44). The resulting higher plasma SHBG levels in individuals who carry the rs6259 SNP have been negatively associated with the risk of developing breast cancer (166, 167) and type 2 diabetes (161).

Another SNP (rs6258) located in exon 4 of *SHBG* results in a P156L substitution. This SNP was identified more than a decade ago in a woman who presented with extreme virilisation during pregnancy (24), and it is present in about 4% of French-Canadian Caucasians (168). The plasma SHBG levels in this patient were exceptionally low due to a second novel single nucleotide deletion within the exon 8 sequence of her other *SHBG* allele that resulted in premature translation termination and a complete loss of SHBG production.

In a genome-wide meta-analysis study, rs6258 was recently found in ~2% of European men, and was associated with low serum testosterone levels (169). In my initial studies, I therefore performed biochemical analysis of the SHBG P156L mutant to investigate why its presence is associated with low plasma testosterone levels. I followed this with a more comprehensive interrogation of recent releases of SNP databases in which more than 49 non-synonymous SHBG SNPs had been identified. Of these, 32 were located within the coding region for the SHBG N-terminal LG domain that contains the steroid-binding site, as well as the dimerization and fibulin-interaction domains. I prioritized SNPs for analysis based on our knowledge of SHBG structures in order to focus on naturally occurring amino acid substitutions that might be structurally or functionally important.

2.2 Material and methods

2.2.1 Antibodies and reagents

Two mouse monoclonal anti-human SHBG antibodies (7H9 and S1B5) were used that recognize epitopes within the SHBG N-terminal LG domain. The 7H9 antibody was kindly provided by Dr. John Lewis (170) while the S1B5 antibody was prepared in house (171), as was the rabbit anti-human SHBG antibody (172). PNGase F was purchased from New England BioLabs (Ipswich, MA). Kallikrein-related peptidase 4 was kindly provided by Dr. Jonathan Harris (Queensland University of Technology). [³H]5 α -Dihydrotestosterone ([³H]DHT;

specific activity 110 Ci/mmol) was purchased from PerkinElmer (Waltham, MA). [³H]Testosterone (specific activity 50 Ci/mmol) [³H]2-methoxyestradiol ([³H]2-MeOE2; specific activity 60 Ci/mmol) were purchased from American Radiolabeled Chemicals (St. Louis, MO). Unlabeled steroids were obtained from Steraloids, and used without further purification.

2.2.2 Cell culture

Cell culture reagents were from Life Technologies (Burlington, Ontario). Chinese hamster ovary (CHO) cells were routinely cultured in Minimum Essential Medium alpha (MEM α) supplemented with 10% fetal bovine serum (FBS) and antibiotics (100 U penicillin/mL and 100 μ g streptomycin/mL).

2.2.3 Production of human SHBG mutants

Human *SHBG* cDNA in the pRC/CMV vector was used for site-directed mutagenesis (47) using the QuickChange II Site-Directed Mutagenesis Kit (Agilent Technologies, Santa Clara, CA) and site-specific mutagenic oligonucleotide primers (**Table 2.1**). The mutated plasmids were sequenced to ensure that only the targeted mutations were present. I transfected CHO cells with these plasmids using Lipofectamine 2000® (Life Technologies). After selection in the presence of 1 mg/mL Geneticin® (Life Technologies), stably transfected cells were grown to near confluence, then washed twice with phosphate-buffered saline to remove

FBS, and cultured in MEM α supplemented with antibiotics (100 U penicillin/mL and 100 μ g streptomycin/mL) and 100 nM DHT. Culture media containing recombinant human SHBG were filtered with a Millex-GP Filter Unit (Millipore, Etobicoke, Ontario), concentrated 10-fold using an Amicon Ultra-4 Centrifugal Filter with an Ultracel-3 membrane (Millipore), and then equilibrated and stored in Tris-buffered saline, pH 7.5, containing 100 nM DHT and 0.05% sodium azide.

2.2.4 Immuno-fluorometric assay (IFA)

A modified version of a time-resolved IFA (173) was used to measure SHBG concentrations in culture media. Briefly, 96-well plates were coated overnight with 150 μ L rabbit antiserum against SHBG (1:500 diluted in filtered 0.5M NaHCO₃) at 4°C, and then blocked with 300 μ L blocking buffer (1% casein in 20 mM Tris-HCl, pH 8, 150 mM NaCl) for 2 h at room temperature. Diluted (1:1,000) aliquots (100 μ L) of the concentrated culture media samples and 50 μ L Europium-labelled S1B5 antibody (2,000X diluted in DELFIA® assay buffer (PerkinElmer)) were then co-incubated for 3 h at room temperature. Wells were washed 6 times with washing buffer (50 mM Tris-HCl pH 7.5, 150 mM NaCl), and 150 μ L DELFIA® enhancement solution (PerkinElmer) was added to each well. Time-resolved fluorescence was measured using a VICTOR™ X4 Multimode Plate Reader (PerkinElmer).

2.2.5 Steroid-binding capacity measurements

A standard ligand saturation analysis (174) was used to determine the steroid-binding capacity, affinity, and specificity of SHBG and SHBG mutants. Briefly, concentrated and buffer-exchanged media were pre-incubated with dextran-coated charcoal (DCC) to remove steroids prior to incubation with [³H]DHT or [³H]testosterone in the presence or absence of 100-fold molar excess of unlabeled DHT to monitor nonspecific binding. Unbound steroids were removed by exposure to DCC for 10 min at 0°C followed by centrifugation to allow SHBG-bound [³H]DHT or [³H]testosterone to be measured. Affinity constants were determined by the Scatchard analysis (174), and the relative binding affinities of steroids were determined using [³H]DHT as the labeled ligand and increasing amounts of DHT, testosterone, or 17β-estradiol as competitors (174).

2.2.6 Steroid-binding kinetics

Equal amounts of SHBG or SHBG mutants of interest were first incubated with DCC to remove steroids from the binding sites. The stripped SHBG samples and reagents were cooled on ice to ensure the following reactions occurred at 0°C. The association rate kinetics of DHT to SHBG were determined by incubating ~1.5 nM SHBG with 10 nM [³H]DHT for 15 sec to 10 min, while dissociation rate kinetics were determined by pre-incubating SHBG with 10 nM of

[³H]DHT for 1 h followed by the addition of 3 μM DHT for 0 to 20 min. SHBG-bound [³H]DHT was separated and measured, as described above.

The methods described above were modified to examine the effects of S1B5 antibody on steroid-binding kinetics. The association kinetics of steroid-binding to SHBG were determined in the presence or absence of S1B5 antibody by incubating unliganded SHBG with or without S1B5 antibody for 1 h at room temperature followed by [³H]DHT or [³H]2-MeOE2 incubation for 30 sec to 1 h at 0°C. The dissociation of steroids from SHBG was also measured by incubating [³H]DHT or [³H]2-MeOE2 saturated SHBG with or without S1B5 antibody for 1 h at room temperature followed by DCC treatment for 2.5 to 30 min at 10°C.

2.2.7 Western blotting

Recombinant human SHBG from culture media or CHO cell lysates were resolved by 10% PAGE under non-denaturing or denaturing conditions and transferred to 0.45 μm Immobilon-P PVDF membranes (Millipore) by electroblotting. The membranes were blocked in 5% skim milk for 1 h, followed by incubation with 1:6,000 diluted rabbit anti-human SHBG antiserum or 1:200 diluted 7H9 antibody. Immunoreactive proteins were detected with 1:10,000 diluted horseradish peroxidase-conjugated goat anti-rabbit or anti-mouse IgG as secondary antibody (Sigma-Aldrich, St. Louis, MO).

2.2.8 SHBG dimerization assay

Equal amounts of SHBG or SHBG mutants were first incubated with DCC to remove steroids, and 1 mM of EGTA was added to remove calcium. In some samples, 2 mM CaCl₂ and/or 500 nM DHT was then added and incubated at room temperature for 3 h. Non-denaturing PAGE and Western blot analysis were used to detect dimeric versus monomeric SHBG (47).

2.2.9 GST pull-down assays

We used a GST pull-down assay to assess SHBG interactions with fibulin-2 (164). Briefly, 10 µg of a GST-fibulin-2 fusion protein, which includes 77 C-terminal residues of fibulin-2 that contain the SHBG binding site (164), was incubated overnight with 20 nM SHBG or SHBG mutants at 4°C in binding buffer (20 mM Tris-HCl, pH 8.0, 0.02% Nonidet P-40, and 0.2 mg/mL bovine serum albumin). Equilibrated aliquots (50 µL) of glutathione-agarose (Thermo Fisher Scientific, Waltham, MA) were added and samples were incubated at room temperature for 1 h. Sedimented glutathione-agarose beads were then washed 3 times in ice-cold buffer (20 mM Tris-HCl, pH 8.0, 0.02% Nonidet P-40), and proteins bound to the washed beads were extracted by boiling in SDS sample-loading buffer for 5 min, and SHBG was detected by Western blot analysis.

2.2.10 Statistical analysis

Data are reported as the mean \pm S.D. of at least three independent experiments for all measurements. Differences between mean values were evaluated by the Student's *t*-test using GraphPad Prism® (GraphPad) software.

2.3 Results

2.3.1 The rs6258 polymorphism affects SHBG binding affinity for testosterone

The non-synonymous SNP, rs6258, is located in exon 4 of SHBG, and it encodes the SHBG P156L mutant. We therefore first evaluated the serum SHBG testosterone-binding capacity in men with different rs6258 genotypes using Scatchard plots (**Figure 2.1A**). Carriers with the rs6258 genotype (Table 2.2) revealed a higher mean dissociation constant (*K_d*) for testosterone indicative of a lower affinity in TT (*K_d* = 4.9 nM) and CT (*K_d* = 4.5 nM) individuals than in CC individuals (*K_d* = 2.8 nM) (**Figure 2.1B**). To confirm this we expressed the SHBG P156L mutant (rs6258) and SHBG (WT) in CHO cells. When their affinities for testosterone were determined by Scatchard analysis, the SHBG P156L mutant displayed a lower affinity (*K_d* = 2.5 nM) for testosterone when compared to SHBG (*K_d* = 1.2 nM) (**Figure 2.1C and Table 2.3**).

2.3.2 Comparison between immuno-reactivity and DHT-binding activity of SHBG versus the selected non-synonymous SHBG mutants

From entries in the SNP databases, I selected seventeen non-synonymous SNPs within the SHBG N-terminal LG domain and one in the signal polypeptide sequence for analysis (**Table 2.2**). These SNPs were studied because the substituted residues are either conserved across several mammalian species or located in regions of the molecule that could potentially alter the biological properties of SHBG according to crystal structure predictions (**Figure 2.2**). Recombinant SHBGs were expressed in CHO cells, and culture media were concentrated 10-fold for DHT-binding capacity assays and IFA measurements to assess their levels of production. SHBG was analysed at different dilutions and this demonstrated a near perfect correlation between these two assays, which compare the functional property of SHBG in terms of steroid-binding capacity with respect to its immunoassay value (**Figure 2.3**).

Most SHBG mutants, including the mutant with an Arg to His substitution at position 22 in the signal polypeptide sequence were produced at about the same concentration as SHBG, and their DHT-binding capacity and immunoassay values correlate well. However, one of them (SHBG G195E) was present in the culture media at very low levels, as determined by both assay methodologies, and this implies that SHBG G195E is produced at abnormally low levels (**Figure 2.3**). Three other mutants displayed a discrepancy in DHT-binding capacity

with respect to the IFA value. One (SHBG R135C) exhibited a low immunoassay value when compared to its DHT-binding capacity, which suggests that the recognition of SHBG R135C by the labeled S1B5 antibody in the IFA is impaired, while the other two (SHBG T48I and SHBG R123H) mutants had lower than expected DHT-binding capacity values when compared to their IFA values (**Figure 2.3**), suggesting that these mutants have abnormal steroid-binding properties.

2.3.3 Steroid-binding properties of SHBG and previously uncharacterized non-synonymous SHBG mutants

To further evaluate the steroid-binding affinities of SHBG T48I and SHBG R123H, as well as other SHBG mutants, a Scatchard analysis was performed (**Table 2.3**). As anticipated from the above results (**Figure 2.3**), SHBG T48I and SHBG R123H have a 2.5- and 4-fold lower binding affinity for DHT than SHBG, respectively (**Table 2.3**). In addition, the SHBG G195E mutant that was produced at very low levels (**Figure 2.3**) was also found to have 5-fold lower affinity for DHT than SHBG (**Table 2.3**). All of the other SHBG mutants had affinities for DHT similar to SHBG, apart from another mutant with an amino acid substitution at residue 123 (SHBG R123C), which had a significantly reduced affinity for DHT although this was less pronounced than SHBG R123H (**Table 2.3**). To further understand the steroid-binding kinetics responsible for reduced DHT-binding affinity of these SHBG mutants,

association rate (**Figure 2.4A**) and dissociation rate (**Figure 2.4B**) assays were performed using [³H]DHT as a labeled ligand. When compared with SHBG, the association rate of DHT for SHBG R123H is normal (**Figure 2.4A**), while its dissociation rate is faster (**Figure 2.4B**). By contrast, the association rates of DHT for SHBG T48I or SHBG G195E are markedly reduced (**Figure 2.4A**), while their dissociation rates are similar to SHBG (**Figure 2.4B**).

Interestingly, substitutions of R123 by either His or Cys both result in a small but significant increases in estradiol binding affinity relative to those of DHT or testosterone (**Table 2.3**). Moreover, three other SHBG mutants with essentially normal affinities for DHT (SHBG R135C, SHBG L165M, SHBG E176K) have approximately 2-fold higher relative binding affinities for estradiol when compared to either DHT or testosterone (**Table 2.3**).

2.3.4 Mutations that influence steroid-binding through abnormal calcium binding or dimerization

It is known that human SHBG contains two calcium-binding sites (45), and that a calcium-binding site within the N-terminal LG domain is important for stabilizing the steroid-binding and dimerization of SHBG (47, 48). In a crystal structure of the human SHBG LG domain (50), Thr48 is located close to key residues that interact with calcium while Arg123 is located within the dimerization interface. While dimerization is not essential for the formation of a functional steroid-binding site (58), we investigated if the reduced DHT-binding affinity

that characterizes SHBG T48I is related to a defect in calcium binding. To assess this, we added 1 mM CaCl₂ to saturate the calcium-binding sites of SHBG mutants with lower affinities to DHT (SHBG T48I, SHBG R123H and SHBG G195E) prior to steroid-binding capacity assays (**Figure 2.5A**). This demonstrated that calcium supplementation restored the DHT-binding affinity of SHBG T48I to values approaching those observed for SHBG (**Figure 2.5A**). By contrast, the relatively low DHT binding affinities of SHBG R123H and SHBG G195E were unaltered by calcium supplementation (**Figure 2.5A**). Moreover, supplementation of calcium or DHT also reversed a marked defect in SHBG T48I dimer formation, as assessed by a mobility shift in a native polyacrylamide gel electrophoresis, and this was accentuated when calcium and DHT were added together (**Figure 2.5B**). The SHBG R123H mutant exhibited a minor disruption of dimer formation only in absence of steroid ligands and calcium, but this was resolved by calcium or DHT supplementation (**Figure 2.5B**).

2.3.5 SHBG mutations that influence interaction with fibulin-2

Human SHBG has been reported to interact with the C-terminal domain of fibulin-2 in a steroid-ligand dependent manner (164), and we therefore used a GST-fusion protein comprising the C-terminal domain of fibulin-2 as bait in GST pull-down assays to determine whether the various SHBG mutants interact differently with fibulin-2. This revealed that interactions between SHBG T48I, SHBG G195E or SHBG R135C and fibulin-2 were

significantly increased in the presence of DHT, when compared with SHBG or the other mutants (**Figure 2.6A**). The increased interactions between fibulin-2 and SHBG T48I or SHBG G195E were surprising because they both have abnormally low affinities for DHT (**Table 2.3**). Moreover, given that calcium restores the DHT-binding affinity and dimerization of SHBG T48I (**Figure 2.5**), we examined whether calcium supplementation specifically alters the pronounced interaction between SHBG T48I and fibulin-2. Paradoxically, while calcium supplementation increased the DHT-binding affinity of this mutant (**Figure 2.5A**), the enhanced interaction with fibulin-2 was lost (**Figure 2.6B**). These results suggest that global conformational alterations of SHBG T48I and SHBG G195E may over-ride any effects of steroid-binding on the fibulin-2 interaction. The enhanced interaction between fibulin-2 and the SHBG R135C mutant (**Figure 2.6A**) is of particular interest because this mutant is secreted normally and is characterized by an increased relative binding affinity for estradiol when compared to DHT (**Table 2.3**).

The electrophoretic micro-heterogeneity of SHBG subunits during SDS-PAGE (**Figure 2.6**) is due to variations in the complexity of carbohydrate structures attached at specific glycosylation sites, whereas the macro-heterogeneity is a reflection of the utilization of individual O-linked and N-linked glycosylation sites (41, 175). For instance, the two distinct SHBG subunits of ~46kDa and ~48kDa typically observed in SHBG reflect occupancy of one

or both of the N-linked glycosylation sites within the C-terminal LG domain of SHBG, respectively (41, 175). In the Western blot of the GST fibulin-2 pull-down assay (**Figure 2.6**), SHBG R(22)H, SHBG T7N, SHBG E119D and SHBG R123H also differed in their micro-heterogeneity when compared to SHBG, while SHBG R135C exhibited an obvious difference in macro-heterogeneity, indicative of the predominant utilization of both N-linked glycosylation sites. Moreover, SHBG T48I and SHBG G195E showed differences in both micro- and macro-heterogeneity when compared to SHBG.

2.3.6 Flux of steroids into and out of the SHBG steroid-binding site

Crystal structure studies have shown that the type of ligand within the steroid-binding site influences the conformation of a flexible loop positioned above the steroid-binding site (53), and that the R135C substitution is located within this loop region. It was therefore of interest that the R135C substitution not only changed the SHBG steroid-binding specificity, but also interfered with the ability of the S1B5 monoclonal antibody to recognize this mutant in the IFA. The latter observation, together with previous reports that S1B5 recognizes SHBG H136Q poorly (176), indicates that the epitope for S1B5 antibody includes the loop above the steroid-binding site.

This prompted us to examine whether the binding of S1B5 to SHBG alters the association or dissociation of steroids from the steroid-binding site. We found that pre-

incubation of S1B5 antibody with unliganded SHBG markedly delayed the association of [³H]DHT with SHBG (**Figure 2.7A**), while binding of S1B5 antibody after saturation of SHBG with [³H]DHT essentially blocked its dissociation (**Figure 2.7B**). Given that estrogens occupy the steroid-binding pocket in an opposite orientation when compared to androgens (53), we also examined whether S1B5 antibody has the same effects on the association and dissociation of estrogens. We used [³H]2-MeOE2 rather than [³H]E2 for this purpose because 2-MeOE2 has much higher binding affinity to SHBG than estradiol, while both estrogens bind in the same orientation (53). Surprisingly, S1B5 also hinders the entrance and exit of [³H]2-MeOE2 into and out of SHBG (**Figure 2.7C and 2.7D**), but this is less pronounced than that observed using [³H]DHT (**Figure 2.7A and 2.7B**).

2.3.7 Characterization of SHBG glycosylation variants

In the SHBG T7N mutant, the Thr that is normally O-glycosylated (177) is replaced by an Asn residue that creates a novel N-glycosylation consensus sequence. The observed lower subunit sizes of SHBG T7N compared to SHBG (**Figure 2.6A**) was therefore surprising because the potential N-glycosylation would be expected to introduce a larger and more complex oligosaccharide. To assess the potential glycosylation at this site in SHBG T7N, we first treated SHBG and SHBG T7N with PNGase-F to remove N-linked glycans, and examined their mobility by SDS-PAGE and Western blotting (**Figure 2.8A**). The apparent molecular

size of T7N SHBG after treatment with PNGase-F is slightly lower than SHBG, most likely due to the lack of the O-linked glycan at residue 7 (**Figure 2.8A**; lane 3 vs. lane 4). To further determine if the O-linked glycan is replaced by an N-linked glycan on residue 7, Kallikrein-related peptidase 4 was used to specifically cleave the SHBG molecules at a site between their two LG domains, as described previously (165). The 7H9 anti-human SHBG monoclonal antibody was then used in a Western blotting experiment to detect the separated N-terminal LG domain (**Figure 2.8A**; lane 5 vs. lane 8). In this experiment, Kallikrein-related peptidase 4 cleavage was terminated prematurely to prevent cleavage at non-specific sites, and there is no difference in the apparent sizes of the separated N-terminal LG domain of SHBG T7N before and after PNGase-F treatment (**Figure 2.8A**; lane 6 vs. lane 8). Furthermore, the difference in apparent molecular sizes of the N-terminal LG domains of SHBG and SHBG T7N is consistent with the presence of an O-linked oligosaccharide at this position on SHBG but not SHBG T7N (**Figure 2.8A**; lanes 5 vs. lane 6). Taken together, I conclude that substitution of Thr7 by an Asn residue eliminates any glycan addition at this position.

As noted above, the subunit macro-heterogeneity of several SHBG mutants differed from SHBG (**Figure 2.6**). In this regard, the SHBG G195E mutant was distinguished by a major subunit size that was greater than that observed for SHBG or any of the other mutants (**Figure 2.6A**). To further characterize this difference, SHBG G195E obtained from cell media

or cell lysates was analyzed by Western blotting (**Figure 2.8B**). In both types of sample, the SHBG G195E exhibited a greater apparent molecular size than observed for SHBG (**Figure 2.8B**; compare lanes 1 and 3 with lanes 5 and 7), but these differences were resolved by removing N-linked glycans (**Figure 2.8B**; compare lanes 2 and 4 with lanes 6 and 8). The greater apparent molecular weight of SHBG G195E therefore reflects the presence of more complex N-glycan structures associated with the C-terminal LG domain. Furthermore, comparison of secreted and intracellular forms of SHBG and G195E SHBG reveals that more incompletely processed glycoforms of G195E SHBG accumulate within CHO cells (**Figure 2.8B**; compare lanes 5 and 6 with lanes 7 and 8). Together, my results indicate that the improper folding of G195E leads to an abnormality in N-glycosylation that restricts its secretion from CHO cells.

2.4 Discussion

Despite the widespread use of plasma SHBG measurements for clinical assessments of biologically active androgen levels, only a few genetic differences that result in defects in SHBG production or function have been recorded. Several regulatory sequence variants appear to influence plasma SHBG levels, presumably as a consequence in altered *SHBG* transcription, including a pentanucleotide (TAAAA_n) repeat (178), rs1799941 in the *SHBG* promoter (151), and rs6257 within intron 1 of *SHBG* that may additionally influence nascent transcript

processing (161). By contrast, only the non-synonymous rs6259 SNP in the *SHBG* coding sequence has been reported to alter SHBG function by introducing an additional N-glycosylation site and increasing the half-life and consequently the plasma levels of SHBG (44). In the present study, I found that SHBG P156L has a lower binding affinity for testosterone, which would imply that it has a reduced ability for protection of testosterone from metabolic clearance. Also, this would explain the association between rs6258 and low serum total testosterone concentrations in men (169).

In SHBG, residue Pro156 is located far from the steroid-binding pocket of SHBG (**Figure 2.9**). However, it is positioned close to the calcium binding site and may cause a structural perturbation of this site. Consequently, calcium binding and the overall structural stability of SHBG may be affected, and this may contribute to a reduced binding affinity for testosterone. Furthermore, our extended study demonstrated that eight uncharacterized non-synonymous SNPs alter SHBG production or function in previously unrecognized ways (**Table 2.4**), which provide insight into the structure and function of this major plasma transport protein for sex steroids.

The most important functional property of human SHBG is its ability to bind both androgens and estrogens with high affinity. Seven of the new SHBG mutants studied displayed an abnormality in steroid-binding affinity or specificity. The G195E substitution caused a

general reduction in steroid-binding affinity and this was surprising because of its location within the linker region between the SHBG LG domains. However, this mutant was also secreted at very low levels, and our results suggest that this is due to a cellular accumulation of incompletely processed glycoforms. Given that oligosaccharides do not directly influence the steroid-binding activity of SHBG (41), the G195E mutation may disturb the normal spatial configuration of the two LG domains with respect to each other, and thereby influence both the steroid-binding activity and the processing of N-linked oligosaccharides attached to sites within the C-terminal LG domain.

Within the N-terminal LG domain, one of the three critical residues responsible for calcium binding (**Figure 2.9**) is substituted by Gln in SHBG E52Q, but this has no effect on the structure or function of SHBG most likely because the carbonyl oxygens of either Glu or Gln will support the coordination of calcium at this site. The Thr48 in human SHBG is also located close to this calcium-binding site (**Figure 2.9**). However, while Thr48 does not directly interact with calcium in human SHBG crystal structures (50), its substitution with isoleucine results in a reduction in both steroid-binding activity and dimerization, and these defects can both be restored by calcium supplementation. This provides evidence for an allosteric link between steroid-binding, dimerization and calcium-binding, and helps explain why the steroid-binding activity of SHBG is unstable in EDTA-treated plasma (46, 48).

As noted above, the secretion of SHBG G195E is severely compromised, and an abnormal interaction with fibulin-2 may not be functionally very important. Two other SHBG mutants (SHBG T48I and SHBG R135C) are produced normally and exhibited enhanced interactions with fibulin-2. The SHBG T48I mutant is characterized by a generalized 2-fold reduction in steroid-binding affinity; it does not dimerize well; it appears to be more extensively glycosylated than SHBG, and its enhanced interaction with fibulin-2 is lost after calcium supplementation. We currently have no explanation for the enhanced interaction between SHBG T48I and fibulin-2, but it may reflect a significant structural alteration in the protein, and it is difficult to predict what the physiological implications of this might be. By contrast, SHBG R135C has an increased affinity for estradiol, when compared to DHT, and this may be physiologically important. This is because SHBG interactions with fibulin-2 are enhanced in a steroid-ligand dependent manner, with occupancy of the SHBG steroid-binding site by estradiol promoting the strongest interaction (11). Moreover, the latter study also demonstrated that the extravascular sequestration and accumulation of plasma SHBG within the endometrial stromal matrix is enhanced by estradiol in both mice treated with human SHBG and in mice that express a human SHBG transgene, and that this accumulation of SHBG occurs in the same location as fibulin-2 within the endometrial stroma (164). Furthermore, the R135C substitution occurs within a flexible loop region that covers what appears to be the

entrance of the SHBG steroid-binding site (**Figure 2.9**). This is of interest because this region appears to be more structured when estrogens are located in the steroid-binding site (7), and it is possible that this loop region represents part of the fibulin-2 interaction domain of SHBG.

Two of the naturally occurring SHBG variants we have studied involve substitutions of Arg123, which is located at the dimer interface (**Figure 2.9**). In contrast to SHBG T48I, we predict that the SHBG R123H and SHBG R123C mutants probably dimerize normally under physiological conditions because dimerization of SHBG R123H could only be destabilized when calcium and steroids are both removed. Interestingly, the DHT-binding affinities of SHBG R123H and SHBG R123C were both reduced while their affinities for estradiol relative to that of DHT are slightly increased. Although the mechanisms responsible for this are not clear, we also found that the rate of DHT association with SHBG R123H is normal while its dissociation rate is abnormally fast. We therefore conclude that amino acid substitutions at the dimer interface exert long-range allosteric effects that influence how specific ligands are accommodated within the steroid-binding pockets of each subunit.

Two of the SHBG mutants that are produced normally, i.e., SHBG T48I and SHBG R123H, have general reductions in affinity for androgens (DHT and testosterone) and estradiol. These reductions in affinity (2.6 and 4.3 fold, respectively) are both greater in magnitude than the 1.8 fold reduction in testosterone binding observed for SHBG P156L (**Figure 2.1**). We

therefore predict that these SHBG mutants will also be associated with reduced serum sex steroid levels, and that these reductions will be even more pronounced than the reductions observed in serum testosterone levels in men with a SHBG P156L mutation (169).

Naturally occurring SHBG variants with abnormal steroid-binding specificity have not been noted previously. It is therefore remarkable that three of the SHBG mutants we studied (SHBG R135C, SHBG L165M and SHBG E176K) bind estradiol with 1.6 - 1.9 fold greater affinities than SHBG, although their affinities for androgens (DHT and testosterone) are normal. It is difficult to accurately predict how these increases in SHBG affinity for estradiol will affect the concentrations or distribution of estradiol in plasma, but it is reasonable to assume that they will reduce the percentage of free estradiol, as well as its metabolic clearance rate, resulting in higher total plasma estradiol concentrations.

The three SHBG mutants with increased affinities for estradiol also provide us with insight into the structural mechanisms that dictate how different classes of steroids are accommodated within the single SHBG steroid-binding site. For instance, we postulate that SHBG R135C may have a different flexible loop conformation that favors estradiol binding, while SHBG L165M and SHBG E176K are of interest because Leu165 and Glu176 flank a β -strand (Arg167 - Trp170) and a series of residues (i.e. Leu171-Lys173) that are specifically displaced when the SHBG steroid-binding site is occupied by estradiol (53). Although L165

and E176 are not located within the steroid-binding site (50), it is possible that they influence the positioning of this β -strand and its C-terminal residues, which appear to specifically influence the accommodation of estradiol within the steroid-binding site.

Our observation that S1B5 differentially hinders the flux of DHT and MeOE2 into and out of SHBG steroid-binding site is also interesting because it suggests that androgens and estrogens enter and exit the steroid-binding site in different ways. In this context, it is possible that either S1B5-binding physically occludes a common entrance and exit to the steroid-binding pocket in a manner that is less effective in blocking the estrogen flux, or that there is an alternative route of entry and/or exit for estrogens when compared with androgens.

The Thr at position 7 in the mature human SHBG sequence is normally the site of attachment for an O-linked oligosaccharide (177), and we were surprised that the SHBG T7N mutant was not N-glycosylated because an Asn residue in this position introduces a consensus tripeptide (Asn-X-Thr/Ser) site for N-glycosylation (179). One explanation for this is that the close proximity of this Asn to the N-terminus of the nascent SHBG polypeptide limits the enzymatic transfer of the precursor glycan to it during synthesis in the endoplasmic reticulum (180, 181). As a result, the SHBG T7N mutant has no oligosaccharide attached at this position at all but this has no impact on the steroid-binding properties of SHBG, as expected from previous studies (41). Furthermore, based on other previous studies, the loss of an

oligosaccharide at this position is not expected to influence the plasma half-life of SHBG appreciably (42). In contrast, utilization of the two N-glycosylation sites in the C-terminal LG domain will have a more significant impact on the half-life of the protein (42). It is therefore of interest that some of the SHBG mutants appear to differ significantly from SHBG with respect to their subunit macro-heterogeneity, and this might influence the plasma half-life and consequently the concentrations of these SHBG variants in the blood circulation.

In our initial characterization of recombinant SHBG mutants, a comparison of their DHT-binding capacity and immunoassay values enabled us to identify mutants produced at low levels, as well as mutants that exhibit defects in steroid-binding activity and/or recognition in our immunoassay. A comparison of the values obtained by these two different assays also highlights the inherent limitations of the respective methodologies. This is important because SHBG values obtained by these methods are widely used to calculate the free concentrations of sex steroids in clinical samples (182). Moreover, formulas used for this purpose rely on assumptions that immunoassays accurately reflect SHBG concentrations and that SHBG has the same affinity for steroid ligands in all samples. Our results demonstrate that these assumptions are flawed. While it may be argued that these assay limitations are not a serious concern if SHBG variants occur rarely, the SNP databases from which these data are drawn include healthy individuals in general populations, and it is possible that some of the variants

we have identified are more highly represented in specific patient or ethnic groups. For instance, the SHBG P156L variant with a reduced affinity for testosterone occurs in ~2% of European populations (169), but is enriched in French Canadians (168). Moreover, the SHBG D327N that is associated with risk for several different diseases occurs less frequently in African Americans than in individuals of European descent (151).

In an era of increasing emphasis on personalized medicine, our studies highlight the importance of defining how specific non-synonymous SNPs affect the biochemical properties of widely used biomarkers, such as SHBG. In the case of *SHBG* SNPs, this will not only facilitate identification of individuals at risk for a variety of hormone-dependent diseases but may shed light on how the plasma levels or functional properties of SHBG are linked to predisposition to diseases including reproductive tissue cancers (151), osteoporosis (183) and type 2 diabetes (184).

Table 2.1 Oligonucleotide sequences for site-directed mutagenesis to produce SHBG mutants with specific amino acid substitutions

a.a. substitutions	mutagenic oligonucleotides ^a
R(22)H	5'-GTTGCTACTACTGC <u>A</u> TCACACCCGCCAGG
T7N	5'-GACCTGTTCTCCCCA <u>A</u> CCAGAGTGCCAC
T48I	5'-CTCCTCCTTTGAGGTTCGAA <u>T</u> CTGGGACCCAG
E52Q	5'-GGTTCGAACCTGGGACCCA <u>C</u> AGGGAGTGAT
R94Q	5'-GGTGCTGGACCAC <u>A</u> GCTGGATGATGGG
L95M	5'-GTGCTGGACCACGG <u>A</u> TGGATGATGGGAGA
D110N	5'-GTCAAGATGGAGGGG <u>A</u> ACTCTGTGCTGCTGG
E119D	5'-GGTGGATGGGG <u>A</u> TGAGGTGCTGCGC
R123C	5'-GGAGGAGGTGCTG <u>T</u> GCCTGAGACAGGT
R123H	5'-GAGGAGGTGCTGC <u>A</u> CCTGAGACAGGTC
R135C	5'-GGCCCCTGACCAGCAA <u>A</u> TGCCATCCCA
A150P	5'-GCTGCTCTTCCCC <u>C</u> CTTCCAACCTTCG
N152K	5'-TCCCCGCTTCCAA <u>A</u> CTTCGGTTGCCGC
R154W	5'-CCCGCTTCCAACCT <u>T</u> TGGTTGCCGCTG
P156L	5'-CAACCTTCGGTTG <u>C</u> TGCTGGTTCCTGCC
L165M	5'-CCTGGATGGCTGC <u>A</u> TGCGCCGGGATTC
E176K	5'-GCTGGACAAACAGGCC <u>A</u> AGATCTCAGCATCTGC
S192L	5'-CCTCAGAAGCTGTGATGTAGAAT <u>T</u> AAATCCCGGGATATT
G195E	5'-ATGTAGAATCAAATCCCG <u>A</u> GATATTTCTCCCTCCAGG

^aDeviations from DNA sequences complementary to the coding sequences spanning amino acids to be modified are indicated in boldface type and underlined.

Table 2.2 Non-synonymous single nucleotide polymorphisms (SNPs) within human *SHBG* are identified by their corresponding rs numbers

The nucleotides of SNP/ancestral alleles and the corresponding amino acid substitutions for each SNP are listed. The amino acid positions in the mature human SHBG sequence are indicated. However, R(22)H refers to a substitution at position 22 in the signal peptide of the human SHBG precursor.

SNP Identification No.	Alleles	Amino Acid Position
rs9282845	A/G	R(22)H
rs373254168	A/C	T7N
rs143521188	T/C	T48I
rs374583574	C/G	E52Q
rs148001698	A/G	R94Q
rs143452836	A/C	L95M
rs147130840	A/G	D110N
rs186960957	T/G	E119D
rs373769356	T/C	R123C
rs143269613	A/G	R123H
rs368589266	T/C	R135C
rs115336700	C/G	A150P
rs143134553	A/C	N152K
rs139379650	T/C	R154W
rs6258	T/C	P156L
rs145273466	A/C	L165M
rs372114420	A/G	E176K
rs189578288	T/C	S192L
rs146779355	A/G	G195E

Table 2.3 Steroid-binding affinities and specificities of SHBG and SHBG mutants

The dissociation rate constant (K_d) was determined by Scatchard analysis for SHBG (WT) and SHBG mutants using [3 H]DHT as a labeled ligand, apart from SHBG P156L which was compared to WT SHBG in a Scatchard analysis using [3 H]testosterone as a labeled ligand. The relative binding affinity (RBA) values of SHBG and SHBG mutants for testosterone (T) and estradiol (E2) were determined as percentages by dividing the IC_{50} of DHT (i.e., the concentration of DHT required to displace 50% of [3 H]DHT from SHBG) with the corresponding IC_{50} values of unlabeled T or E2 in standard competitive steroid binding assays (27). The K_d and RBA values are expressed as means \pm SD of three independent assays. *= p <0.05, **= p <0.01, ***= p <0.001

SHBG	K_d (nM)	RBA (% of DHT)	
		T	E2
WT	1.2 (testosterone)		
P156L	2.5 (testosterone)		
WT	0.30 \pm 0.08	24.02 \pm 4.18	4.52 \pm 0.57
R(22)H	0.33 \pm 0.02	23.23 \pm 5.34	4.64 \pm 0.87
T7N	0.30 \pm 0.07	21.83 \pm 1.72	4.75 \pm 1.65
T48I	0.78 \pm 0.10 ***	23.88 \pm 4.69	5.32 \pm 0.58
E52Q	0.24 \pm 0.03	21.43 \pm 2.04	4.50 \pm 0.54
R94Q	0.35 \pm 0.01	24.80 \pm 4.82	4.73 \pm 0.88
L95M	0.30 \pm 0.02	24.50 \pm 4.54	4.86 \pm 0.52
D110N	0.39 \pm 0.19	21.14 \pm 0.12	4.51 \pm 0.16
E119D	0.31 \pm 0.04	24.81 \pm 3.94	4.53 \pm 0.89
R123C	0.49 \pm 0.05 ***	24.48 \pm 3.53	5.82 \pm 0.36 **
R123H	1.29 \pm 0.23 ***	26.26 \pm 4.49	5.42 \pm 0.34 *
R135C	0.27 \pm 0.01	25.93 \pm 3.36	7.64 \pm 0.94 ***
A150P	0.40 \pm 0.17	25.58 \pm 4.41	5.13 \pm 0.97
N152K	0.28 \pm 0.06	23.91 \pm 1.99	4.97 \pm 0.70
R154W	0.33 \pm 0.03	24.38 \pm 4.36	3.97 \pm 0.71
L165M	0.24 \pm 0.04	22.93 \pm 1.71	7.37 \pm 0.32 ***
E176K	0.35 \pm 0.04	23.59 \pm 0.44	8.62 \pm 0.47 ***
S192L	0.27 \pm 0.07	25.79 \pm 1.13	4.53 \pm 0.61
G195E	1.52 \pm 0.08 ***	21.72 \pm 3.34	3.94 \pm 0.62

Table 2.4 Summary of the abnormal properties associated with SHBG mutants

T7N	Loss of glycosylation at residue 7.
T48I	2.6-fold lower binding affinity for DHT; increased fibulin-2 interaction, inefficient dimerization, probably due to conformational change caused by defect in calcium binding.
R123C	1.6-fold lower binding affinity for DHT; 1.3-fold higher relative binding affinity for E2.
R123H	4.3-fold lower binding affinity for DHT; 1.2-fold higher relative binding affinity for E2; minor defect in dimerization.
R135C	Reduced S1B5 antibody recognition; 1.7-fold relative higher binding affinity for E2; increased fibulin-2 interaction.
P156L	2-fold lower binding affinity for testosterone
L165M	1.6-fold higher relative binding affinity for E2.
E176K	1.9-fold higher relative binding affinity for E2.
G195E	High complexity of N-glycosylation leading to inefficient secretion in CHO cells; 5-fold lower binding affinity for DHT; increased fibulin-2 interaction, probably due to global change of conformation caused by abnormal protein folding.

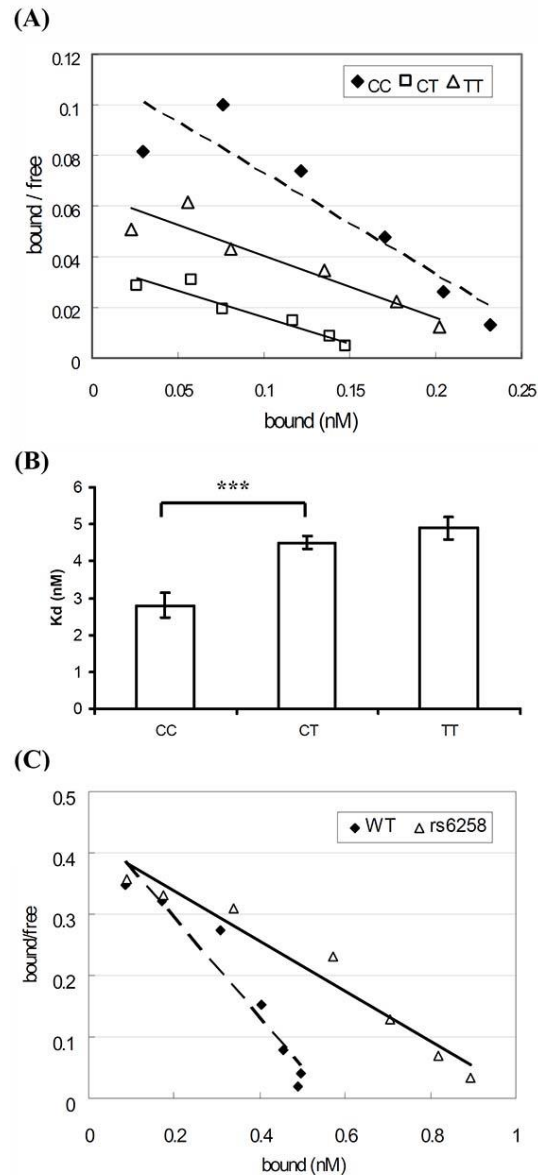


Figure 2.1 Affinities of serum or recombinant SHBG and SHBG mutant for testosterone
 (A) Representative Scatchard plots of serum SHBG binding to $[^3\text{H}]$ testosterone. Serum from individuals homozygous for the common SHBG allele (CC dashed line) or the rs6258 variant allele (TT, solid line), or heterozygous for these alleles (CT, solid line). (B) Dissociation constant (K_d) of serum SHBG according to rs6258 genotype (CC, $n = 4$ subjects; CT, $n = 4$ subjects; TT [variant] $n = 1$ and the variation for the TT subject is derived from three separate analyses). ***= $p < 0.001$. (C) Representative Scatchard plots of recombinant SHBG binding to $[^3\text{H}]$ testosterone. Recombinant SHBG (WT, C genotype; dashed line) or mutant SHBG (rs6258, T genotype; solid line) expressed by CHO cells was diluted 1:10 and subjected to Scatchard analysis, as in panel A.

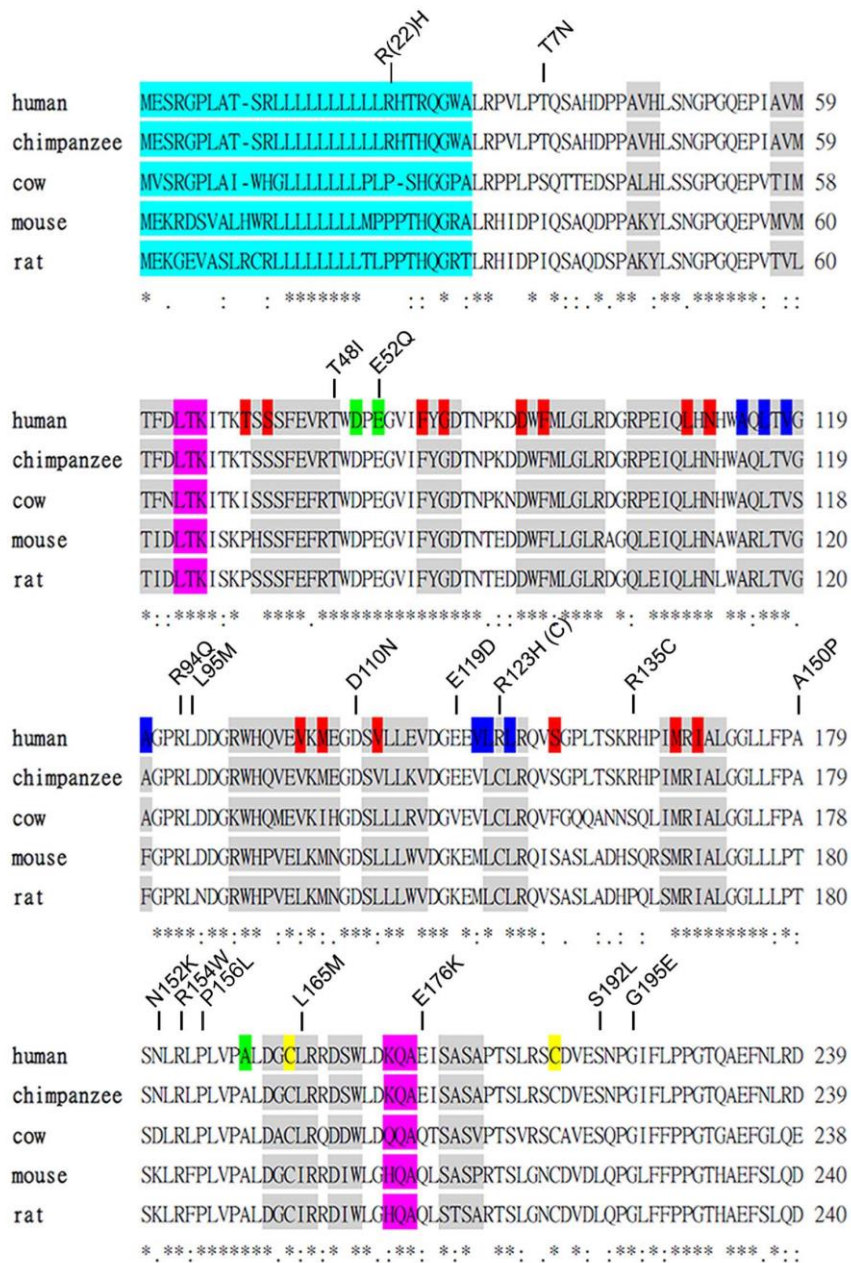


Figure 2.2 Sequence alignment of the N-terminal LG domains of human SHBG and its orthologues in other mammals showing the positions of amino acid substitutions associated with the non-synonymous SNPs studied

Amino acid sequences between human and other species of SHBG N-terminal LG domain were aligned. Secondary structure of α -helix and β -strands are shown as pink and grey box respectively. Residues known to be involved in steroids binding (red), dimerization (blue), calcium binding (green) and disulfide bridge formation (yellow) are highlighted. Signal peptide is also highlighted as light-blue color. Amino acid substitutions are presented on top of the sequences. *= conserved residues between species.

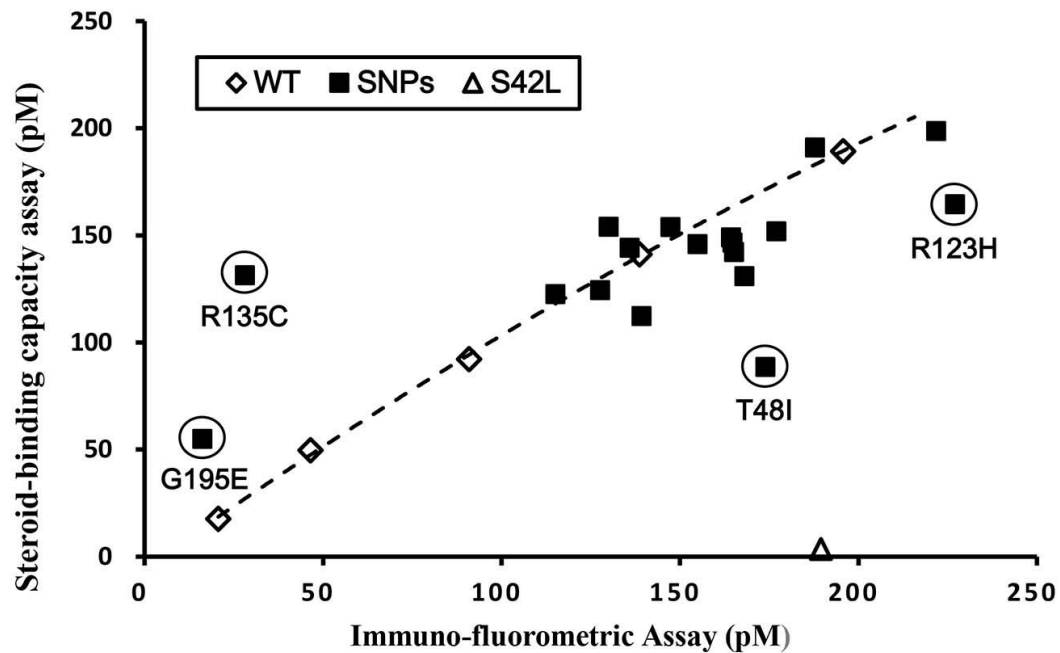


Figure 2.3 Comparison of DHT-binding capacity assay and immuno-fluorometric assay (IFA) values of recombinant SHBG and SHBG mutants

Values for SHBG mutants in which amino acid substitutions introduced by non-synonymous SNPs (solid squares) are compared with a reference line generated using the values for SHBG (WT) determined at five different concentrations (open diamonds). For reference, the corresponding values for a known DHT-binding deficient mutant, SHBG S42L (50), are shown (open triangle). Mutants suspected of exhibiting abnormal DHT-binding affinity or immune-recognition in the IFA are circled, and are positioned below or above the WT reference line, respectively.

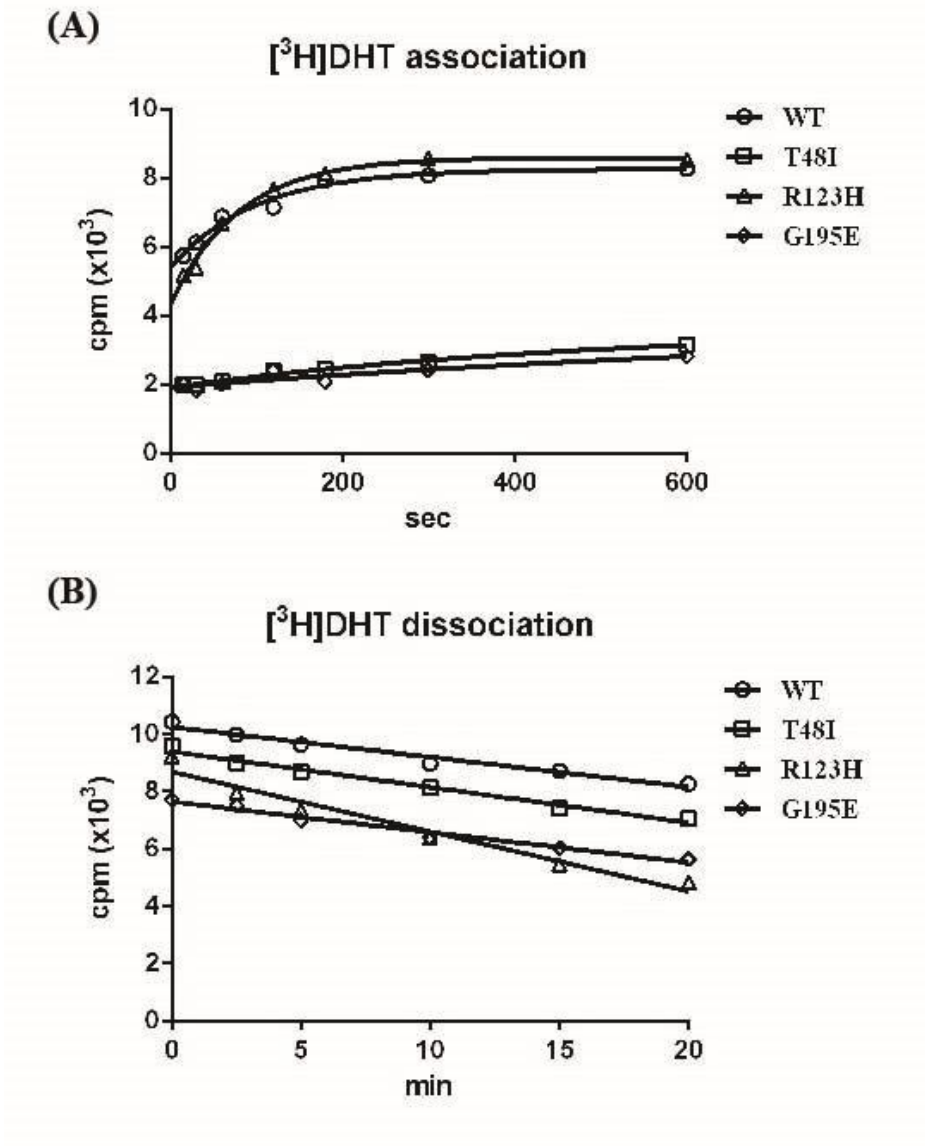


Figure 2.4 Kinetics of DHT binding to SHBG (WT) and SHBG mutants with a suspected abnormally low DHT-binding affinity (SHBG T48I, SHBG R123H, and SHBG G195E)
 (A) Association rates were determined by measuring the occupancy of unliganded SHBG samples by $[^3\text{H}]\text{DHT}$ over time at 0°C . (B) Dissociation rates were determined in a pulse-chase experiment by pre-incubating SHBG with 10 nM of $[^3\text{H}]\text{DHT}$ for 1 h followed by adding 3 μM DHT for 0 to 20 min at 0°C .

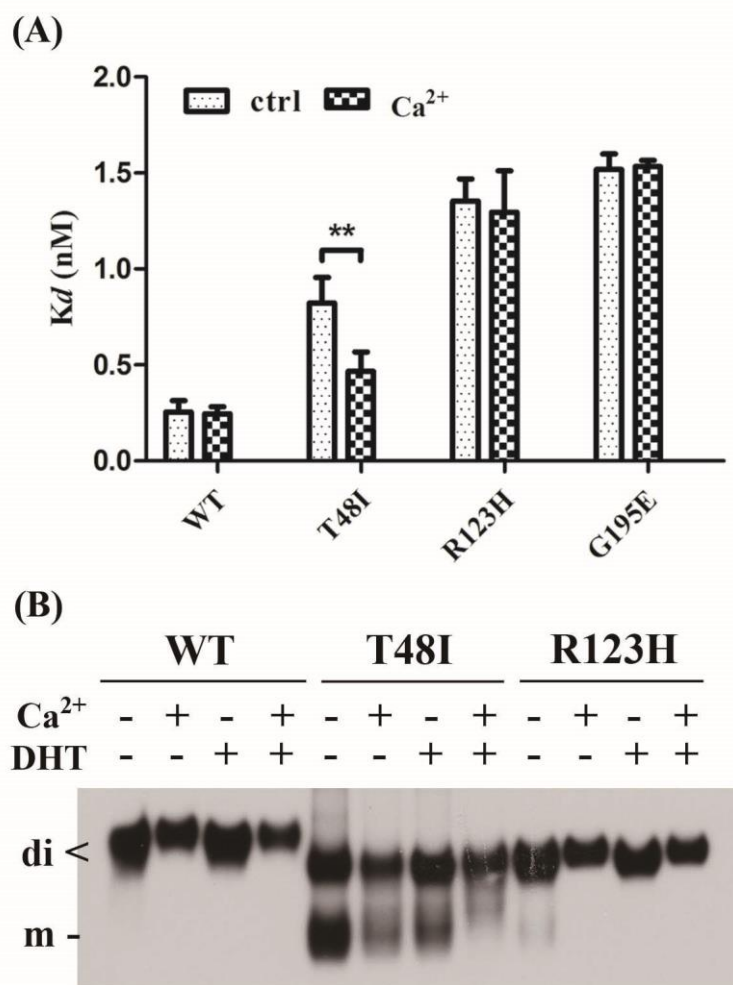
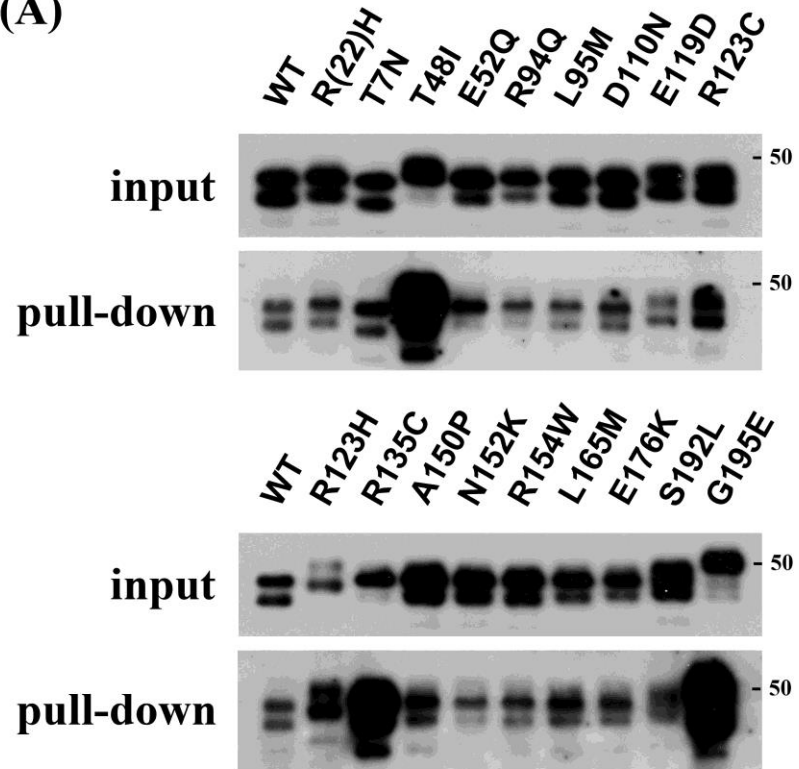


Figure 2.5 Influence of calcium supplementation on SHBG mutants with abnormally low DHT-binding affinity

(A) Calcium partially restores DHT-binding affinity of SHBG T48I, but has no effect on other DHT-binding defective variants (SHBG R123H and SHBG G195E). Dissociation constants (K_d) of SHBG (WT), SHBG T48I, SHBG R123H and SHBG G195E for [³H]DHT were determined by Scatchard analysis in the presence or absence (control) of 1 mM CaCl₂. **= $p < 0.01$ (B) Calcium and/or DHT stabilizes SHBG T48I and SHBG R123H homodimers. Western blotting analysis under non-denaturing conditions was performed in the presence or absence of DHT or calcium using rabbit anti-human SHBG antiserum as the primary antibody.

(A)



(B)

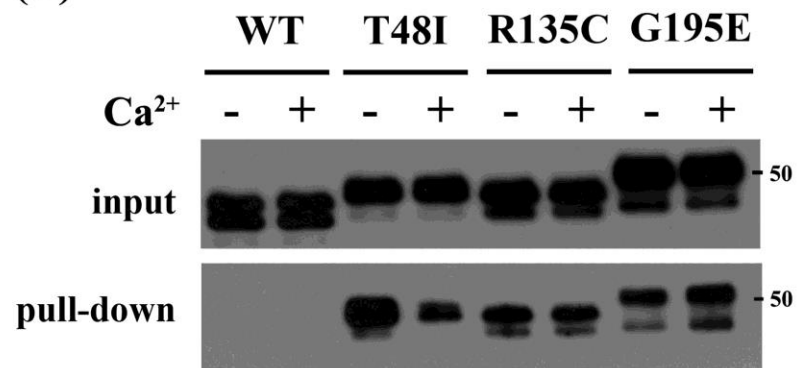


Figure 2.6 Identification of SHBG mutants with abnormal interactions with fibulin-2

(A) Interaction of SHBG or SHBG mutants with the C-terminal domain of fibulin-2. A GST pull-down assay was performed by using 10 μg of a GST-fibulin-2 fusion protein as bait, and the relative amounts of interacting SHBG were determined by SDS-PAGE and Western blotting using rabbit anti-human SHBG antiserum as the primary antibody. Exposure of the Western blots was adjusted in order to compare the relative amounts of different SHBG mutants that interacted fibulin-2 in the GST pull-down assay, against SHBG as a reference. (B) Calcium partially restored the interaction of T48I SHBG with fibulin-2 when the GST pull-down assay was performed in the presence or absence of 1 mM CaCl_2 . Note that this Western blot was under-exposed in order to see the effect of calcium supplementation on fibulin-2 interaction with SHBG mutants with enhance ability to interact with fibulin-2, and at this exposure the pull-down of SHBG is not detectable. In all of these Western blots, the denatured recombinant SHBG monomers migrate during SDS-PAGE as a doublet, the sizes and intensities of which reflect differential utilization of the two N-linked glycosylation sites in the C-terminal LG domain (41). A 50 kDa molecular weight size marker is shown on the right of the Western blots, which are representative examples of three independent experiments.

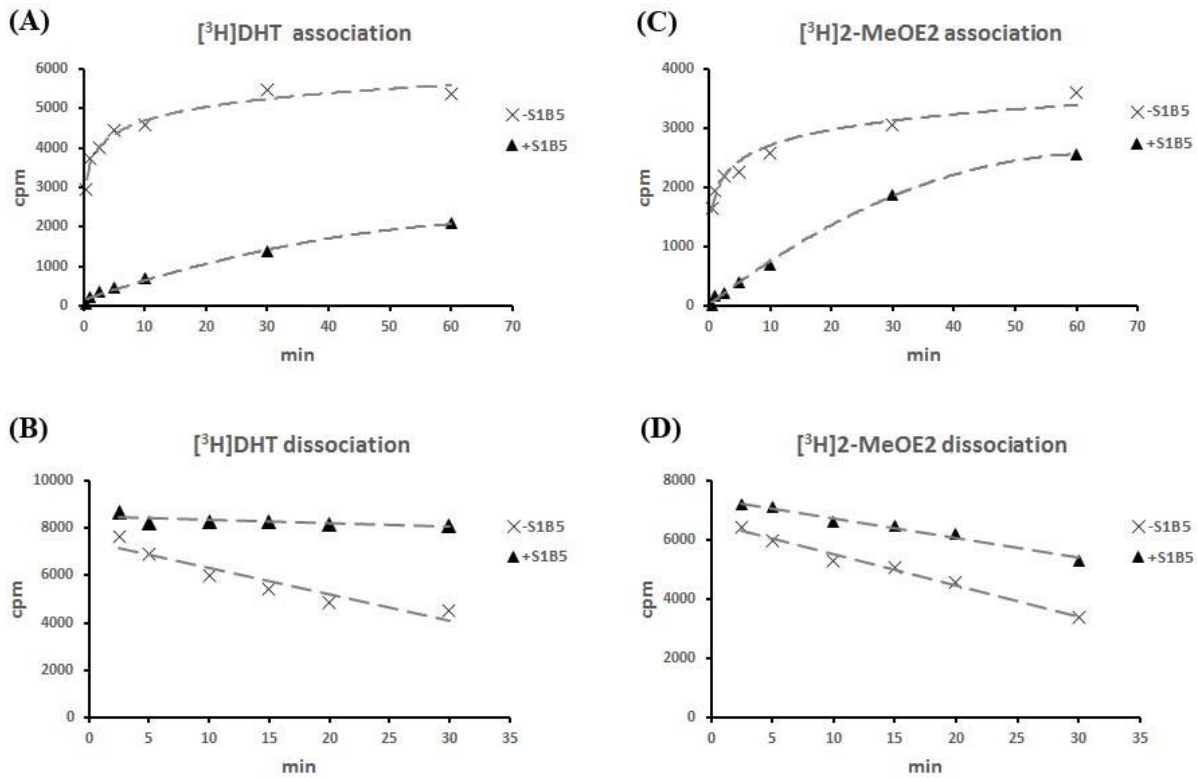


Figure 2.7 Effects of S1B5 antibody binding to SHBG on steroid-binding kinetics

Steroid association rates were determined by incubating unliganded SHBG with or without S1B5 antibody for 1 h at room temperature followed by incubation (30 sec to 1 h at 0°C) with either [3H]DHT (A) or [3H]2-MeOE2 (C). Dissociation rates were determined by first saturating SHBG with [3H]DHT (B) or [3H]2-MeOE2 (D) followed by an incubation (1 h at room temperature) in the presence or absence of S1B5 antibody. The irreversible loss of radiolabeled steroids from SHBG over time was then assessed by DCC exposure for 2.5 to 30 min at 10°C.

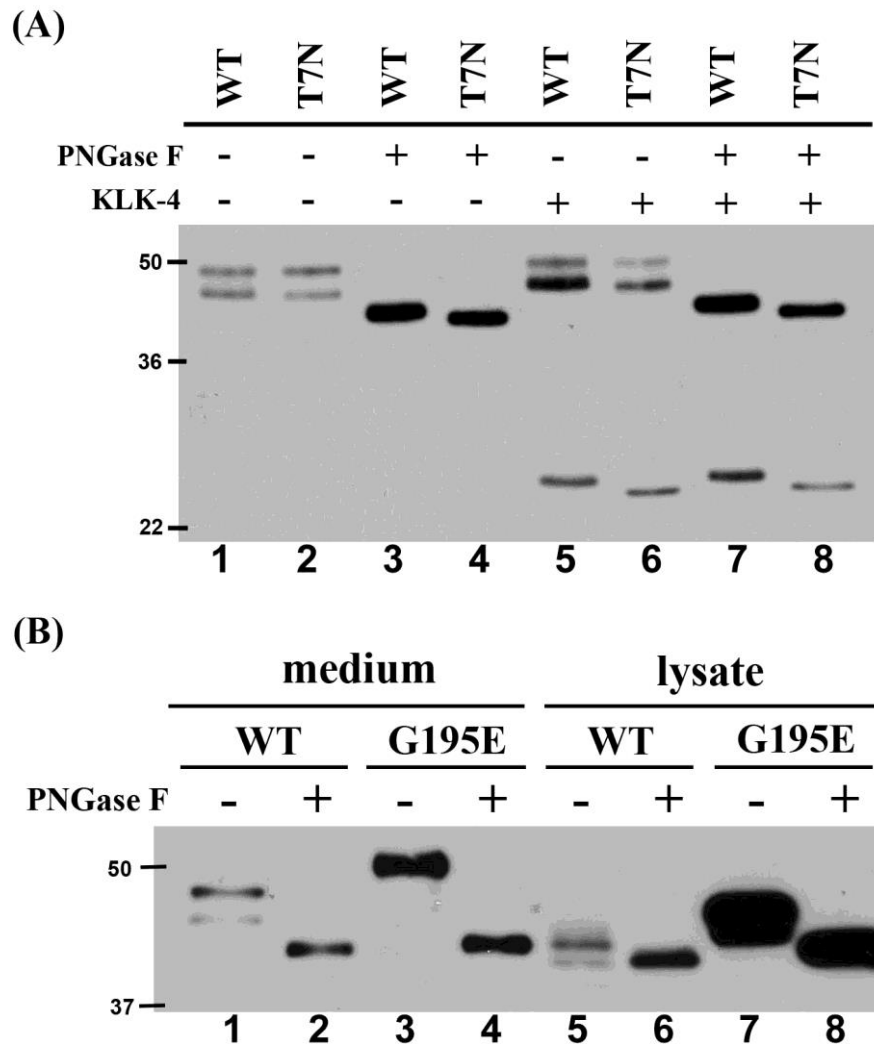


Figure 2.8 Glycosylation status of SHBG T7N and SHBG G195E

(A) Lack of glycosylation at Asn 7 of SHBG T7N. SHBG (WT) or SHBG T7N were treated with PNGase F and/or Kallikrein-related peptidase 4 (KLK-4) for 3 h at 37°C. (B) SHBG G195E mostly accumulated in CHO cells with more complexed N-linked glycans. Equal amount of SHBG (WT) and SHBG G195E from media, or 20 µg or 5 µg total cell lysate from SHBG or SHBG G195E stably expressed CHO cells were treated with PNGase F at 37°C for 3 h. Deglycosylated and/or KLK-4 cleaved SHBGs were detected by SDS-PAGE and Western blotting analysis using mouse 7H9 monoclonal antibody. Molecular weight size markers (kDa) are shown on the left of each Western blot.

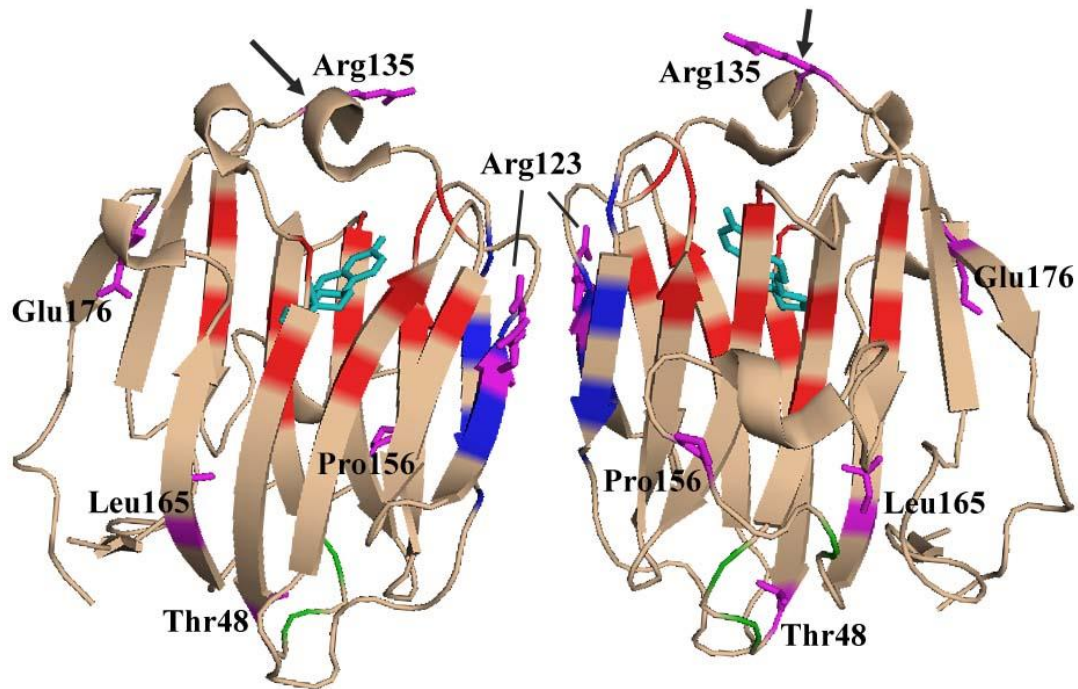


Figure 2.9 Crystal structure of the N-terminal LG domain of human SHBG in complex with estradiol (PDB code: 1LHU, estradiol shown in cyan) showing the residues where amino acid substitutions were found to alter the functional properties of SHBG

The positions of residues previously reported (5) to be involved in steroid binding (red), dimerization (blue) and calcium binding (green) are highlighted. The loop structure positioned above the steroid-binding pocket is indicated with an arrow. The residues where substitutions result in altered steroid binding (Thr48, Arg123, Arg135, Pro156, Leu165, Glu176), dimerization (Arg123, Thr48), calcium binding (Thr48) or fibulin-2 binding (Thr48, Arg135) are shown in purple. Note that Gly195 is not included in this crystal structure of the SHBG N-terminal LG domain.

Chapter 3 : Crystal structure analysis of the SHBG R123H and SHBG E176K mutant N-terminal LG domains

3.1 Introduction

The crystal structures of the N-terminal Laminin G-like (LG) domain of SHBG in complex with DHT (50), estradiol (53) or several other steroids (53, 56) have been solved. These structures revealed a dimer interface composed by β -strand 7 and 10 (50), and a steroid-binding site that androgens occupy in an opposite orientation when compared with estrogens (53). In addition, a disordered segment from Pro130 to Arg135 forms a flexible loop that covers the entrance to the steroid-binding site (60). This loop segment can be clearly visible in the electron density maps when SHBG is in complex with estradiol (53). On the contrary, this loop segment cannot be defined in SHBG crystals in complex with DHT (50) unless the crystals were soaked in EDTA to remove zinc ions, or were formed in tetragonal space group (60). These results imply that this loop region is more stable under conditions that SHBG is in complex with estradiol, and removal of zinc ion from SHBG increases the homogeneity of this region because binding of zinc levers His136 away from the protein surface and causes disorder of the loop region (51, 185). In **Chapter 2**, functional analysis of the naturally occurring non-synonymous SNPs within this domain informed us that several genetic

variations alter the production and/or biochemical properties of SHBG. In this study, I set out to determine the crystal structures of the N-terminal LG domains of two of these mutants (SHBG R123H and SHBG E176K) in order to gain insight into the molecular mechanisms that mediate their abnormal steroid-binding properties.

In **Chapter 2**, I provided evidence that substitution of Arg123 by His causes a 4.3-fold reduction in affinity for DHT and testosterone, while the reduction in the relative affinity for estradiol was less marked (**Table 2.3**). I also showed that the reduced affinities of SHBG R123H for these steroids was due to a higher dissociation rate, while the association rate stayed the same as that of SHBG (**Figure 2.4**). This was unexpected because the Arg123 residue is located within the dimer interface of human SHBG and not in the steroid-binding site *per se*. Moreover, despite previous reports that dimerization and steroid binding activity are in some way linked (118), the dimer deficient mutant (V89E) exhibits normal steroid binding affinity and specificity (58), and I also noted that substitution of Arg123 by His did not disrupt SHBG dimerization in the presence of calcium or steroid ligands (**Figure 2.5**), indicating that SHBG R123H likely exists as a dimer under physiological conditions.

In the case of SHBG E176K, substitution of Glu176 by Lys specifically resulted in 1.9-fold increase of affinity for estradiol, but not for DHT or testosterone (**Table 2.3**). Again this was somewhat surprising because although Glu176 is not located within the steroid-binding

site of SHBG, it is adjacent to a β -strand (Arg167-Trp170) and a series of residues (Leu171-Lys173) that are specifically displaced when estradiol binds to SHBG (53).

To gain further insight into these questions, crystal structures of the SHBG R123H and SHBG E176K N-terminal LG domains were obtained and compared with existing crystal structures of the corresponding region of SHBG in the presence of relevant steroid ligands. The resulting data provide molecular explanations for how these naturally occurring non-synonymous SNPs affect the ligand-binding properties of SHBG.

3.2 Material and methods

3.2.1 Recombinant protein overproduction

A human *SHBG* cDNA encoding the N-terminal LG domain (amino acid residues 1-205) was cloned into the pGEX-2T vector. A glutathione S-transferase (GST) cDNA was fused in frame with the *SHBG* cDNA and with a linker encoding a thrombin-cleavage site inserted between them for removing the GST tag from the GST-SHBG fusion proteins. Mutagenesis was performed to generate mutant constructs for producing the N-terminal LG domains of SHBG R123H and SHBG E176K using QuickChange II Site-Directed Mutagenesis Kit (Agilent Technologies, Santa Clara, CA). Plasmids were introduced into the *E. coli* host strain Rosetta and transformed cells were grown in LB medium containing 100 $\mu\text{g}/\text{mL}$ of ampicillin at 37°C to an optical density of 0.6 at 600 nm. To induce production of GST-SHBG fusion

proteins, 0.4 mM of isopropyl β -D-1-thiogalactopyranoside (IPTG) was added to the medium and cells were grown at 30°C for an additional 4 h.

3.2.2 Protein purification

Bacterial pellets from 12 L of culture were harvested and re-suspended in a lysis buffer containing 50 mM Tris-HCl pH 7.5, 300 mM NaCl, 2.5 mM CaCl₂ and 5 μ M steroid ligands (DHT for SHBG R123H and estradiol for SHBG E176K). Immediately before cell lysis, 0.2 mM phenylmethylsulfonyl fluoride (PMSF) and 250 μ g/mL lysozyme were added. Cells were lysed at 4°C by sonication and the cell lysate was filtered with 0.45 μ m filters. The clear cell lysate was applied to a column packed with 20 mL of equilibrated Pierce Glutathione Superflow Agarose (Thermo Fisher Scientific, Waltham, MA) at a constant flow rate of 1 mL/min at room temperature. The column was washed with 2x100 mL of wash buffer (20 mM Tris-HCl pH 8.0, 100 mM NaCl, and 2.5 mM CaCl₂) to rinse off the remained cell lysate and weakly bound non-specific proteins. An ~70 kDa *E. coli* chaperon protein, DnaK, was washed off by 3x60 mL of MgATP buffer (Tris-buffered saline with 5 mM ATP, 5 mM MgSO₄, and 0.1 mg/mL denatured *E. coli* proteins) (**Figure 3.1, lane 1 and 2**) (186). After a final rinse with 100 mL of wash buffer, 10 mL of 20 unit/mL thrombin (GE Healthcare Life Sciences, Baie d'Urfe, Quebec) was added to Glutathione Superflow Agarose beads and incubated at room temperature overnight. The drained elute and the subsequent 20 mL of rinse with wash buffer

were pooled and concentrated by Millipore Amicon® Ultra-15 centrifugal filter concentrators (**Figure 3.1, lane 3**).

The N-terminal LG domain of SHBG was further purified by gel-filtration and anion-exchange chromatography using an Ä KTA FPLC system (GE Healthcare). In brief, a Superdex 75 10/300 GL column (GE Healthcare Life Sciences) was equilibrated with 50 mM Tris-HCl pH 7.5, 150 mM NaCl, and 2.5 mM CaCl₂. The concentrated protein samples were applied to the column and eluted in fractions using the same buffer for column equilibration. Fractions containing the N-terminal LG domain of SHBG were pooled (**Figure 3.1, lane 4**) and dialyzed overnight against 20 mM Tris-HCl pH 8.0 at 4°C. Dialyzed samples were applied to a Mini Q 4.6/50 PE column (GE Healthcare Life Sciences) equilibrated with 20 mM Tris-HCl pH 8.0, and eluted by a linear gradient of NaCl (0 to 1 M). Fractions containing the N-terminal LG domain of SHBG were pooled and exchanged with a buffer containing 50 mM HEPES pH 7.5, 2.5 mM CaCl₂, and 5 µM DHT or estradiol (**Figure 3.1, lane 5**).

3.2.3 Crystallization

The N-terminal LG domain of SHBG R123H and SHBG E176K were both crystallized by the hanging-drop vapor diffusion method at room temperature. For SHBG R123H, 1 µL of protein solution (10 mg/mL protein, 50 mM HEPES pH 7.5, 2.5 mM CaCl₂, and 5 µM DHT) was mixed with 1 µL of reservoir solution (0.2 M lithium nitrite and 20% PEG 3350) and the

droplet was equilibrated against 1 mL of reservoir solution (**Figure 3.2A**). For SHBG E176K, 1 μ L of protein solution (10 mg/mL protein, 50 mM HEPES pH 7.5, 2.5 mM CaCl₂, and 5 μ M estradiol) was mixed with 1 μ L of reservoir solution (0.2 M potassium thiocyanate and 20% PEG 3350) and the droplet was equilibrated against 1 mL of reservoir solution (**Figure 3.2B**).

3.2.4 Crystallographic analysis

Crystals of the N-terminal LG domain of SHBG R123H or SHBG E176K were soaked in appropriate reservoir solutions containing 14 μ M DHT and 30% glycerol, or 14 μ M estradiol and 30% ethanol, respectively, as cryo-protectants before being flash-frozen in liquid nitrogen. The X-ray diffraction data sets were collected on BL 7-1 beamline at the SSRL synchrotron in Stanford, USA. Data sets were reduced with the program HKL3000.

The crystal structures of SHBG R123H and SHBG E176K were solved by the molecular replacement method present in the PHENIX package using the previously reported SHBG structures (PDB accession number 1KDM and 1LHU respectively) as research models. The models were refined in PHENIX. The conformation of the loop segment (Leu131-His136) covering the steroid-binding site was further refined. The X-ray diffraction data and the refinement statistics are listed in **Table 3.1**. All structures are depicted using Pymol (DeLano Scientific; <http://www.pymol.org>).

3.3 Results

3.3.1 Characteristics of the SHBG R123H and SHBG E176K N-terminal LG domain

crystals

In our previous studies of crystal structures of the SHBG in complex with different steroid ligands, SHBG N-terminal LG domains (amino acid residue 1-205) without a polyhistidine tag were crystalized previously in a trigonal space group $R32$ rapidly within one week (50, 53, 187). By contrast, SHBG crystals with polyhistidine tag were crystalized in a tetragonal space group $P4_322$ slowly within three months (60, 187). Under the new conditions with PEG3350 as a precipitant for crystallization, we were able for the first time to get crystals of the SHBG N-terminal LG domain without a polyhistidine tag in a $P4_322$ tetragonal space group (**Table 3.1**).

Calcium was coordinated with crystals of both SHBG R123H and SHBG E176K N-terminal LG domain mutants due to the supplementation of 2.5 mM calcium chloride during the preparation of SHBG proteins and crystals. By contrast, zinc was not supplemented; therefore, there were no zinc ion signals in the electron density maps of both crystals. The previous crystal structure of SHBG in complex with DHT in the same space group of $P4_322$ (1KDM), and SHBG in complex with estradiol (1LHU), although in a different space group, were chosen for comparisons with the crystal structures of SHBG R123H and SHBG E176K,

respectively.

3.3.2 The steroid-binding pocket and dimerization domain of SHBG R123H are structurally similar to those of SHBG

The crystal structure of the N-terminal domain of SHBG R123H revealed that the orientation of the His123 side chain did not disrupt the dimerization interface, and the dimer formed properly within the crystals (**Figure 3.3A**). In a previous biochemical study, SHBG R123H possessed a reduced binding affinity for DHT, testosterone, and estradiol (**Table 2.3**) due to a faster steroid dissociation rate (**Figure 2.4B**). However, the bound DHT and the four critical residues, Ser42, Asp65, Asn82, and Val105, that interact with it within the steroid-binding site are essentially superimposable in the crystal structures of N-terminal LG domain of SHBG R123H and SHBG (**Figure 3.3B**).

3.3.3 The Arg135 of SHBG R123H replaces the space occupied by Lys134 in SHBG

Affinity-labeling experiments and crystal structure studies of SHBG have shown that Lys134 is the only residue that makes contact with steroid directly within the flexible loop region that covers the entrance to the steroid-binding site (60, 61). Removal of the side chain of Lys134 by substitution with alanine only marginally reduced the SHBG binding-affinity for DHT (60). In our new crystal structure of the amino-terminal LG domain of SHBG R135H we see a different conformation of the flexible loop region, with a space replacement of SHBG

Lys134 by Arg135 of SHBG R123H (**Figure 3.4**). In addition, a relative lower thermal displacement factor was observed in association with Arg135 of SHBG R123H, indicating that the loop region of SHBG R123H is more rigid than that of SHBG.

3.3.4 Substitution of Glu176 with lysine caused a local conformational change at the SHBG N-terminal LG domain surface

Human SHBG E176K exhibits a higher binding affinity specifically for estradiol (**Table 2.3**). The crystal structure of the N-terminal LG domain of SHBG E176K revealed that estradiol resides normally within the steroid-binding pocket (**Figure 3.5A**). The flexible loop region on top of the steroid-binding pocket also behaved in essentially the same way as in the SHBG conformation (**Figure 3.5B**). One observable structural difference between SHBG and the SHBG E176K mutant locates near a series of residues (Leu171-Lys173) that are specifically displaced when estradiol binds to SHBG (**figure 3.5B**) (53). A detailed examination of the structure reveals that the side chain of Lys176 repels the side chain of Lys173 by about 3.6 Å away from the center of a rim at the lateral side of the N-terminal domain of SHBG (**Figure 3.6**).

3.4 Discussion

To further investigate the molecular basis of my findings in **Chapter 2**, SHBG R123H and SHBG E176K were prioritized for crystal structure analysis because their dimerization

and/or steroid-ligand binding properties are different from SHBG. The crystals of these SHBG mutants formed under a new condition using PEG3350 as precipitant. As a result, SHBG mutants were arranged in a tetragonal space group $P4_322$ in crystals, which differs from a trigonal space group $R32$ obtained from the previous studies of the same domain of SHBG.

The crystal structures of the N-terminal domain of SHBG R123H in complex with DHT, and SHBG E176K in complex with estradiol were compared with crystal structures of the same domain of SHBG in complex with these same ligands (53, 60). Our results revealed that substitution of Arg123 by histidine resulted in distal alterations of the position and the flexibility of the loop region above the steroid binding pocket of SHBG. By contrast, substitution of Glu176 to lysine locally displaced the side chain of Lys173 at the lateral side of the N-terminal domain of SHBG.

It is of interest that the abnormal steroid-binding properties of SHBG R123H and SHBG E176K were not due to conformational changes of their steroid-binding pockets. By contrast, other important characteristics of SHBG that affect the stability and/or the dynamics of steroid-ligand binding may account for the abnormal steroid-binding properties. For example, a space replacement of Lys134 in SHBG by Arg135 in SHBG R123H stabilizes the flexible loop region and the lack of a proper flexibility of this region may reduce the ability of SHBG to

accommodate the bound steroid ligands and cause their easier dissociation as observed in the dissociation rate study in **Chapter 2 (Figure 2.4B)**.

Moreover, my studies described in **Chapter 2** revealed that estradiol associates with and dissociates from SHBG differently from DHT in a way independent of S1B5 antibody steric hindrance (**Figure 2.7**). Whether an alternative pathway exists specifically for the entrance of estradiol into the steroid-binding pocket is an interesting possibility. The Glu176 of SHBG locates at the lateral surface of the N-terminal LG domain of SHBG (**Figure 2.9**). When looking from this side, the N-terminal LG domain resembles a “hollow tube” that could act as a pathway for the influx or efflux of steroids (**Figure 3.6**). In this case, both Glu176 and Lys173 locate at the opening rim of the entrance to this “hollow tube”. Testing this possibility by investigating whether substitution of Glu176 with lysine results in removal of the hindrance by Lys173 from the opening of this alternative pathway for estradiol movement into and/or out of the steroid-binding pocket will be an interesting future direction to pursue.

Besides the above assumptions that may account for the abnormal steroid binding properties associated with both SHBG mutants, several possibilities should also be taken into consideration carefully. First, SHBG proteins are confined in a rigid structure within crystals and their motion is limited when compared to the proteins in solution. The binding of steroids to SHBG is very dynamic, so an artificially fixed conformation of the steroid-binding pocket

in the confined crystals with saturated steroid ligands may occur. Second, the structure of SHBG in a ligand-free (apo) state has not yet been solved. Therefore, with information only for ligand-bound (holo) SHBG, we are not able to know how the protein conformation changes from the apo to holo state. For instance, SHBG R123H in solution possesses a normal association rate, but a faster dissociation rate for DHT (**Figure 2.4B**). While the conformation of the steroid-binding pocket of SHBG R123H is almost the same as that of SHBG when they are in complex with DHT, differences in conformational changes as they transit from ligand-bound to ligand-free state may account for SHBG R123H's faster dissociation rate for DHT. Third, the affinities of SHBG for steroids were measured using full-length SHBG. However, all SHBG crystal structures were obtained using the N-terminal LG domain of SHBG. Whether the intact full-length SHBG influences the way these two SHBG mutants bind steroids remains to be determined.

In addition, the positions of residues between His123 and the flexible loop region of the SHBG R123H mutant were not changed when compared with those of SHBG (**Figure 3.4**). How substitution of Arg123 with histidine caused a long range effect on the flexibility of this loop region, and whether this apparent change in its flexibility is simply due to the different conditions for crystal formation or differences in how the final structures were refined need to be further examined.

While we have previously focused on structures of SHBG in complex with different steroid ligands, or on structures in the presence or absence of zinc ions, this is the first structural analysis of SHBG mutants. My results provided insights into molecular mechanisms that explain how genetic polymorphisms affect steroid-binding properties of SHBG.

Table 3.1 X-ray diffraction data and refinement statistics for SHBG R123H and SHBG E176K versus SHBG (WT) N-terminal LG domain crystals

	SHBG R123H	SHBG WT (1KDM*)	SHBG E176K	SHBG WT (1LHU**)
Data collection				
Space group	<i>P</i> ₄ ₃ ₂ ₂	<i>P</i> ₄ ₃ ₂ ₂	<i>P</i> ₄ ₃ ₂ ₂	<i>R</i> ₃ ₂
Cell dimensions				
<i>a</i> , <i>b</i> , <i>c</i> (Å)	52.0, 52.0, 148.5	52.2, 52.2, 148.5	52.0, 52.0, 149.7	103.6, 103.6, 84.5
α , β , γ (°)	90, 90, 90	90, 90, 90	90, 90, 90	90, 90, 120
Resolution (Å)	50-1.68 (1.73-1.68) ^a	40-2.35 (2.4-2.35)	50-1.7 (1.73-1.7)	20-1.8 (1.82-1.8)
<i>R</i> _{sym} or <i>R</i> _{merge}	10.9 (86.9)	9.1 (37.9)	8.8 (56.9)	3.2 (28.0)
Completeness (%)	100 (100)	94.9 (99.1)	99.3 (90.8)	96.6 (70.4)
Redundancy	10.4 (7.5)		10.4 (5.6)	
Refinement				
Resolution (Å)	50-1.68 (1.73-1.68)	40-2.35 (2.4-2.35)	50-1.7 (1.73-1.7)	20-1.8 (1.82-1.8)
<i>R</i> _{work} / <i>R</i> _{free}	16.8/18.2	19.3/26.4	15.6/17.7	20.4/23.7
No. of atoms				
protein	2978	1374	3022	1394
water	388	72	576	96
Average <i>B</i> -factor (Å ²)	24.5	35.6	20.3	29.9
r.m.s. deviations				
Bond lengths (Å)	0.009	0.01	0.009	0.01
Bond angles (°)	1.396	0.039	1.391	1.58

^a Values for the highest-resolution shell are given in parenthesis

* protein data bank ID for crystal structure of His-tagged N-terminal LG domain of SHBG in complex with DHT

** protein data bank ID for crystal structure of N-terminal LG domain of SHBG in complex with estradiol

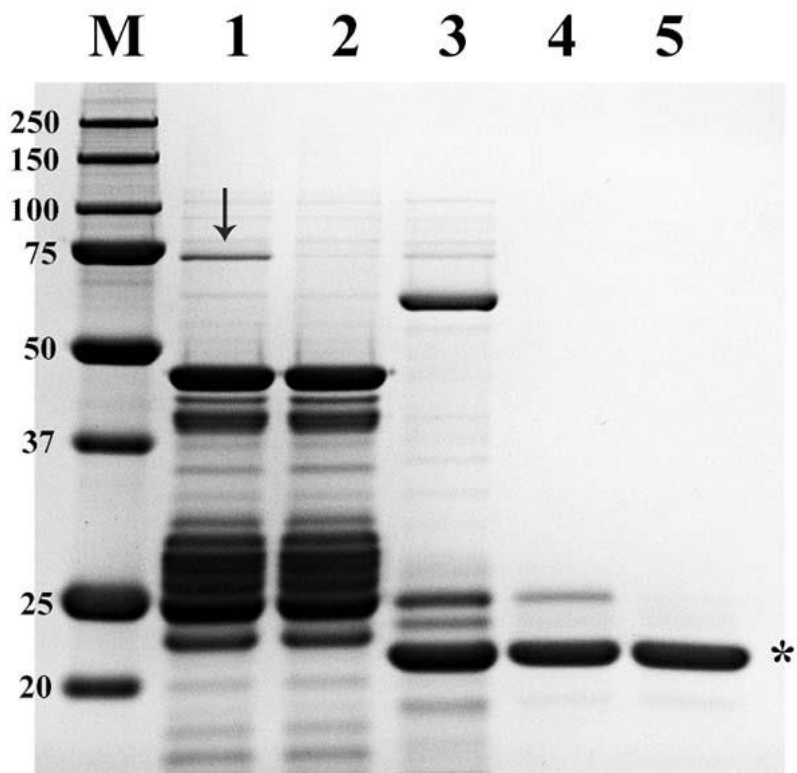


Figure 3.1 Purification of the N-terminal LG domain of SHBG

Protein samples from each purification step were resolved by 10% SDS-PAGE and stained with coomassie blue. Glutathione agarose beads before (lane 1) and after (lane 2) MgATP buffer washing were boiled in SDS protein sample buffer. The majority of DnaK (arrow) was washed off by the MgATP buffer. The thrombin cleaved fractions (lane 3) were subjected to following Superdex gel-filtration (lane 4) and Mini Q anion-exchange (lane 5) chromatography. Markers (M) with molecular sizes (kDa) were shown on the left. *, N-terminal LG domain of SHBG

(A)

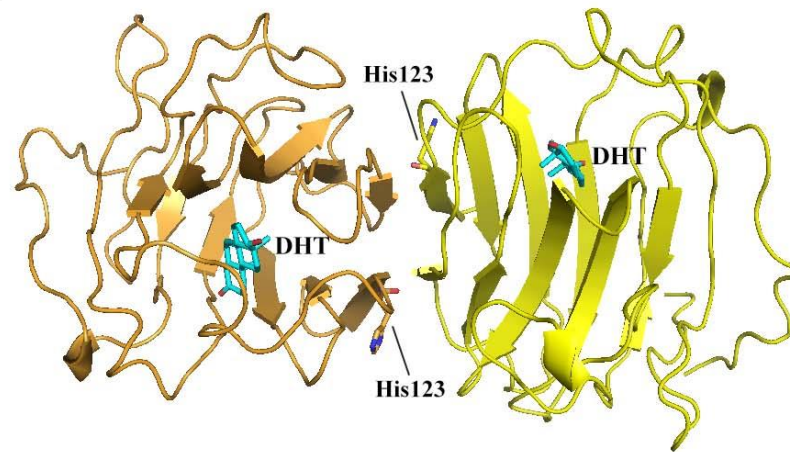


(B)



Figure 3.2 Crystals of the N-terminal LG domain of SHBG R123H and SHBG E176K
The N-terminal LG domains of (A) SHBG R123H (B) SHBG E176K were crystallized in 20% PEG3350 solutions by hanging-drop vapor diffusion method at room temperature.

(A)



(B)

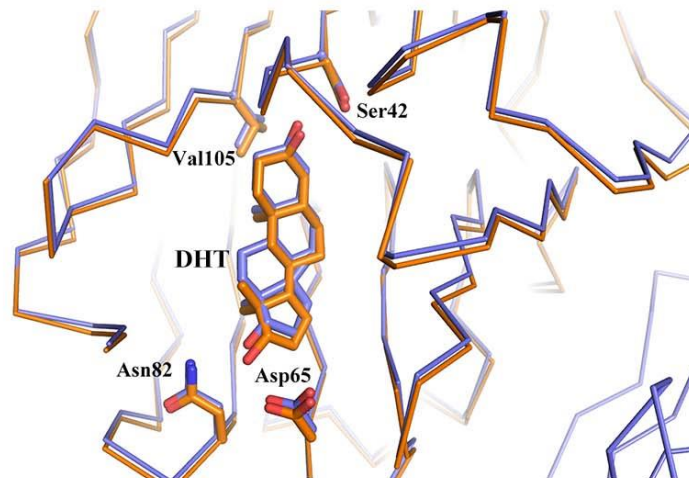


Figure 3.3 Molecular properties of DHT-bound SHBG and SHBG R123H revealed by the crystal structures of their N-terminal LG domains

(A) In crystals, the SHBG R123H bound DHT and dimerized properly. The left (orange) and the right (yellow) half represent each monomer of the N-terminal LG domain of SHBG R123H. (B) A superimposed image of the steroid-binding pockets of SHBG (1KDM, blue) and SHBG R123H (orange). The positions of DHT and four residues, Ser42, Asp65, Asn82, and Val105 that are responsible for hydrogen bond formation with DHT almost overlap in SHBG and SHBG R123H.

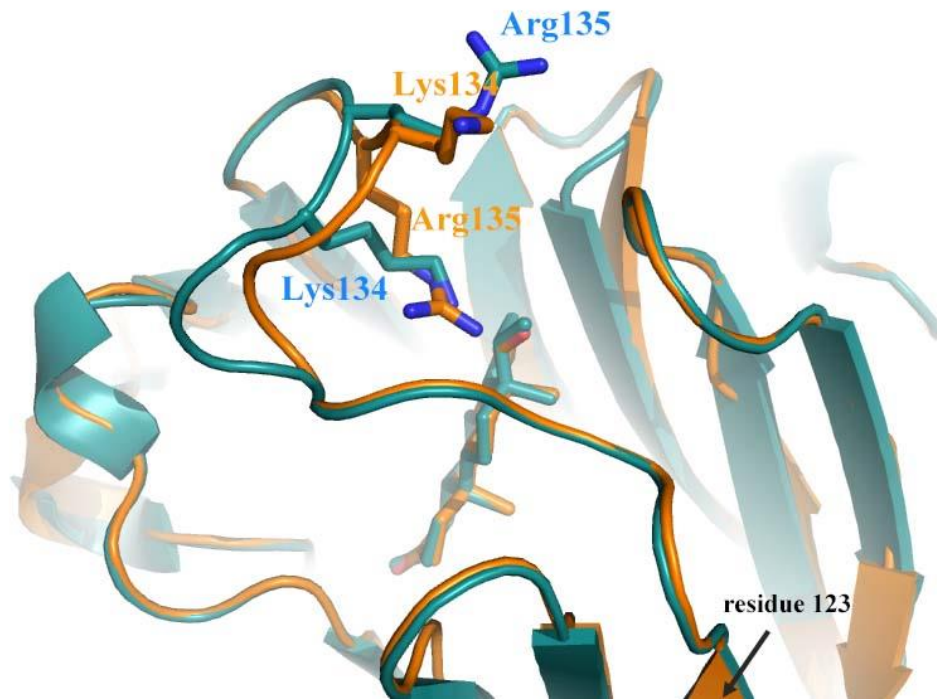


Figure 3.4 The flexible loop region above the steroid-binding pocket of SHBG and SHBG R123H

A superimposed image revealing the flexible loop region above steroid-binding pockets of SHBG (1KDM, blue) and SHBG R123H (orange) shows the displacement of Lys134 of SHBG by Arg135 of SHBG R123H that protrudes into the steroid-binding pocket.

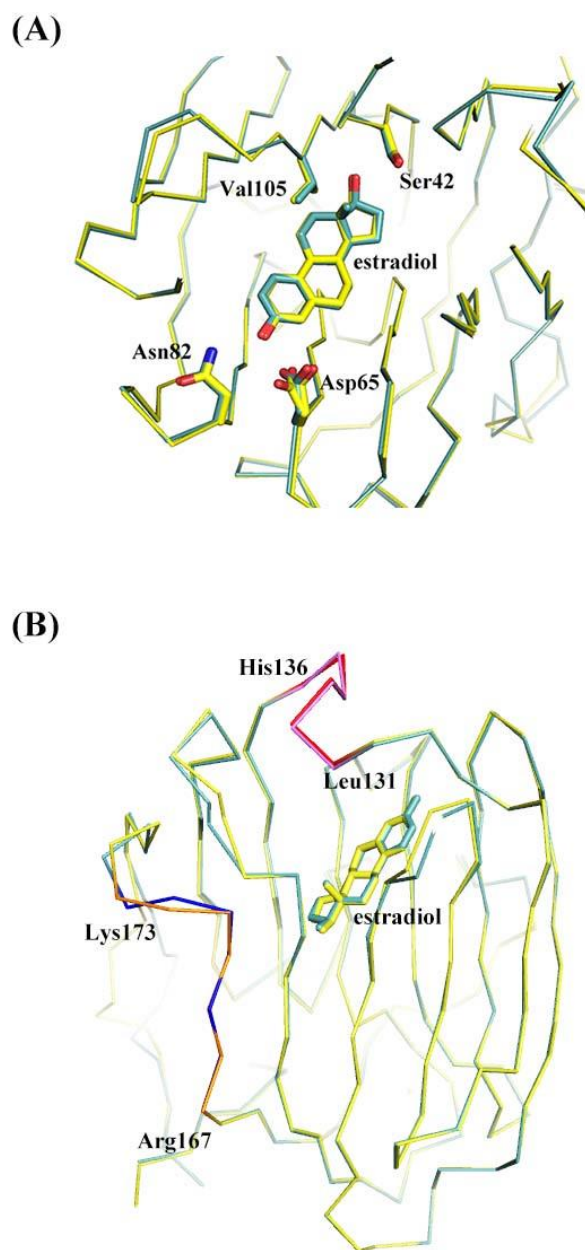


Figure 3.5 Estradiol-binding properties of the SHBG E176 N-terminal LG domain

Superimposed images of SHBG (1LHU, light blue) and SHBG E176K (yellow). (A) The positions of estradiol and four residues, Ser42, Asp65, Asn82, and Val105 that are responsible for hydrogen bond formation with estradiol almost overlap in SHBG and SHBG R123H. (B) The flexible loop region (Leu131-His136) above the steroid-binding pockets of SHBG and SHBG R123H were represented in pink and red, respectively. A region (Arg167-Lys173) that is specifically pushed out from the steroid binding pocket while SHBG is in complex with estradiol is represented in dark blue for SHBG and in orange for SHBG R123H.

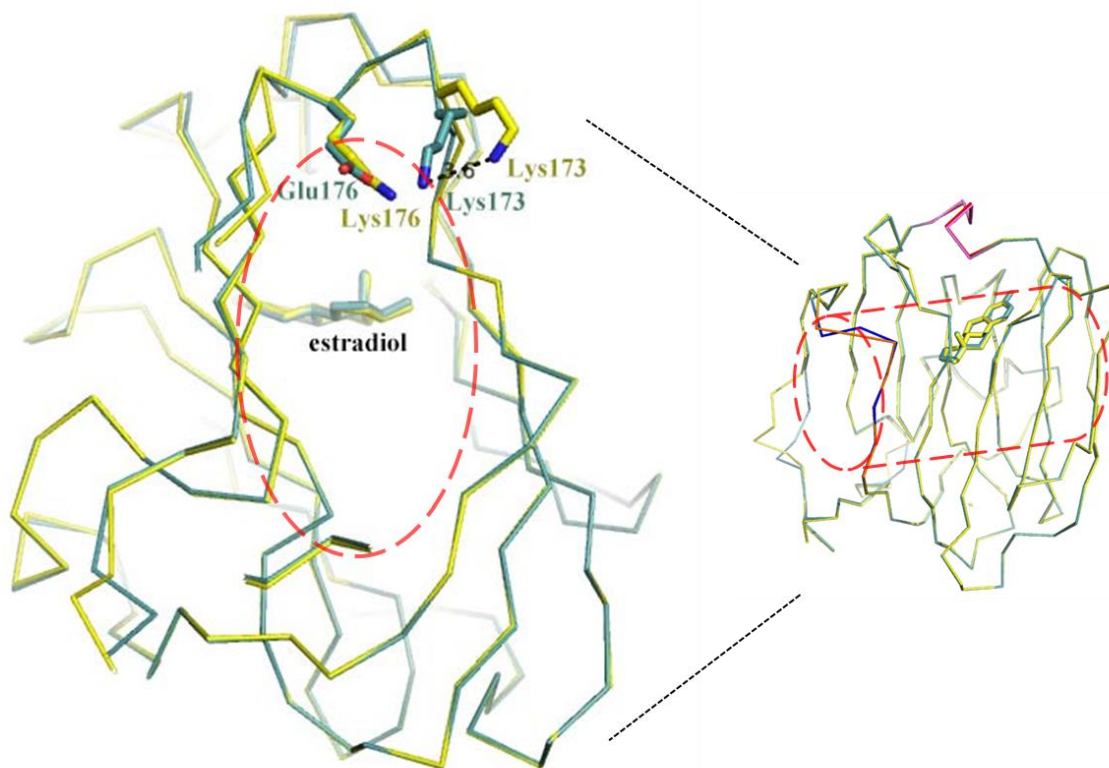


Figure 3.6 Lys176 pushed Lys173 outward from the “hollow tube” of SHBG E176K

A superimposed image from the lateral side of the N-terminal LG domain of SHBG (1LHU, light blue) and SHBG E176K (yellow) shows that substitution of Glu176 to Lys176 displaces Lys173 about 3.6 Å away from the center of the opening rim (left red dash line) at a putative entrance to the “hollow tube” (right red dash line).

Chapter 4 : Functional characterization of naturally occurring genetic polymorphism in *SHBG* regulatory sequences

4.1 Introduction

Fluctuations of plasma human sex hormone-binding globulin (SHBG) levels in response to changes in physiological or metabolic states ensures the appropriate plasma distribution and accessibility of sex steroids to their target tissues (163). On the other hand, dysregulation of SHBG production is associated with reproductive or metabolic disorders (148, 188). Changes in SHBG production are mainly controlled by an “on-off switch” mechanism, where the orphan nuclear hormone receptor, HNF4 α and COUP-TF1, compete for the same *cis*-element close to the transcriptional start site of *SHBG* promoter to activate and repress its transcriptional activity, respectively (34). Although nutritional and hormonal differences may account for most inter-individual differences in plasma SHBG levels, there is increasing evidence that genetic variations in regulatory regions of the human *SHBG* gene influence its transcription (24, 148).

The most well studied genetic polymorphism is a variable (TAAAA)_n pentanucleotide repeat located within an *Alu* element upstream of the *SHBG* promoter (178). Individuals carrying more than 8 TAAAA repeats have lower serum SHBG levels and higher free androgen levels (189, 190). Importantly, this polymorphism has been associated with the age of

menarche (191), coronary artery disease (192), semen quality (193), and hip bone mineral density (194). Other single nucleotide polymorphisms (SNPs) exist in *SHBG* regulatory regions, including the common rs1799941 located close to the transcription start site, for which the A and G alleles are associated with higher and lower plasma SHBG levels, respectively (194). Another interesting C/T SNP (rs6257) located in intron 1 of *SHBG* has been associated with lower serum SHBG levels and a higher risk of development of breast cancer (152) and type 2 diabetes (161, 184).

To date, there are more than 20 uncharacterized SNPs within *SHBG* proximal promoter in the NCBI SNP database. To investigate their potential influence on *SHBG* transcriptional activity, 7 SNPs within the proximal promoter, as well as rs6257 in intron 1, were selected for this study. These SNPs are conserved across several mammalian species and are located near regions of the *SHBG* promoter that are DNase I footprinted by liver nuclear protein extracts (34), or they have high minor allele frequency or strong clinical relevance to diseases (**Figure 4.2** and **Table 4.1**). Two of these SNPs, rs138097069 and rs6257, are particularly interesting because they are located at the critical positions within a putative farnesoid X receptor (FXR) and a putative forkhead box protein A2 (FOXA2) binding element, respectively. Therefore, the effects of FXR or FOXA2 on *SHBG* expression were also assessed.

4.2 Material and methods

4.2.1 Antibodies and reagents

The S1B5 monoclonal antibody (171) and a rabbit anti-human SHBG antiserum (172) were used in a time-resolved immuno-fluorometric assay (IFA) (173). Rabbit anti-FXR (H-130, sc-13063), mouse anti-FXR (D-3, sc-25309), goat anti-HNF4a (C-19, sc-6556), goat anti-GAPDH (V-18, sc-20357), normal goat IgG (sc-2028), and normal rabbit IgG (sc-2027) antibodies were from Santa Cruz Biotechnology (Santa Cruz, CA). Mouse anti COUP-TF1 (PP-H8132) was from R&D Systems (Minneapolis, MN). The L-Thyroxine and FXR agonist GW4064 were from Sigma-Aldrich (St. Louis, MO). Reagents for luciferase reporter gene assays were purchased from Promega (Madison, WI).

4.2.2 Cell culture and transient transfection

Cell culture reagents were from Life Technologies (Burlington, Ontario). Human HepG2 hepatoblastoma cells (HB-8065, ATCC) were routinely cultured in low-glucose DMEM supplemented with 10% fetal bovine serum (FBS), antibiotics (100 U penicillin/mL and 100 µg streptomycin/mL) at 37 °C, 100% humidity, and 5% CO₂. L-Thyroxine (100 nM) was routinely added to culture medium to maintain HepG2 cells in a more differentiated state (195) with higher SHBG production (79).

HepG2 cells were transiently transfected with plasmids using GenJet™ In Vitro DNA

Transfection Reagent (SignaGen Laboratories, Rockville, MD), or with ON-TARGET^{plus} SMARTpool siRNA (GE Healthcare Dharmacon, Lafayette, CO) using Lipofectamine[®] RNAiMAX Transfection Reagents (Life Technologies) according to instructions provided by the manufacturers.

4.2.3 Expression plasmids and luciferase reporter gene constructs

Two *SHBG* fragments of different DNA regions that included sequences of the proximal promoter, exon 1, intron 1, and part of exon 2 (-266~+366 bp and -849~+366 bp) were generated by PCR amplification and were cloned into the pGL3-Basic vector (Promega) (**Figure 4.1**). In both constructs, a stop codon was introduced immediately downstream of the translation initiation codon in *SHBG* exon 1. This was done to disrupt translation from the normal *SHBG* translation start site in exon 1 to ensure efficient translation initiation at the luciferase gene inserted within exon 2. The *FOXA2* cDNA clone for expression in mammalian cells was purchased from OriGene Technologies (Rockville, MD). All mutants and variants corresponding to *SHBG* SNPs were generated using a QuickChange II Site-Directed Mutagenesis Kit (Agilent Technologies, Santa Clara, CA) with site-specific mutagenic oligonucleotide primers (**Table 4.2**).

4.2.4 Luciferase reporter gene assay

HepG2 cells were co-transfected with the luciferase reporter plasmids and the β -

galactosidase expression plasmids as an internal control for transfection efficiency. Forty-eight hours post transfection, cells were lysed with the Reporter Lysis Buffer (Promega). In a well of the white opaque 96-well plate, 75 μL of the luciferase substrate solution (Promega) was added to 25 μL of cell lysate and immediately taken for luminescence measurement. β -galactosidase activity was determined after incubation of 25 μL of cell lysate with 25 μL of the Assay 2X Buffer (Promega) for 15 min at 37°C. Luminescent light units from the luciferase assay were divided by the absorbance reading from the β -galactosidase assay to determine the relative luciferase activity, and both were measured using a VICTOR X4 Multimode Plate Reader (PerkinElmer, Waltham, MA).

4.2.5 Immuno-fluorometric assay (IFA)

A modified version of a time-resolved IFA (173) was used to measure SHBG concentrations in culture media. Briefly, 96-well plates were coated overnight with 150 μL rabbit antiserum against SHBG (1:500 diluted in filtered 0.5M NaHCO_3) at 4°C, and then blocked with 300 μL blocking buffer (1% casein in 20 mM Tris-HCl, pH 8, 150 mM NaCl) for 2 h at room temperature. Diluted (1:1,000) aliquots (100 μL) of concentrated culture media samples and 50 μL Europium-labelled S1B5 antibody (2,000X diluted in DELFIA® assay buffer (PerkinElmer)) were then co-incubated for 3 h at room temperature. Wells were washed 6 times with wash buffer (50 mM Tris-HCl pH 7.5, 150 mM NaCl), and 150 μL DELFIA®

enhancement solution (PerkinElmer) was added to each well. Time-resolved fluorescence was measured using a VICTOR™ X4 Multimode Plate Reader (PerkinElmer).

4.2.6 Western blotting

HepG2 cells were lysed with Cell Lysis Buffer (Cell Signaling Technology, Danvers, MA). The nuclear and the cytoplasmic proteins were separated into fractions using the NEPER Nuclear Protein Extraction Kit (Thermo Fisher Scientific, Waltham, MA). Whole cell lysates or nuclear/cytoplasmic fractions were resolved by 8% SDS-PAGE and transferred to 0.45 µm Immobilon-P PVDF membranes (Millipore, Etobicoke, Ontario) by electroblotting. The membranes were blocked in 5% skim milk for 1 h, followed by an overnight incubation with primary antibodies at 4°C. Western Blots were incubated with 1:10,000 diluted horseradish peroxidase-conjugated secondary antibodies (Sigma-Aldrich) and the immunoreactive proteins were detected by ImageQuant LAS 4000 (GE Healthcare Life Sciences, Baie d'Urfe, Quebec).

4.2.7 RNA isolation and quantitative reverse transcription polymerase chain

reaction (RT-PCR)

Total RNA was extracted using the RNeasy Mini Kit (Qiagen, Toronto, Ontario) and the concentrations were determined using a NanoDrop 2000 spectrophotometer (Thermo Fisher Scientific). Total RNA (2.5 µg) was reverse transcribed to first strand cDNA using

SuperScript® II Reverse Transcriptase together with oligo(dT) and random primers (Life Technologies) according to the manufacturer's instructions. Oligonucleotide primers for quantitative PCR were validated with an amplification efficiency more than 90 % and their sequences are listed in **Table 4.2**. A 20 µL mixture containing 5 µL of 1:40 diluted cDNA, 300 nM of each of forward and reverse primers, and 10 µL of 2X SYBR Green PCR master mix (Life Technologies) was made in the 96-well optical reaction plate. Reactions were performed using the ABI Prism 7000 Sequence 10 detection system (Life Technologies). All experiments were run in triplicate and relative mRNA levels were determined using the $2^{-\Delta\Delta C_T}$ method (196).

4.2.8 Chromatin Immunoprecipitation (ChIP) assays

The ChIP assays were performed using the Magna ChIP™ A/G Chromatin Immunoprecipitation Kit (Millipore). HepG2 cells were fixed in 1% formaldehyde for 10 min at room temperature and unreacted formaldehyde was quenched by addition of Glycine. Cells were rinsed, scraped, and collected with ice-cold PBS, then re-suspended in the Cell Lysis Buffer containing Protease Inhibitor Cocktail II. After 15 min incubation on ice, cells were spun down and pellets were re-suspended in the Nuclear Lysis Buffer. Chromatin was sheared mainly into lengths between 200~500 bp using a Microson Ultrasonic Cell Disruptor under a condition of 12 cycles of 5 sec sonication at an output of 7 Watts and 25 sec rest on ice. Sheared

chromatin was incubated overnight at 4°C with 4 µg of FXR, HNF4a or FOXA2 antibody, or the species-matched IgG as a control. Protein A/G magnetic beads were added into the mixture and were incubated for 2 h at room temperature before being washed with the Low Salt, High Salt, LiCl, and TE Buffer provided in the kit for 5 min at room temperature. Chromatin was eluted and reverse cross-linked by incubation of beads with the ChIP Elution Buffer plus Proteinase K for 2 h at 62°C. DNA was recovered using the QIAquick PCR Purification Kit (Qiagen) and analyzed by PCR with primers listed in **Table 4.2**. The resulting PCR products were analyzed by 2% agarose gel electrophoresis and visualized by an ImageQuant LAS 4000 (GE Healthcare Life Sciences).

4.2.9 Statistical analysis

Data were represented as mean ± S.D. of at least three independent experiments for all measurements. Differences between two means were evaluated using the paired Student *t* test. Differences between multiple means were evaluated using one-way ANOVA followed by the Dunnett's test, or two-way ANOVA followed by the Bonferroni test.

4.3 Results

4.3.1 Effects of the SNPs within the *SHBG* proximal promoter regulatory region on transcriptional activity

To investigate how SNPs within *SHBG* proximal promoter or intron 1 influence *SHBG*

expression, *SHBG* sequences with the SNPs under investigation (**Figure 4.2**) were inserted into luciferase reporter plasmids and their promoter activities were assessed in relation to the *SHBG* sequence in HepG2 cells. This revealed that only one of them (rs138097069) significantly increased *SHBG* transcriptional activity in HepG2 cells (**Table 4.1**). In previous genome-wide association studies, rs858518, rs3760213, and rs6257 were associated with higher or lower serum SHBG levels (**Table 4.1**), but they had no significant effects on *SHBG* promoter activity in luciferase reporter assays.

4.3.2 SNP rs138097069 is located within a putative FXR binding element

To investigate the underlying mechanism by which SNP rs138097069 increases *SHBG* promoter activity, sequences adjacent to this SNP were subjected to *in silico* prediction of binding sites for transcriptional factors. This revealed that rs138097069 is located at a critical position (position 12) within a putative FXR binding element (FXRE) (**Figure 4.3A**). To analyze this potential FXRE in detail, two other nucleotides at critical positions (position 2 and 6) and their combinations with rs138097069 were mutated and examined in the luciferase reporter assay (**Figure 4.3A**). The results showed that the mutation at position 6 in the FXR binding sequence had no effect on either basal or the rs138097069-induced increase of *SHBG* promoter activity (**Figure 4.3B**, compare mut-2 with mut-5). By contrast, mutation at position 2 marginally decreased the basal *SHBG* promoter activity but very effectively negated the

rs138097069-induced increase of *SHBG* promoter activity (**Figure 4.3B**, compare mut-3 with mut-6).

4.3.3 FXR agonist GW4064 reduces SHBG production independent of HNF4 α

To examine whether *SHBG* expression is regulated by FXR, HepG2 cells were treated with a synthetic (non-bile acid) FXR agonist GW4064 at doses of up to 2 μ M. The results showed that a dose of 0.1 μ M GW4064 is sufficient to effectively suppress SHBG production (**Figure 4.4A**) and *SHBG* mRNA levels (**Figure 4.6A**), and this therefore suggests that the suppression occurs at the transcriptional level. Importantly, the inhibitory effects of GW4064 on *SHBG* expression are not due to altered HNF4 α or COUP-TF1 levels (**Figure 4.4B**), or to loss of HNF4 α occupancy on *SHBG* promoter (**Figure 4.4C**).

GW4064 treatment at the same dose (0.1 μ M) that is sufficient to repress SHBG production and *SHBG* mRNA levels had no effect on *SHBG* promoter activity in luciferase reporter gene assays (**Figure 4.5**). Although a slightly increase in luciferase activity was observed when cells were treated with GW4064 at 1 μ M or above (**Figure 4.5**), this induction is independent of FXR activation because it was not mitigated when FXR was knocked-down (**Figure 4.5**). Also, the induction is likely non-specific because high-dose of GW4064 (over 1 μ M) non-specifically activate other receptors (197, 198). In light of the limitations of luciferase reporter gene assays (see Discussion), I conclude that the FXR agonist, GW4064, has an

inhibitory effect on *SHBG* expression without affecting HNF4 α levels and its occupancy on *SHBG* promoter.

4.3.4 Knockdown of FXR reduces *HNF4 α* and *SHBG* expression

To verify the regulation of FXR on SHBG production in a different way, the levels of FXR in HepG2 cells were knocked down using siRNAs (**Figure 4.6D**). Unexpectedly, *SHBG* mRNA levels (**Figure 4.6A**) and SHBG levels (**Figure 4.6B**) were reduced when FXR was knocked down. However, an analysis of *HNF4 α* expression revealed that in contrast to an HNF4 α independent regulation of GW4064 on *SHBG* expression, knockdown of FXR decreased *HNF4 α* mRNA (**Figure 4.6C**) and protein levels (**Figure 4.6D**). Moreover, the ability of GW4064 to suppress *SHBG* expression was mitigated when FXR is knocked down (**Figure 4.6A and 4.6B**), further supporting the conclusion that GW4064 reduces *SHBG* expression through activation of FXR.

4.3.5 GW4064-activated FXR binds the FXRE within the *SHBG* promoter

The observation that the inhibitory effect of GW4064 on *SHBG* expression may occur specifically through activation of FXR prompted us to investigate whether the FXRE within the *SHBG* promoter is a direct target of GW4064-activated FXR. As for other FXRE within the *SHP* (199) and *APOC3* (114) regulatory regions, the FXRE in the *SHBG* promoter region is occupied by GW4064-activated FXR (**Figure 4.7**). In conclusion, while knockdown of FXR

indirectly down-regulates *SHBG* expression by reducing HNF4 α , GW4064-activated FXR binds to the *SHBG* promoter and represses its activity in an HNF4 α -independent manner.

4.3.6 Overexpression of FOXA2 suppresses SHBG production in an HNF4 α -independent manner

In silico predictions revealed that rs6257 is located within a putative FOXA2 binding element. To examine whether FOXA2 regulates SHBG production, we overexpressed FOXA2 or FOXA2-T156A, a constitutive active form that cannot be phosphorylated at Thr156 and is excluded from the nucleus upon insulin stimulation, in HepG2 cells (145).

Under low glucose (1 g/L) culture conditions, endogenous and overexpressed FOXA2 or FOXA2-T156A localize in the nucleus of HepG2 cells (**Figure 4.8A**). While overexpression of FOXA2 or FOXA2-T156A had no effect on HNF4 α (**Figure 4.8A**) and *HNF4 α* mRNA (**Figure 4.8B**) levels, *SHBG* mRNA levels (**Figure 4.8B**) and SHBG production (**Figure 4.8C**) were repressed. Luciferase reporter gene assays revealed that *SHBG* promoter activity was also reduced when FOXA2 or FOXA2-T156A were overexpressed in HepG2 cells (**Figure 4.8D**). However, these inhibitory effects were not attenuated by rs6257 (**Figure 4.8D**). Moreover, the inhibitory effects of overexpressed FOXA2 on *SHBG* expression are not due to alterations of HNF4 α occupancy on the *SHBG* promoter (**Figure 4.8E**). These results indicate that

overexpression of FOXA2 negatively regulates *SHBG* expression in an HNF4 α -independent manner.

4.3.7 Knockdown of FOXA2 induces HNF4 α and SHBG production

In contrast to the observations that the expression of *HNF4 α* was unaltered by overexpressed FOXA2 or FOXA2-T156A, levels of *HNF4 α* mRNA (**Figure 4.9A**) and HNF4 α (**Figure 4.9B**) were increased when FOXA2 was knocked down in HepG2 cells. As expected, *SHBG* promoter activity (**Figure 4.9C**) and SHBG production (**Figure 4.9D**) were both up-regulated by the increase of HNF4 α .

4.3.8 FOXA2 directly binds to SHBG intron1

To investigate the HNF4 α -independent mechanism by which FOXA2 negatively regulates *SHBG* expression, binding of FOXA2 to its putative binding site within *SHBG* intron1 was examined by ChIP assays. Endogenous FOXA2 binds to the intron1 of *SHBG*, as well as a control target, *FABP1* (200), to limited extents (**Figure 4.10**). By contrast, the FOXA2 binding sites in *SHBG* intron 1 and *FABP1* were occupied by overexpressed FOXA2 or FOXA2-T156A to a much greater extent (**Figure 4.10**). In summary, FOXA2 down regulates *SHBG* expression indirectly through altering HNF4 α levels, and/or directly through binding to *SHBG* intron1.

4.4 Discussion

Plasma levels of SHBG have been used as a biomarker for diseases associated with the metabolic syndrome, such as cardiovascular diseases (201) and type 2 diabetes (161). While nutritional and hormonal factors contribute to most inter-individual differences of plasma SHBG levels, genetic variations in both the regulatory sequences (**Table 4.1**) and coding sequences (153, 169) of *SHBG* have been linked to plasma SHBG levels in clinical studies. Therefore, the early observations that SHBG levels are an inherited trait (160) can now be in part explained. While it is relatively easy to determine how genetic variants in the coding sequences of *SHBG* influence the production and function of SHBG, the molecular mechanisms by which polymorphism in regulatory sequences are associated with different plasma SHBG levels are more challenging to define and remain less understood. In this study, 8 SNPs within the SHBG regulatory sequences near the transcriptional start site were selected and examined by luciferase reporter gene assays. In contrast to what has been observed in clinical association studies, only one SNP (rs138097069) exhibited an influence on *SHBG* promoter activity (**Table 4.1**). However, the limitations of clinical association studies, in which the observed associations could be due to linkage disequilibrium or a population specific effects, should be taken into consideration.

Similar issues regarding discrepancies between results of luciferase reporter gene assays and results from other measurements have highlighted the limitations of interpreting the results of luciferase reporter assays as definitive explanations for altered transcriptional regulation of *SHBG* under physiological conditions. For example, higher numbers (more than 8 repeats) of the variable (TAAAA)_n pentanucleotide repeat in the *SHBG* promoter are associated with lower serum levels of SHBG (189, 190), whereas *SHBG* promoter activities were reduced only by six TAAAA pentanucleotide repeats in luciferase reporter gene assays (178). In the present study, treatment of GW4064 at very high doses that are known to activate other receptors (197, 198), may enhance *SHBG* promoter activities in an FXR-independent manner (**Figure 4.5**). To overcome the limitations that the naked *SHBG* promoter driven-luciferase reporter plasmid DNA may not accurately reflect the transcriptional regulation imposed at chromatin structure levels, it will be necessary to use the CRISPR-Cas9 genome engineering system (202) to mutate specific nucleotides in the genome of HepG2 cells. This will help determine if a SNP is causative or simply a marker due to the linkage disequilibrium, and investigate the allele-specific mechanisms by which SNPs affect *SHBG* transcriptional activity under a more physiological condition.

Both FXR and FOXA2 respond to certain metabolic or hormonal stimuli by regulating the expression of a wide range of genes (105, 126). In our study, we observed that while neither

GW4064 activation of FXR or overexpression of FOXA2 affected *HNF4α* expression, knockdown of FXR or FOXA2 altered HNF4α levels in HepG2 cells significantly. This indicated that in HepG2 cells, deprivation of FXR or FOXA2 triggered global metabolic changes to a greater extent than activation or overexpression of them. In fact, studies in FXR or FOXA2 null mice demonstrated that deprivation of FXR resulted in elevated blood glucose (119) and hyper-triglyceridaemia (104), whereas deprivation of FOXA2 predisposed mice in a fasting state (135). Such metabolic changes that are associated with down-regulation or up-regulation of HNF4α levels are reflected in decreases or increases of hepatic SHBG production, respectively (34).

Both activation of FXR and overexpression of FOXA2 suppressed *SHBG* expression in an HNF4α-independent manner (**Figure 4.4** and **Figure 4.8**). The inhibitory effects were direct, as demonstrated by ChIP assays under conditions of GW4064 treatment or FOXA2 overexpression in HepG2 cells (**Figure 4.7** and **Figure 4.10**). Suppression of target genes by activated nuclear receptors has been demonstrated in other cases. A common mechanism for the *trans*-repression by nuclear receptors is to replace the transcription factors and co-activators necessary for target gene expression, and concomitantly recruit co-repressors to the regulatory region. For example, ligand-bound FXR negatively regulates one of glucose-induced glycolytic genes, liver-type pyruvate kinase gene (*L-PK*), by releasing carbohydrate

response element binding protein (ChREBP) and co-activator p300, and recruitment of silencing mediator of retinoic acid and thyroid hormone receptor (SMRT) co-repressor to *L-PK* promoter (203). Nevertheless, binding of either GW4064-activated FXR or overexpressed FOXA2 to *SHBG* promoter or intron1, respectively, did not alter the occupancy of HNF4 α (**Figure 4.4C** and **Figure 4.8E**) and the underlying molecular mechanisms remain to be determined.

In conclusion, rs138097069 and rs6257 are located within functional binding sites for FXR and FOXA2 in the *SHBG* proximal promoter and intron 1, respectively. Besides the indirect effects through alteration of HNF4 α levels, direct binding of either FXR or FOXA2 to *SHBG* suppressed its expression without altering HNF4 α levels and occupancy on the *SHBG* promoter. This and ongoing studies of allele-specific effects of SNP rs138097069 or rs6257 on FXR or FOXA2 binding and *SHBG* expression under more physiological conditions will help understand how these genetic polymorphisms involved in etiologies of diseases that associated with serum SHBG levels.

Table 4.1 Properties of SNPs selected within the *SHBG* promoter and intron1 region

ID	common/variant alleles	MAF ^a	luciferase activity ^b (fold change)	clinical relevance	ref.
rs146797612	G/C	0.004	1.02 ± 0.07		
rs112885647	-/insertion G	0.046	1.03 ± 0.06		
rs62059839	C/T	0.124	1.18 ± 0.04		
rs858518	A/G	0.426	1.26 ± 0.07	associated with lower serum SHBG levels	(152)
rs3760213	G/A	0.085	1.06 ± 0.20	associated with higher serum SHBG and total testosterone levels, and a lower risk of metabolic syndrome	(204)
rs145624328	G/C	0.0005	0.96 ± 0.03		
rs138097069	C/T	0.0009	2.18 ± 0.32 ***		
rs6257	T/C	0.051	1.06 ± 0.01	associated with lower serum SHBG levels and a higher risk of development of type II diabetes	(161)

^aminor allele frequency

^bmean of three independent measurements ± S.D.

Mean differences were analyzed using student *t* test. ***, $p < 0.001$

Table 4.2 Oligonucleotide sequences (5' to 3') for molecular cloning, site-directed mutagenesis, quantitative RT-PCR, or ChIP assay

molecular cloning	
SHBG -849F	GCTTGA ^A ACTCGAGAGGCAG
SHBG -266F	GAGTGGACAGAAATCTTGGAG
SHBG +366R	GACAGCGATAGGCTCTTGTC
mutagenesis^a	
rs146797612	GTGATTTCTACTGCTAGACT <u>CTTT</u> AGGCCCTGTAATAAATG
rs112885647	ATAACTGAGAGGC <u>CGGGGG</u> GCAGGTCC
rs62059839	TTATTTTCCTCATTTTACAGACAAGGACA <u>TTGA</u> AGCACAAAGGTG
rs858518	ACAGACAAGGACACTGAAGCACAGAGGTGAAGTGAC
rs3760213	GGCCCTAGAGGAGGAGAA <u>AGGG</u> GAGATGG
rs145624328	CTGGGCCCTGG <u>ACAGGG</u> GTC AAGG
rs138097069	GTCAAGGGTCAGTGCC <u>ICTG</u> TTTCTTTACCCC
rs6257	GTCCCTACTCAGCTTTGTTTG <u>CTTT</u> CTTTCTTGATAGAG
FXRE-mut1	GGCAGGGGTCAAG <u>ITGTC</u> AGTGCCCTG
FXRE-mut2	GGGGTCAAGGGTC <u>CGGTG</u> CCCTGTTTC
FXRE-mut4	GGCAGGGGTCAAG <u>ITGTC</u> GGTGCCCTGTTTC
FXRE-mut5	GGGGTCAAGGGTC <u>CGGTG</u> CCICTGTTTCTTTACC
FXRE-mut6	GGGCAGGGGTCAAG <u>ITGTC</u> CGGTGCCICTGTTTCTTTACC
FOXA2 T156A	CAGGCGCAGCTAC <u>GCGC</u> ACGCAAAGCC
quantitative RT-PCR	
q-SHBG-ex2F	GCCCAGGACAAGAGCCTATC
q-SHBG-ex3R	AGTCCCAGCATAAACCAGTCAT
q-HNF4a-1F	CAGGCTCAAGAAATGCTTCC
q-HNF4a-1R	ATCTGTCGGGACAGGACCTC
q-GAPDH-F	CTGCACCACCAACTGCTTAG
q-GAPDH-R	GCAGGGATGATGTTCTGGAG
ChIP assays	
SHBG -204F	CAGTGGAGGATGATAGTGGAG
SHBG -2R	ACTCTGGGAGAATGTGTAGAG
SHP -343F	GGACACCTGCTGATTGTGC
SHP -176R	ACGTGGCACTGATATCACCT
APOC3 -765F	CCAGACATGAGACCAGCTC
APOC3 -546R	AATCCAGGCAGGCGAGTG
FABP1 -277F	ACCGATGTACAAACACATACGC
FABP1 -54R	CTCCTGAGAGCAATGGTCAATG

^aMutated DNA sequences are indicated in boldface type and underlined.

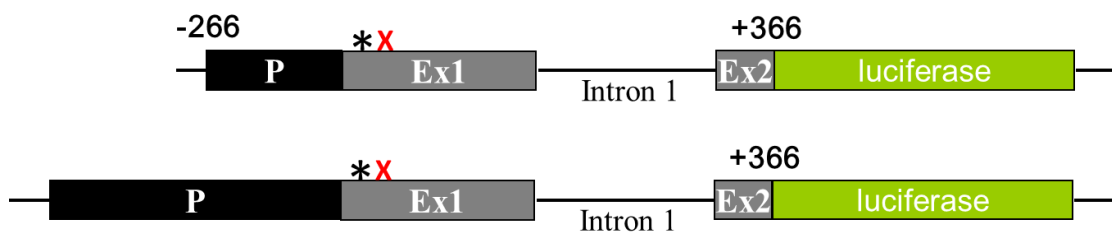


Figure 4.1 Diagrams of *SHBG* luciferase reporter gene constructs

DNA fragments ranging from -266 to +366 bp or from -849 to +366 bp relevant to the transcriptional start site of human *SHBG* gene were cloned into a pGL3-Basic vector. A stop codon (red x) was introduced immediately downstream of the translation initiation codon (star) in both constructs. P=promoter; Ex1=exon1; Ex2=exon2

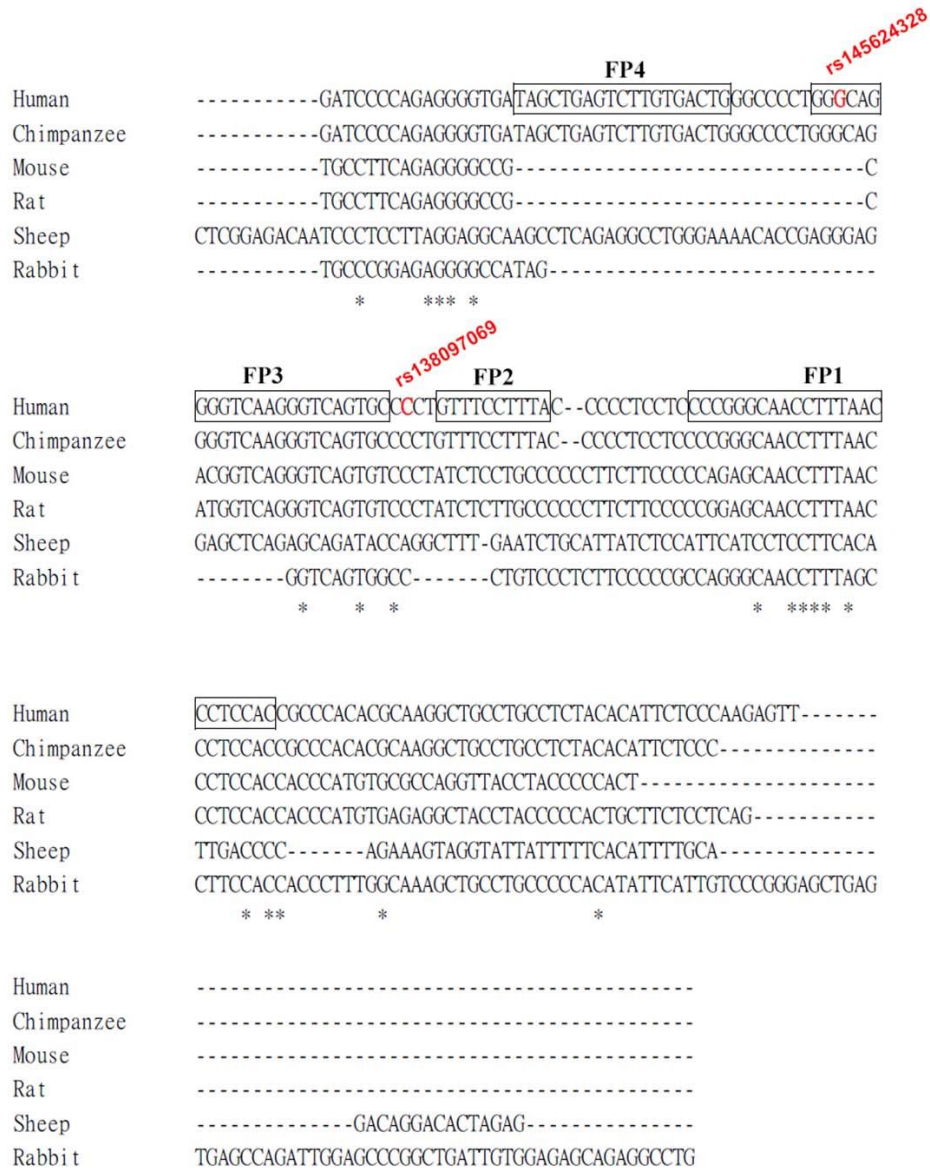


Figure 4.2 Orthologous sequence alignment of the *SHBG* proximal promoter

Nucleotide sequences between human and other species *SHBG* proximal promoter were aligned. Selected non-synonymous SNPs were shown in red color. Footprints were shown in boxes and labeled as FP1 to FP17 according to previous DNaseI footprinting studies (34). *= conserved nucleotide sequences between species

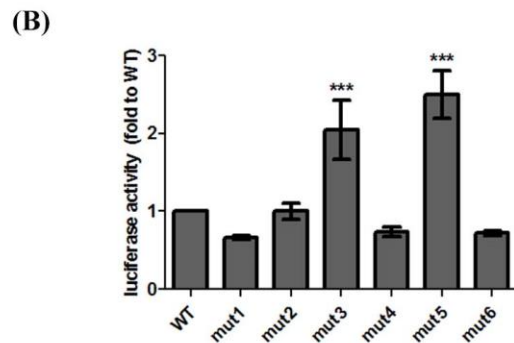
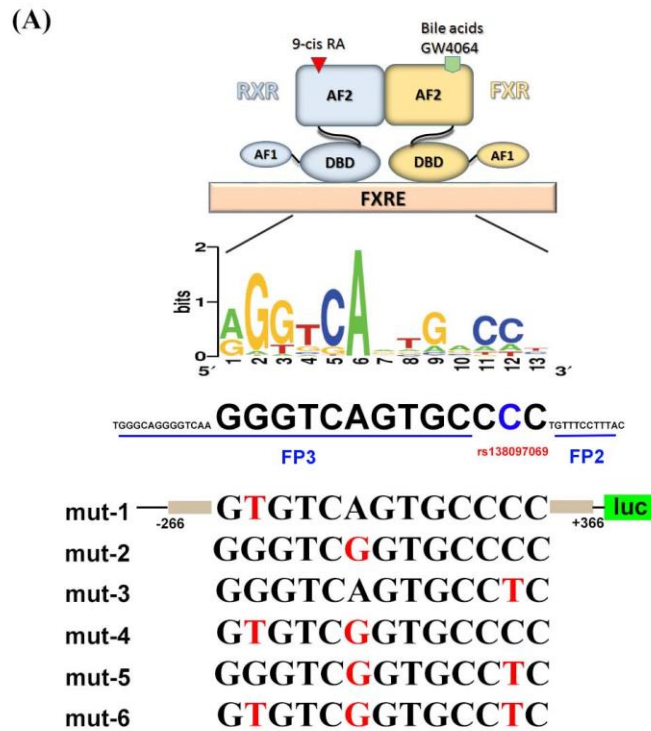


Figure 4.3 Location of SNP rs138097069 within a putative FXR binding element (FXRE) and luciferase reporter gene activities for mutants within FXRE

(A) A diagram shows the N-terminal domain with activation function 1 (AF1), the DNA-binding domain (DBD), and the ligand binding domain with activation function 2 (AF2) of FXR and RXR nuclear receptors. FXR-RXR heterodimer binds to a consensus DNA sequence called FXR binding element (FXRE). The sequences of the region where SNP rs138097069 is located are well matched to a FXRE and compose the footprint 2 (FP2) and footprint 3 (FP3) of *SHBG* proximal promoter. Mutations in constructs containing a region from *SHBG* -266 to +366 nt for luciferase reporter gene assays were shown in red letters. (B) HepG2 cells were transfected with the constructs above and cell lysates were harvest 48 h post transfection for luciferase reporter gene assays. Mean differences were analyzed using one-way ANOVA followed by the Dunnett's test. ***, $p < 0.001$

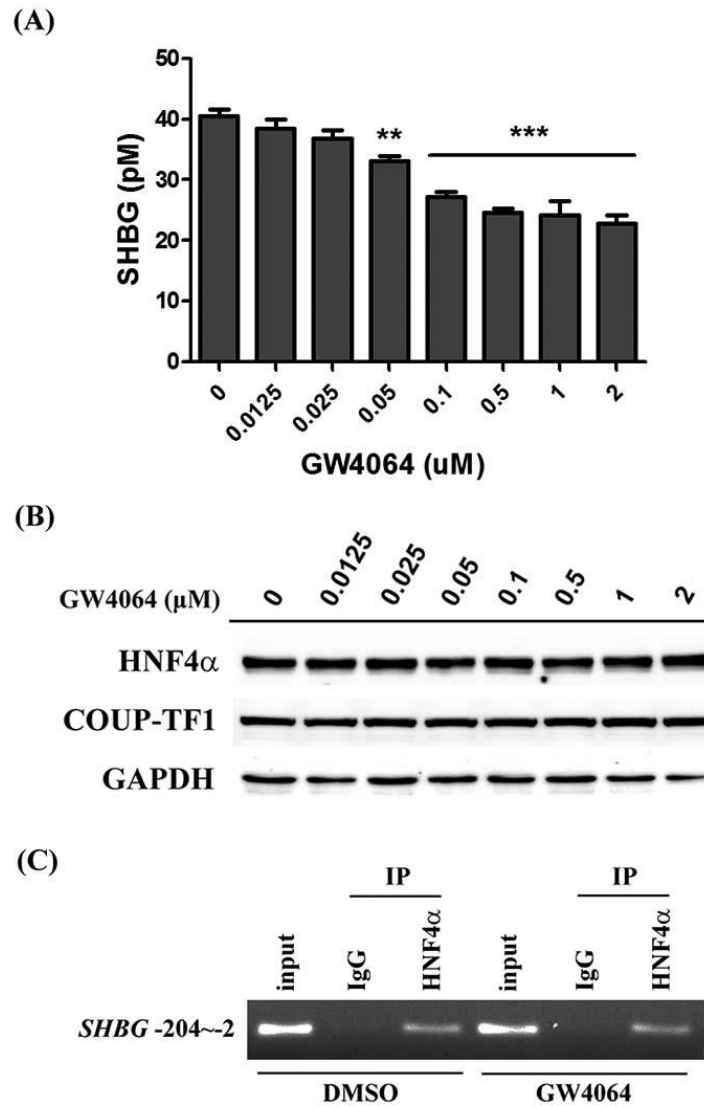


Figure 4.4 FXR agonist GW4064 reduces SHBG production in an HNF4 α -independent manner

HepG2 cells were treated with 0 to 2 μ M GW4064 for 72 h. (A) Cultured medium were harvested and SHBG levels were measured by immune-fluorometric assays. (B) Cell lysates were harvested and levels of HNF4 α and COUP-TF were determined by Western blotting analysis. GAPDH levels were used for an internal control. (C) HepG2 cells were treated with vehicle (DMSO) or 1 μ M GW4064 for 6 h and the association of HNF4 α to *SHBG* promoter (-204 to -2 nt relative to the transcriptional starting site) was examined by ChIP assays. One percent of sheared chromatin (input) and appropriate amount of immunoprecipitated (IP) chromatin were used for PCR amplification. Mean differences were analyzed using one-way ANOVA followed by the Dunnett's test. **, $p < 0.01$; ***, $p < 0.001$

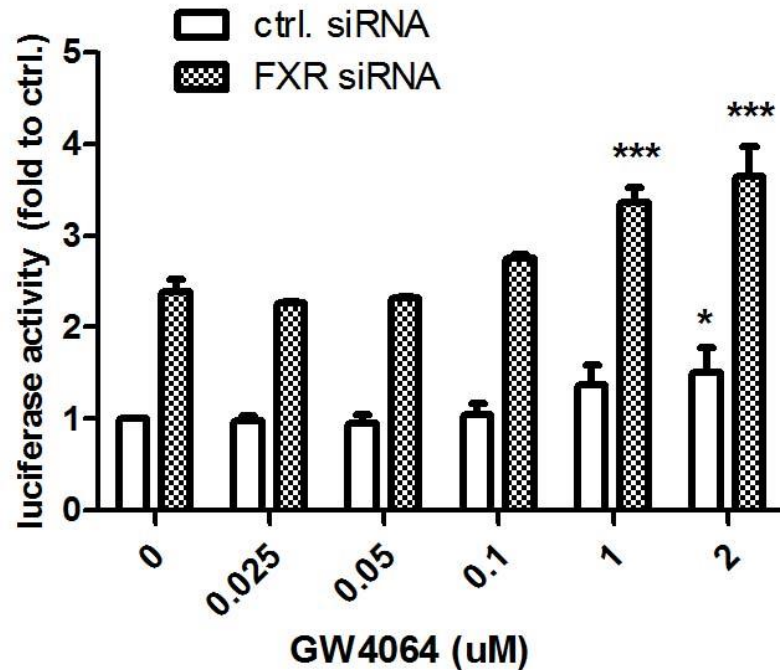


Figure 4.5 Effects of FXR agonist GW4064 on *SHBG* promoter activity

HepG2 cells were first transfected with control (ctrl.) siRNA or FXR siRNA. Twelve hours after transfection, cells were incubated with fresh medium containing 0 to 2 μ M of GW4064. Forty-eight hours later, cell lysates were harvested and subjected to luciferase reporter gene assays. Values from measurements were represented as fold changes to the value from the control (ctrl.) siRNA transfected HepG2 cells without GW4064 treatment. Mean differences between GW4064 treatments were analyzed using two-way ANOVA followed by the Bonferroni post-tests. *, $p < 0.05$; ***, $p < 0.001$

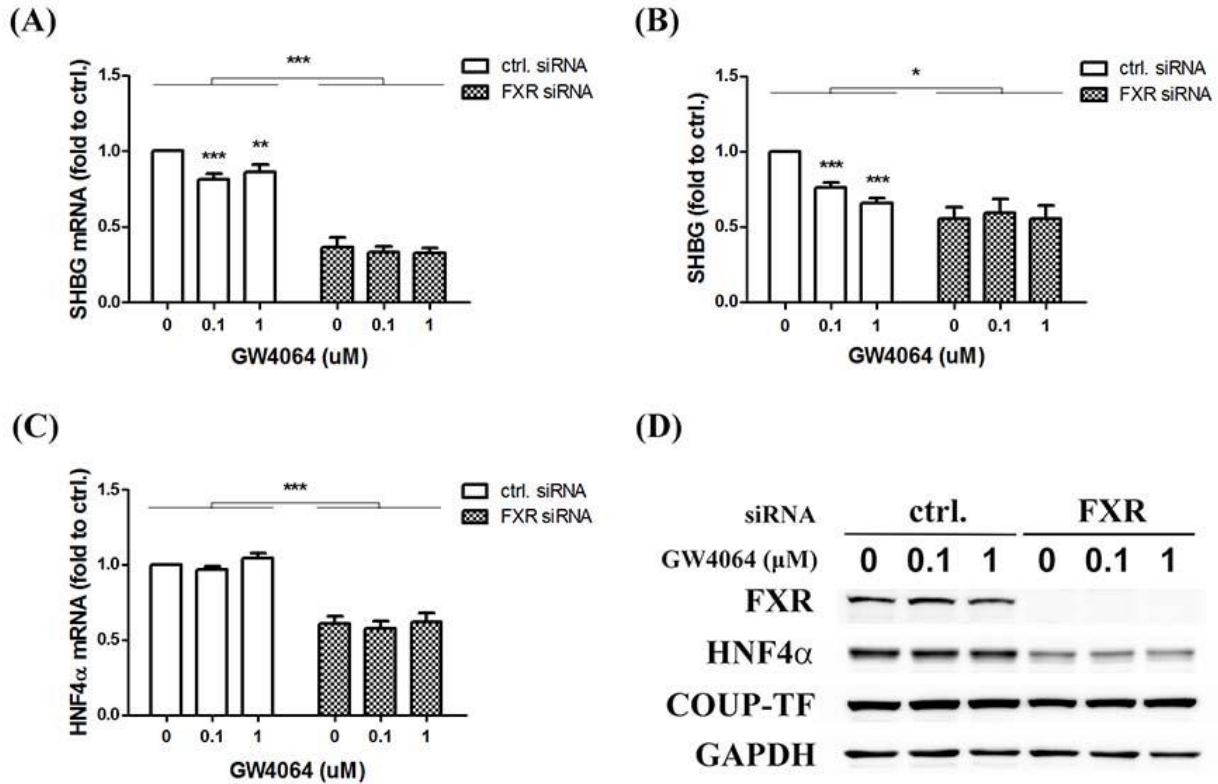


Figure 4.6 Effects of knock-down of FXR on *SHBG* and *HNF4α* expression

HepG2 cells were transfected with scrambled control (ctrl.) or FXR siRNA and 24 h post transfection, cells were treated with vehicle, 0.1, or 1 μM GW4064 for 48 h. (A) *SHBG* mRNA levels and (B) secreted SHBG levels in cultured medium were measured by quantitative RT-PCR and immuno-fluorometric assays respectively. (C) *HNF4α* mRNA levels were measured by quantitative RT-PCR. (D) Levels of FXR, *HNF4α*, COUP-TF, and GAPDH were assessed by Western blotting, and GAPDH was used as an internal control. Mean differences between control and FXR siRNA treatments were analyzed using two-way ANOVA, and mean differences between GW4064 treatments were analyzed using two-way ANOVA followed by the Bonferroni post-tests. *, $p < 0.05$; **, $p < 0.01$; ***, $p < 0.001$

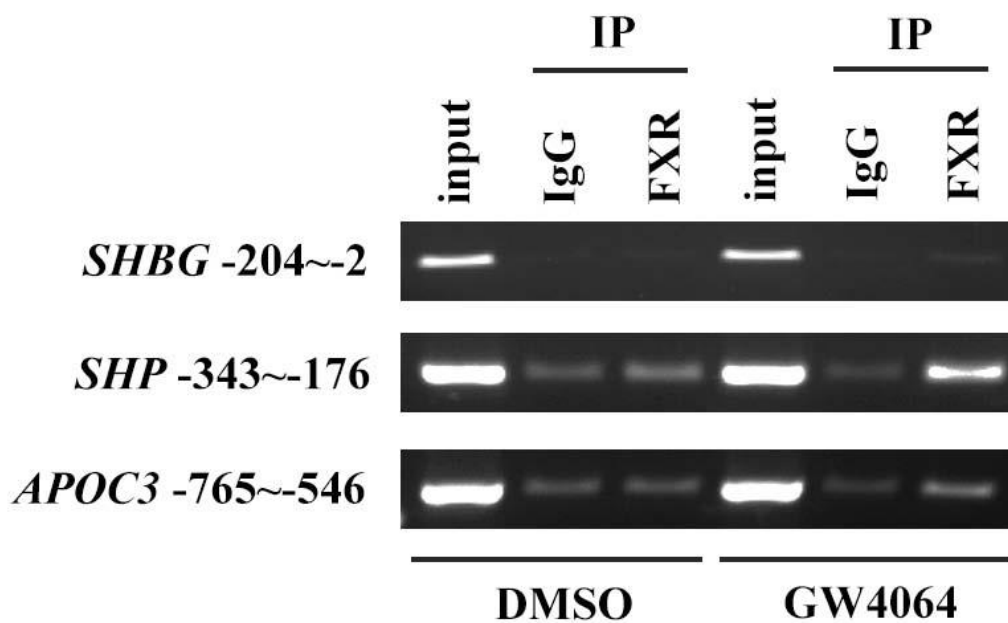


Figure 4.7 GW4064 activated FXR directly binds to the *SHBG* promoter

HepG2 cells were treated with vehicle (DMSO) or 1 μ M GW4064 for 6 h and association of FXR to *SHBG* promoter (-204 to -2 nt relative to the transcriptional starting site) was examined by ChIP assays. Association of FXR to *SHP* (-343 to -176 nt) and *APOC3* (-765~-546 nt) were also examined as positive controls of the assays. One percent of sheared chromatin (input) and appropriate amount of immunoprecipitated (IP) chromatin were used for PCR amplification.

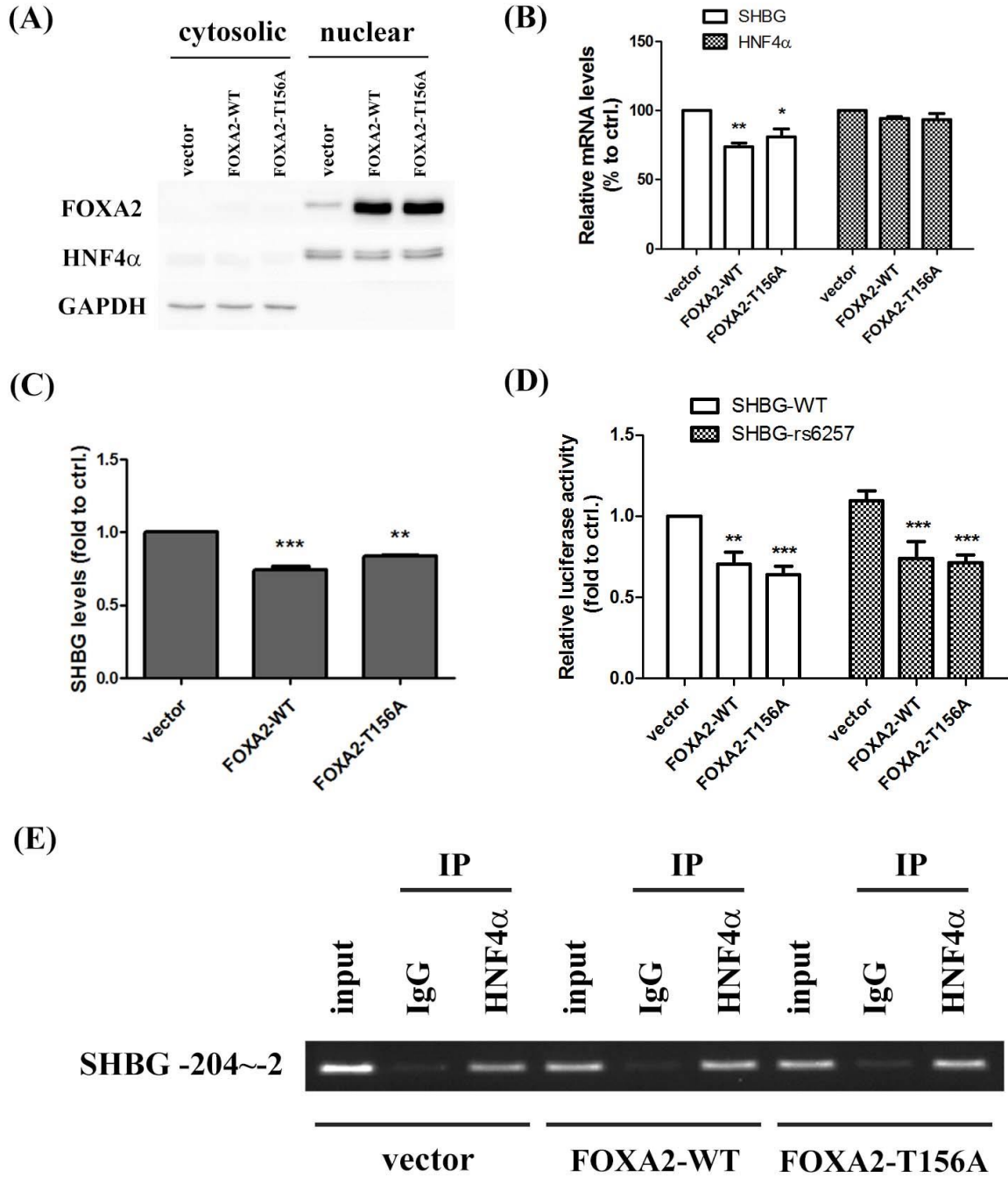


Figure 4.8 Overexpression of FOXA2 or FOXA2-T156A represses *SHBG* expression in an HNF4a-independent manner

HepG2 cells were transfected with vector plasmids as controls, or plasmids for overexpression of FOXA2 or FOXA2-T156A. (A) 48 h post transfection, the cytosolic and nuclear proteins of HepG2 cells were separated in fractions and analyzed by Western blotting. GAPDH (cytosolic protein) was used as an internal and sub-cellular control. (B) 48 h post transfection, total RNA was extracted and *SHBG* and *HNF4 α* mRNA levels were determined using quantitative RT-PCR analysis. (C) 72 h post transfection, SHBG levels in cultured medium were determined using immune-fluorometric assays. (D) Luciferase constructs containing a region of -266 to +366 nt of *SHBG*, or the same region with SNP rs6257, were co-transfected along with vector or FOXA2 overexpression plasmids into HepG2 cells. 48 h post transfection, cells were lysed and luciferase reporter gene assays were performed. (E) 48 h post transfection, One percent of sheared chromatin (input) and appropriate amount of immunoprecipitated (IP) chromatin were used for PCR amplification. (B) (C) Mean differences were analyzed using one-way ANOVA followed by the Dunnett's test. **, $p < 0.01$ (D) Mean differences were analyzed using two-way ANOVA followed by the Bonferroni post-tests. ***, $p < 0.001$

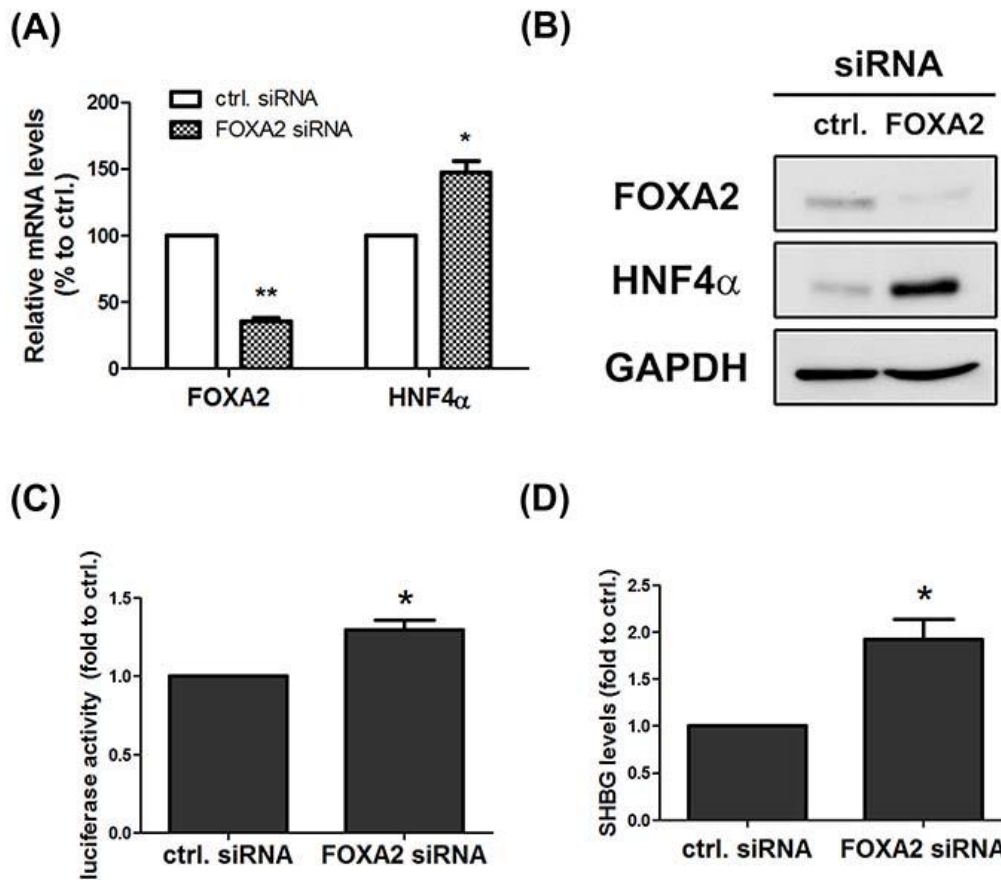


Figure 4.9 Knock-down of FOXA2 induces *HNF4 α* and *SHBG* expression

HepG2 cells were transfected with scrambled control (ctrl.) siRNA or FOXA2 siRNA. 72 h post transfection, multiple examinations were performed. (A) Total RNAs were extracted for determination of *FOXA2* and *HNF4 α* mRNA levels using quantitative RT-PCR. (B) Cell lysates were harvested and levels of FOXA2 and HNF4 α were determined by Western blotting analysis. GAPDH levels were used for an internal control. (C) 24 h post transfection of siRNAs, cells were transfected with luciferase constructs containing a region of -266 to +366 nt of *SHBG*. 48 h after, cells were lysed and luciferase reporter gene assays were performed. (D) SHBG levels in cultured medium were determined by immune-fluorometric assays. Mean differences were analyzed using student *t* test. *, $p < 0.05$; **, $p < 0.01$

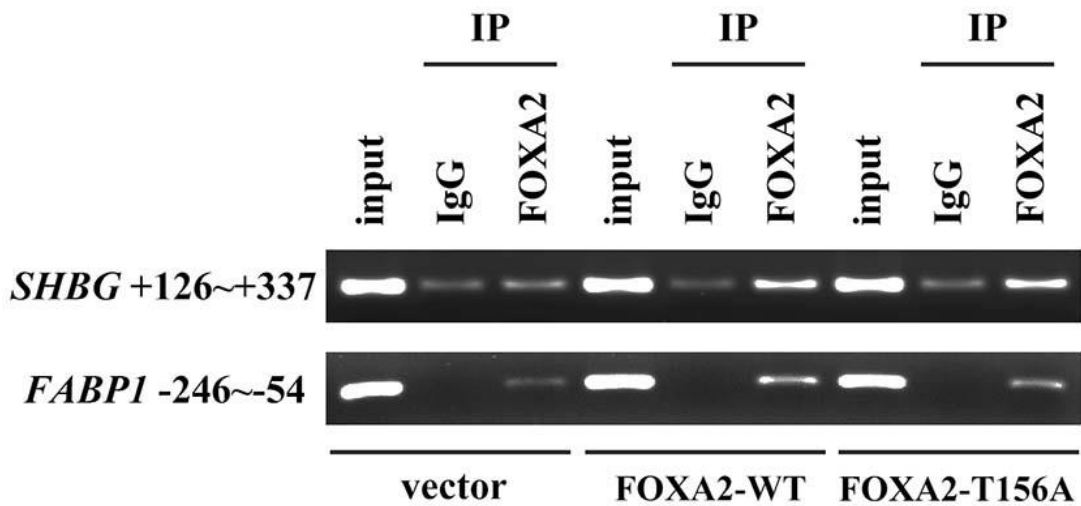


Figure 4.10 Endogenous and overexpressed FOXA2 directly binds to *SHBG* intron 1

HepG2 cells were transfected with vector plasmids, or plasmids for overexpression of FOXA2 or FOXA2-T156A. Forty-eight hours post transfection, association of FOXA2 to *SHBG* promoter (+126 to +337 nt) was examined by ChIP assays. Association of FOXA2 to *SHP* (-343 to -176 nt) and *APOC3* (-765~-546 nt) were also examined as positive controls of the assays. One percent of sheared chromatin (input) and appropriate amount of immunoprecipitated (IP) chromatin were used for PCR amplification.

Chapter 5 : Conclusion

It has been well established that plasma SHBG produced by the liver transports biologically active sex steroids and determines their availability to target tissues (9). In addition, studies of the production and/or sequestration of SHBG in other tissues, such as testis, kidney and uterus, or in other species have extended our knowledge of SHBG as a simple binding protein for sex steroids to its diverse roles in reproduction (66). Moreover, SHBG levels have been widely utilized as a biomarker for metabolic and sex steroid-dependent diseases, as well as a parameter for calculating free testosterone levels (148). However, how genetic variation contributes to inter-individual differences in SHBG levels and etiology of disease, especially the molecular mechanisms of which, are not as well known.

In my studies, I therefore focused my attention on genetic polymorphisms within *SHBG* regulatory and coding sequences, and investigated their effects on SHBG production and function. The conclusions drawn from the results of my research are described in the following sections. Collectively, biochemical and structural characterization of *SHBG* non-synonymous SNPs that encode SHBG mutants with abnormal molecular properties provides explanations for clinical observations, such as the association of the SNP rs6258 with low testosterone levels in men (169). In addition, the values I obtained for steroid-binding affinity of these SHBG

mutants (**Table 2.3**) may help improve computational methods of estimating free sex steroid hormones levels. Moreover, characterization of FXR and FOXA2 as novel regulators for hepatic *SHBG* expression suggests that a more complex network exists in addition to HNF4 α /COUP-TF to precisely regulate SHBG production in response to changes in metabolic status. This and the ongoing investigation of allele-specific effects of SNP rs138097069 and rs6257 on FXR and FOXA2 binding, respectively, and *SHBG* expression under a more physiological condition will help understand mechanisms that underlie the association between genetic differences, SHBG levels, and metabolic disorders.

With knowledge of the underlying mechanisms that alter SHBG levels/activity, the functional SNPs identified in my studies will facilitate strategies such as Mendelian randomization tests or a genotype first approach in studying the etiology of complex metabolic or endocrine diseases. Furthermore, inter-individual differences of steroid binding affinity of SHBG should be taken into consideration together with serum levels of SHBG when utilizing it as a biomarker. In the era of personalized medicine, these functional SHBG SNPs can be used in genetic background check to modify the current counselling, prognosis, diagnosis, treatment or personalized life-style management of endocrine or metabolic disorders into a more precise way, including a greater precision in the appropriate dosage of sex steroids in hormone replacement therapy in individual patients.

5.1 Non-synonymous *SHBG* genetic polymorphism encoding SHBG variants with altered molecular properties

Biochemical examination of recombinant SHBG mutants encoded by *SHBG* cDNA carrying non-synonymous SNPs was performed (**Chapter 2**). This showed that mutation of the corresponding amino acid residues in the N-terminal LG domain of SHBG can cause changes of its molecular properties (**Table 2.4**). In brief, while SHBG P156L has reduced affinity for testosterone, and SHBG T48I, R123H, R123C, G195E have general reduced affinity for DHT, testosterone and estradiol, SHBG R135C, L165M and E176K have higher affinity specifically for estradiol. I also observed an enhanced interaction of SHBG T48I, or R135C, or G195E with fibulin-2. The effects of SHBG T48I and G195E on ligand binding and fibulin-2 interaction may be due to alterations in their global protein conformation. This is because T48I is deficient in calcium binding, which has been shown to be critical in SHBG's stability and structural integrity (47, 48), and supplementation of calcium partially restores SHBG T48I's normal steroid-binding and fibulin-2 interacting properties, as well as the deficiency of the dimer formation. In the case of SHBG G195E, in which the residue 195 locates at the linking region between N- and C-terminal LG domains, an abnormality in N-glycosylation and a restriction of its secretion from CHO cells suggests that it is misfolded. In addition, instead of introducing an extra N-linked glycan, SHBG T7N loses the glycosylation

at residue 7. Some of our results explain observations in clinical studies. For example, reduced testosterone-binding affinity of SHBG P156L may be one of the reasons that male carriers with rs6258 have lower serum testosterone levels. Moreover, a man with undetectable plasma SHBG and testosterone levels was identified as homozygous for a missense mutation that encodes an Arginine at residue 195 of SHBG (205). This SHBG G195R mutant accumulated in the cells (205) and its deficiency in secretion is very similar to SHBG G195E (**Figure 2.8B**).

5.2 Factors independent of structural integrity of the steroid-binding pocket contribute to normal SHBG ligand-binding properties

To provide explanations for the abnormal biochemical properties of SHBG mutants at an atomic level, crystal structures of the N-terminal LG domain of SHBG R123H and SHBG E176K mutants were analyzed in **Chapter 3**. In both SHBG mutants, the structure of the steroid-binding pocket was normal when compared with that of SHBG. However, a space that is close to the steroid-binding pocket and is occupied by Lys134 in SHBG was replaced with the Arg135 of SHBG R123H (**Figure 3.4**). This, together with the reduced flexibility of the whole flexible loop region, may account for the generally reduced steroid-binding affinity of SHBG R123H mutant. In the case of the SHBG E176K mutant, a subtle conformational change was observed at an open rim from the lateral side of the N-terminal LG domain (**Figure 3.6**). How this subtle change specifically affects estradiol binding to SHBG remains unknown.

However, this and the fact that both Leu165 and Glu176 locate at this lateral open rim, and both SHBG L165M and E176K mutants have higher affinity for estradiol raise an interesting possibility that apart from the entrance covered by the flexible loop, an alternative pathway may exist for flux of estradiol at the lateral side of the SHBG N-terminal LG domain (**Figure 3.6**). Although several limitations of crystal structure analysis should be taken into consideration as described in the discussion of **Chapter 3**, this is the first time that SHBG mutants have been crystallized and analyzed. Conclusively, our structural results provide direct evidence indicating that independent of the integrity of the steroid-binding pocket, conformation of the flexible loop region or the putative entry site for estradiol contributes to normal SHBG ligand-binding properties.

5.3 FXR and FOXA2 both regulate *SHBG* expression in HNF4 α dependent and independent manners

Effects of the genetic polymorphisms in *SHBG* regulatory sequences on *SHBG* expression were investigated in **Chapter 4**. Human *SHBG* promoter activity is enhanced by the SNP rs138097069. In addition, *in silico* prediction revealed FXR and FOXA2 binding elements containing rs138097069 and rs6257, respectively. Their direct binding to human *SHBG* at sites where they were predicted was confirmed by ChIP assay, and their occupancy does not influence binding of HNF4 α to *SHBG* promoter. Activation of FXR and

overexpression of FOXA2 both directly suppress *SHBG* expression in an HNF4 α -independent manner. However, knock-down of FXR inhibits *SHBG* expression unexpectedly, whereas knock-down of FOXA2 up-regulates *SHBG* expression. Importantly, their knock-down effects are both in an HNF4 α -dependent manner, in which HNF4 α levels are altered probably due to global metabolic changes induced by deprivation of FXR or FOXA2 in HepG2 cells. In the future, a CRISPR-Cas9 genome engineering system (202) will be applied in HepG2 cells to investigate the allele-specific mechanisms by which SNPs affect *SHBG* transcriptional activity under more physiological conditions.

References

1. Franchimont, P. 1983. Regulation of gonadal androgen secretion. *Horm Res* 18:7-17.
2. Ryan, K.J. 1979. Granulosa-thecal cell interaction in ovarian steroidogenesis. *J Steroid Biochem* 11:799-800.
3. Jin, J.M., and Yang, W.X. 2014. Molecular regulation of hypothalamus-pituitary-gonads axis in males. *Gene* 551:15-25.
4. Selva, D.M., and Hammond, G.L. 2006. Human sex hormone-binding globulin is expressed in testicular germ cells and not in sertoli cells. *Horm Metab Res* 38:230-235.
5. Tsai, M.J., and O'Malley, B.W. 1994. Molecular mechanisms of action of steroid/thyroid receptor superfamily members. *Annu Rev Biochem* 63:451-486.
6. Gronemeyer, H., Gustafsson, J.A., and Laudet, V. 2004. Principles for modulation of the nuclear receptor superfamily. *Nat Rev Drug Discov* 3:950-964.
7. Falkenstein, E., Tillmann, H.C., Christ, M., Feuring, M., and Wehling, M. 2000. Multiple actions of steroid hormones--a focus on rapid, nongenomic effects. *Pharmacol Rev* 52:513-556.
8. Westphal, U. 1986. Steroid-protein interactions II. *Monogr Endocrinol* 27:1-603.
9. Dunn, J.F., Nisula, B.C., and Rodbard, D. 1981. Transport of steroid hormones: binding of 21 endogenous steroids to both testosterone-binding globulin and corticosteroid-binding globulin in human plasma. *J Clin Endocrinol Metab* 53:58-68.
10. Mendel, C.M. 1989. The free hormone hypothesis: a physiologically based mathematical model. *Endocr Rev* 10:232-274.
11. Hammond, G.L., Underhill, D.A., Rykse, H.M., and Smith, C.L. 1989. The human sex hormone-binding globulin gene contains exons for androgen-binding protein and two other testicular messenger RNAs. *Mol Endocrinol* 3:1869-1876.
12. Pinos, T., Barbosa-Desongles, A., Hurtado, A., Santamaria-Martinez, A., de Torres, I., Morote, J., Reventos, J., and Munell, F. 2009. Identification, characterization and expression of novel Sex Hormone Binding Globulin alternative first exons in the human prostate. *BMC Mol Biol* 10:59.
13. Hryb, D.J., Nakhla, A.M., Kahn, S.M., St George, J., Levy, N.C., Romas, N.A., and Rosner, W. 2002. Sex hormone-binding globulin in the human prostate is locally synthesized and may act as an autocrine/paracrine effector. *J Biol Chem* 277:26618-26622.
14. Joseph, D.R., Power, S.G., and Petrusz, P. 1997. Expression and distribution of androgen-binding protein/sex hormone-binding globulin in the female rodent

- reproductive system. *Biol Reprod* 56:14-20.
15. Vermeulen, A. 1988. Physiology of the testosterone-binding globulin in man. *Ann NY Acad Sci* 538:103-111.
 16. Morisset, A.S., Blouin, K., and Tchernof, A. 2008. Impact of diet and adiposity on circulating levels of sex hormone-binding globulin and androgens. *Nutr Rev* 66:506-516.
 17. Selva, D.M., Hogeveen, K.N., Seguchi, K., Tekpetey, F., and Hammond, G.L. 2002. A human sex hormone-binding globulin isoform accumulates in the acrosome during spermatogenesis. *J Biol Chem* 277:45291-45298.
 18. Selva, D.M., Hogeveen, K.N., and Hammond, G.L. 2005. Repression of the human sex hormone-binding globulin gene in Sertoli cells by upstream stimulatory transcription factors. *J Biol Chem* 280:4462-4468.
 19. Janne, M., Deol, H.K., Power, S.G., Yee, S.P., and Hammond, G.L. 1998. Human sex hormone-binding globulin gene expression in transgenic mice. *Mol Endocrinol* 12:123-136.
 20. Srinivasan, S.R., Myers, L., and Berenson, G.S. 1999. Temporal association between obesity and hyperinsulinemia in children, adolescents, and young adults: the Bogalusa Heart Study. *Metabolism* 48:928-934.
 21. Lakka, H.M., Salonen, J.T., Tuomilehto, J., Kaplan, G.A., and Lakka, T.A. 2002. Obesity and weight gain are associated with increased incidence of hyperinsulinemia in non-diabetic men. *Horm Metab Res* 34:492-498.
 22. Abramovich, D.R., Towler, C.M., and Bohn, H. 1978. The binding of sex steroids in human maternal and fetal blood at different stages of gestation. *J Steroid Biochem* 9:791-794.
 23. Hammond, G.L., Leinonen, P., Bolton, N.J., and Vihko, R. 1983. Measurement of sex hormone binding globulin in human amniotic fluid: its relationship to protein and testosterone concentrations, and fetal sex. *Clin Endocrinol (Oxf)* 18:377-384.
 24. Hogeveen, K.N., Cousin, P., Pugeat, M., Dewailly, D., Soudan, B., and Hammond, G.L. 2002. Human sex hormone-binding globulin variants associated with hyperandrogenism and ovarian dysfunction. *J Clin Invest* 109:973-981.
 25. M.G. Forest, A.B., A. Lecoq, C. Bréban and M. Pugeat. 1986. Ontogenèse de la protéine de liaison des hormones sexuelles (SBP) et de la transcortine (CBG) chez les primates: variations physiologiques et études dans différents milieux biologiques. In: *M. G. Forest and M. Pugeat. Protéines de liaison des hormones stéroïdes : John Libbey Eurotext* 149:263-291.

26. Elmlinger, M.W., Kuhnel, W., Wormstall, H., and Doller, P.C. 2005. Reference intervals for testosterone, androstenedione and SHBG levels in healthy females and males from birth until old age. *Clin Lab* 51:625-632.
27. Leger, J., Forest, M.G., and Czernichow, P. 1990. Thyroid hormones influences sex steroid binding protein levels in infancy: study in congenital hypothyroidism. *J Clin Endocrinol Metab* 71:1147-1150.
28. Apter, D., Bolton, N.J., Hammond, G.L., and Vihko, R. 1984. Serum sex hormone-binding globulin during puberty in girls and in different types of adolescent menstrual cycles. *Acta Endocrinol (Copenh)* 107:413-419.
29. Belgorosky, A., and Rivarola, M.A. 1986. Progressive decrease in serum sex hormone-binding globulin from infancy to late prepuberty in boys. *J Clin Endocrinol Metab* 63:510-512.
30. Pogmore, J.R., and Jequier, A.M. 1979. Sex hormone binding globulin capacity and postmenopausal hormone replacement therapy. *Br J Obstet Gynaecol* 86:568-571.
31. A. VERMEULEN, L.V., M. VAN DER STRAETEN and N. ORIE 1969. Capacity of the Testosterone-Binding Globulin in Human Plasma and Influence of Specific Binding of Testosterone on Its Metabolic Clearance Rate *J Clin Endocrinol Metab* 29.
32. Berube, D., Seralini, G.E., Gagne, R., and Hammond, G.L. 1990. Localization of the human sex hormone-binding globulin gene (SHBG) to the short arm of chromosome 17 (17p12----p13). *Cytogenet Cell Genet* 54:65-67.
33. Hammond, G.L., Underhill, D.A., Smith, C.L., Goping, I.S., Harley, M.J., Musto, N.A., Cheng, C.Y., and Bardin, C.W. 1987. The cDNA-deduced primary structure of human sex hormone-binding globulin and location of its steroid-binding domain. *FEBS Lett* 215:100-104.
34. Janne, M., and Hammond, G.L. 1998. Hepatocyte nuclear factor-4 controls transcription from a TATA-less human sex hormone-binding globulin gene promoter. *J Biol Chem* 273:34105-34114.
35. Walsh, K.A., Titani, K., Takio, K., Kumar, S., Hayes, R., and Petra, P.H. 1986. Amino acid sequence of the sex steroid binding protein of human blood plasma. *Biochemistry* 25:7584-7590.
36. Hammond, G.L., Robinson, P.A., Sugino, H., Ward, D.N., and Finne, J. 1986. Physicochemical characteristics of human sex hormone binding globulin: evidence for two identical subunits. *J Steroid Biochem* 24:815-824.
37. Joseph, D.R., and Baker, M.E. 1992. Sex hormone-binding globulin, androgen-binding protein, and vitamin K-dependent protein S are homologous to laminin A, merosin, and

- Drosophila crumbs* protein. *FASEB J* 6:2477-2481.
38. Petra, P.H., Stanczyk, F.Z., Senear, D.F., Namkung, P.C., Novy, M.J., Ross, J.B., Turner, E., and Brown, J.A. 1983. Current status of the molecular structure and function of the plasma sex steroid-binding protein (SBP). *J Steroid Biochem* 19:699-706.
 39. Gershagen, S., Henningsson, K., and Fernlund, P. 1987. Subunits of human sex hormone binding globulin. Interindividual variation in size. *J Biol Chem* 262:8430-8437.
 40. Petra, P.H., Griffin, P.R., Yates, J.R., 3rd, Moore, K., and Zhang, W. 1992. Complete enzymatic deglycosylation of native sex steroid-binding protein (SBP or SHBG) of human and rabbit plasma: effect on the steroid-binding activity. *Protein Sci* 1:902-909.
 41. Bocchinfuso, W.P., Ma, K.L., Lee, W.M., Warmels-Rodenhiser, S., and Hammond, G.L. 1992. Selective removal of glycosylation sites from sex hormone-binding globulin by site-directed mutagenesis. *Endocrinology* 131:2331-2336.
 42. Cousin, P., Dechaud, H., Grenot, C., Lejeune, H., Hammond, G.L., and Pugeat, M. 1999. Influence of glycosylation on the clearance of recombinant human sex hormone-binding globulin from rabbit blood. *J Steroid Biochem Mol Biol* 70:115-121.
 43. Power, S.G., Bocchinfuso, W.P., Pallesen, M., Warmels-Rodenhiser, S., Van Baelen, H., and Hammond, G.L. 1992. Molecular analyses of a human sex hormone-binding globulin variant: evidence for an additional carbohydrate chain. *J Clin Endocrinol Metab* 75:1066-1070.
 44. Cousin, P., Dechaud, H., Grenot, C., Lejeune, H., and Pugeat, M. 1998. Human variant sex hormone-binding globulin (SHBG) with an additional carbohydrate chain has a reduced clearance rate in rabbit. *J Clin Endocrinol Metab* 83:235-240.
 45. Ross, J.B.A., Contino, P.B., Lulka, M.F., and H., P.P. 1985. Observation and Quantitation of Metal-Binding Sites in the Sex Steroid-Binding Protein of Human and Rabbit Sera Using the Luminescent Probe Terbium. *Journal of Protein Chemistry* 4:299-304.
 46. Fillmore, C.M., Fears, T.R., Hoover, R.N., Falk, R.T., Vaught, J.B., Chandler, D.W., Stanczyk, F.Z., Galmarini, M., and Ziegler, R.G. 2000. Biomarkers (sex-hormone binding globulin (SHBG), bioavailable oestradiol, and bioavailable testosterone) and processing of blood samples in epidemiological studies. *BIOMARKERS* 5:395-398.
 47. Bocchinfuso, W.P., and Hammond, G.L. 1994. Steroid-binding and dimerization domains of human sex hormone-binding globulin partially overlap: steroids and Ca²⁺ stabilize dimer formation. *Biochemistry* 33:10622-10629.
 48. Rosner, W., Toppel, S., and Smith, R.N. 1974. Testosterone-estradiol-binding globulin

- of human plasma: denaturation and protection. *Biochim Biophys Acta* 351:92-98.
49. Hildebrand, C., Bocchinfuso, W.P., Dales, D., and Hammond, G.L. 1995. Resolution of the steroid-binding and dimerization domains of human sex hormone-binding globulin by expression in *Escherichia coli*. *Biochemistry* 34:3231-3238.
 50. Grishkovskaya, I., Avvakumov, G.V., Sklenar, G., Dales, D., Hammond, G.L., and Muller, Y.A. 2000. Crystal structure of human sex hormone-binding globulin: steroid transport by a laminin G-like domain. *Embo J* 19:504-512.
 51. Avvakumov, G.V., Muller, Y.A., and Hammond, G.L. 2000. Steroid-binding specificity of human sex hormone-binding globulin is influenced by occupancy of a zinc-binding site. *J Biol Chem* 275:25920-25925.
 52. Avvakumov, G.V., Cherkasov, A., Muller, Y.A., and Hammond, G.L. 2010. Structural analyses of sex hormone-binding globulin reveal novel ligands and function. *Mol Cell Endocrinol* 316:13-23.
 53. Grishkovskaya, I., Avvakumov, G.V., Hammond, G.L., Catalano, M.G., and Muller, Y.A. 2002. Steroid ligands bind human sex hormone-binding globulin in specific orientations and produce distinct changes in protein conformation. *J Biol Chem* 277:32086-32093.
 54. Hammond, G.L., and Bocchinfuso, W.P. 1996. Sex hormone-binding globulin: gene organization and structure/function analyses. *Horm Res* 45:197-201.
 55. Grenot, C., de Montard, A., Blachere, T., de Ravel, M.R., Mappus, E., and Cuilleron, C.Y. 1992. Characterization of Met-139 as the photolabeled amino acid residue in the steroid binding site of sex hormone binding globulin using delta 6 derivatives of either testosterone or estradiol as unsubstituted photoaffinity labeling reagents. *Biochemistry* 31:7609-7621.
 56. Avvakumov, G.V., Grishkovskaya, I., Muller, Y.A., and Hammond, G.L. 2002. Crystal structure of human sex hormone-binding globulin in complex with 2-methoxyestradiol reveals the molecular basis for high affinity interactions with C-2 derivatives of estradiol. *J Biol Chem* 277:45219-45225.
 57. Moras, D., and Gronemeyer, H. 1998. The nuclear receptor ligand-binding domain: structure and function. *Curr Opin Cell Biol* 10:384-391.
 58. Avvakumov, G.V., Grishkovskaya, I., Muller, Y.A., and Hammond, G.L. 2001. Resolution of the human sex hormone-binding globulin dimer interface and evidence for two steroid-binding sites per homodimer. *J Biol Chem* 276:34453-34457.
 59. Zakharov, M.N., Bhasin, S., Travison, T.G., Xue, R., Ulloor, J., Vasan, R.S., Carter, E., Wu, F., and Jasuja, R. 2015. A multi-step, dynamic allosteric model of testosterone's

- binding to sex hormone binding globulin. *Mol Cell Endocrinol* 399:190-200.
60. Grishkovskaya, I., Avvakumov, G.V., Hammond, G.L., and Muller, Y.A. 2002. Resolution of a disordered region at the entrance of the human sex hormone-binding globulin steroid-binding site. *J Mol Biol* 318:621-626.
 61. Namkung, P.C., Kumar, S., Walsh, K.A., and Petra, P.H. 1990. Identification of lysine 134 in the steroid-binding site of the sex steroid-binding protein of human plasma. *J Biol Chem* 265:18345-18350.
 62. Chambon, C., Bennat, D., Delolme, F., Dessalces, G., Blachere, T., Rolland de Ravel, M., Mappus, E., Grenot, C., and Cuilleron, C.Y. 2001. Photoaffinity labeling of human sex hormone-binding globulin using 17alpha-alkylamine derivatives of 3beta-androstanediol substituted with azidonitrophenylamido, azidonitrophenylamino, or trifluoroazidonitrophenylamino chromophores. Localization of Trp-84 in the vicinity of the steroid-binding site. *Biochemistry* 40:15424-15435.
 63. Jeyaraj, D.A., Grossman, G., Weaver, C., and Petrusz, P. 2002. Dynamics of testicular germ cell proliferation in normal mice and transgenic mice overexpressing rat androgen-binding protein: a flow cytometric evaluation. *Biol Reprod* 66:877-885.
 64. Selva, D.M., Bassas, L., Munell, F., Mata, A., Tekpetey, F., Lewis, J.G., and Hammond, G.L. 2005. Human sperm sex hormone-binding globulin isoform: characterization and measurement by time-resolved fluorescence immunoassay. *J Clin Endocrinol Metab* 90:6275-6282.
 65. Risbridger, G.P., Ellem, S.J., and McPherson, S.J. 2007. Estrogen action on the prostate gland: a critical mix of endocrine and paracrine signaling. *J Mol Endocrinol* 39:183-188.
 66. Hammond, G.L. 2011. Diverse roles for sex hormone-binding globulin in reproduction. *Biol Reprod* 85:431-441.
 67. Pasquali, R. 2006. Obesity, fat distribution and infertility. *Maturitas* 54:363-371.
 68. Azrad, M., Gower, B.A., Hunter, G.R., and Nagy, T.R. 2012. Intra-abdominal adipose tissue is independently associated with sex-hormone binding globulin in premenopausal women. *Obesity (Silver Spring)* 20:1012-1015.
 69. Zhang, S., Liu, Y., Li, Q., Dong, X., Hu, H., Hu, R., Ye, H., Wu, Y., and Li, Y. 2011. Exercise improved rat metabolism by raising PPAR-alpha. *Int J Sports Med* 32:568-573.
 70. Hawkins, V.N., Foster-Schubert, K., Chubak, J., Sorensen, B., Ulrich, C.M., Stanczyk, F.Z., Plymate, S., Stanford, J., White, E., Potter, J.D., et al. 2008. Effect of exercise on serum sex hormones in men: a 12-month randomized clinical trial. *Med Sci Sports*

Exerc 40:223-233.

71. Carlstrom, K., Eriksson, S., and Rannevik, G. 1986. Sex steroids and steroid binding proteins in female alcoholic liver disease. *Acta Endocrinol (Copenh)* 111:75-79.
72. Selva, D.M., Hogeveen, K.N., Innis, S.M., and Hammond, G.L. 2007. Monosaccharide-induced lipogenesis regulates the human hepatic sex hormone-binding globulin gene. *J Clin Invest* 117:3979-3987.
73. Pugeat, M., Crave, J.C., Elmidani, M., Nicolas, M.H., Garoscio-Cholet, M., Lejeune, H., Dechaud, H., and Tourniaire, J. 1991. Pathophysiology of sex hormone binding globulin (SHBG): relation to insulin. *J Steroid Biochem Mol Biol* 40:841-849.
74. Haffner, S.M., Katz, M.S., Stern, M.P., and Dunn, J.F. 1988. The relationship of sex hormones to hyperinsulinemia and hyperglycemia. *Metabolism* 37:683-688.
75. Bonnet, F., Balkau, B., Malecot, J.M., Picard, P., Lange, C., Fumeron, F., Aubert, R., Raverot, V., Dechaud, H., Tichet, J., et al. 2009. Sex hormone-binding globulin predicts the incidence of hyperglycemia in women: interactions with adiponectin levels. *Eur J Endocrinol* 161:81-85.
76. Plymate, S.R., Matej, L.A., Jones, R.E., and Friedl, K.E. 1988. Inhibition of sex hormone-binding globulin production in the human hepatoma (Hep G2) cell line by insulin and prolactin. *J Clin Endocrinol Metab* 67:460-464.
77. Loukovaara, M., Carson, M., and Adlercreutz, H. 1995. Regulation of production and secretion of sex hormone-binding globulin in HepG2 cell cultures by hormones and growth factors. *J Clin Endocrinol Metab* 80:160-164.
78. Crave, J.C., Lejeune, H., Brebant, C., Baret, C., and Pugeat, M. 1995. Differential effects of insulin and insulin-like growth factor I on the production of plasma steroid-binding globulins by human hepatoblastoma-derived (Hep G2) cells. *J Clin Endocrinol Metab* 80:1283-1289.
79. Selva, D.M., and Hammond, G.L. 2009. Thyroid hormones act indirectly to increase sex hormone-binding globulin production by liver via hepatocyte nuclear factor-4alpha. *J Mol Endocrinol* 43:19-27.
80. Krassas, G.E., Poppe, K., and Glinoeer, D. 2010. Thyroid function and human reproductive health. *Endocr Rev* 31:702-755.
81. Selva, D.M., and Hammond, G.L. 2009. Peroxisome-proliferator receptor gamma represses hepatic sex hormone-binding globulin expression. *Endocrinology* 150:2183-2189.
82. Deeb, S.S., Fajas, L., Nemoto, M., Pihlajamaki, J., Mykkanen, L., Kuusisto, J., Laakso, M., Fujimoto, W., and Auwerx, J. 1998. A Pro12Ala substitution in PPARgamma2

- associated with decreased receptor activity, lower body mass index and improved insulin sensitivity. *Nat Genet* 20:284-287.
83. Mousavinasab, F., Tahtinen, T., Jokelainen, J., Koskela, P., Vanhala, M., Oikarinen, J., Laakso, M., and Keinanen-Kiukaanniemi, S. 2006. The Pro12Ala polymorphism of the PPAR gamma 2 gene influences sex hormone-binding globulin level and its relationship to the development of the metabolic syndrome in young Finnish men. *Endocrine* 30:185-190.
 84. Anderson, D.C. 1974. Sex-hormone-binding globulin. *Clin Endocrinol (Oxf)* 3:69-96.
 85. Panzer, C., Wise, S., Fantini, G., Kang, D., Munarriz, R., Guay, A., and Goldstein, I. 2006. Impact of oral contraceptives on sex hormone-binding globulin and androgen levels: a retrospective study in women with sexual dysfunction. *J Sex Med* 3:104-113.
 86. Kraemer, G.R., Kraemer, R.R., Ogden, B.W., Kilpatrick, R.E., Gimpel, T.L., and Castracane, V.D. 2003. Variability of serum estrogens among postmenopausal women treated with the same transdermal estrogen therapy and the effect on androgens and sex hormone binding globulin. *Fertil Steril* 79:534-542.
 87. White, T., Ozel, B., Jain, J.K., and Stanczyk, F.Z. 2006. Effects of transdermal and oral contraceptives on estrogen-sensitive hepatic proteins. *Contraception* 74:293-296.
 88. Ruokonen, A., Alen, M., Bolton, N., and Vihko, R. 1985. Response of serum testosterone and its precursor steroids, SHBG and CBG to anabolic steroid and testosterone self-administration in man. *J Steroid Biochem* 23:33-38.
 89. Pasquali, R., Vicennati, V., Bertazzo, D., Casimirri, F., Pascal, G., Tortelli, O., and Labate, A.M. 1997. Determinants of sex hormone-binding globulin blood concentrations in premenopausal and postmenopausal women with different estrogen status. Virgilio-Menopause-Health Group. *Metabolism* 46:5-9.
 90. Carlstrom, K., Eriksson, A., Gustafsson, S.A., Henriksson, P., Pousette, A., Stege, R., and von Schoultz, B. 1985. Influence of orchidectomy or oestrogen treatment on serum levels of pregnancy associated alpha 2-glycoprotein and sex hormone binding globulin in patients with prostatic cancer. *Int J Androl* 8:21-27.
 91. Toscano, V., Balducci, R., Bianchi, P., Guglielmi, R., Mangiantini, A., and Sciarra, F. 1992. Steroidal and non-steroidal factors in plasma sex hormone binding globulin regulation. *J Steroid Biochem Mol Biol* 43:431-437.
 92. Rose, S.R., Municchi, G., Barnes, K.M., Kamp, G.A., Uriarte, M.M., Ross, J.L., Cassorla, F., and Cutler, G.B., Jr. 1991. Spontaneous growth hormone secretion increases during puberty in normal girls and boys. *J Clin Endocrinol Metab* 73:428-435.

93. Zadik, Z., Chalew, S.A., McCarter, R.J., Jr., Meistas, M., and Kowarski, A.A. 1985. The influence of age on the 24-hour integrated concentration of growth hormone in normal individuals. *J Clin Endocrinol Metab* 60:513-516.
94. Jaffe, C.A., Ocampo-Lim, B., Guo, W., Krueger, K., Sugahara, I., DeMott-Friberg, R., Bermann, M., and Barkan, A.L. 1998. Regulatory mechanisms of growth hormone secretion are sexually dimorphic. *J Clin Invest* 102:153-164.
95. Bichell, D.P., Kikuchi, K., and Rotwein, P. 1992. Growth hormone rapidly activates insulin-like growth factor I gene transcription in vivo. *Mol Endocrinol* 6:1899-1908.
96. Woelfle, J., Chia, D.J., and Rotwein, P. 2003. Mechanisms of growth hormone (GH) action. Identification of conserved Stat5 binding sites that mediate GH-induced insulin-like growth factor-I gene activation. *J Biol Chem* 278:51261-51266.
97. Rudd, B.T., Rayner, P.H., and Thomas, P.H. 1986. Observations on the role of GH/IGF-1 and sex hormone binding globulin (SHBG) in the pubertal development of growth hormone deficient (GHD) children. *Acta Endocrinol Suppl (Copenh)* 279:164-169.
98. Sieminska, L., Lenart, J., Cichon-Lenart, A., Niedziolka, D., Marek, B., Kos-Kudla, B., Kajdaniuk, D., and Nowak, M. 2005. [Serum adiponectin levels in patients with acromegaly]. *Pol Merkur Lekarski* 19:514-516.
99. Kalme, T., Koistinen, H., Loukovaara, M., Koistinen, R., and Leinonen, P. 2003. Comparative studies on the regulation of insulin-like growth factor-binding protein-1 (IGFBP-1) and sex hormone-binding globulin (SHBG) production by insulin and insulin-like growth factors in human hepatoma cells. *J Steroid Biochem Mol Biol* 86:197-200.
100. Forman, B.M., Goode, E., Chen, J., Oro, A.E., Bradley, D.J., Perlmann, T., Noonan, D.J., Burka, L.T., McMorris, T., Lamph, W.W., et al. 1995. Identification of a nuclear receptor that is activated by farnesol metabolites. *Cell* 81:687-693.
101. Makishima, M., Okamoto, A.Y., Repa, J.J., Tu, H., Learned, R.M., Luk, A., Hull, M.V., Lustig, K.D., Mangelsdorf, D.J., and Shan, B. 1999. Identification of a nuclear receptor for bile acids. *Science* 284:1362-1365.
102. Parks, D.J., Blanchard, S.G., Bledsoe, R.K., Chandra, G., Consler, T.G., Kliewer, S.A., Stimmel, J.B., Willson, T.M., Zavacki, A.M., Moore, D.D., et al. 1999. Bile acids: natural ligands for an orphan nuclear receptor. *Science* 284:1365-1368.
103. Wang, H., Chen, J., Hollister, K., Sowers, L.C., and Forman, B.M. 1999. Endogenous bile acids are ligands for the nuclear receptor FXR/BAR. *Mol Cell* 3:543-553.
104. Sinal, C.J., Tohkin, M., Miyata, M., Ward, J.M., Lambert, G., and Gonzalez, F.J. 2000. Targeted disruption of the nuclear receptor FXR/BAR impairs bile acid and lipid

- homeostasis. *Cell* 102:731-744.
105. Lee, F.Y., Lee, H., Hubbert, M.L., Edwards, P.A., and Zhang, Y. 2006. FXR, a multipurpose nuclear receptor. *Trends Biochem Sci* 31:572-580.
 106. Calkin, A.C., and Tontonoz, P. 2012. Transcriptional integration of metabolism by the nuclear sterol-activated receptors LXR and FXR. *Nat Rev Mol Cell Biol* 13:213-224.
 107. Eloranta, J.J., and Kullak-Ublick, G.A. 2008. The role of FXR in disorders of bile acid homeostasis. *Physiology (Bethesda)* 23:286-295.
 108. Lu, T.T., Makishima, M., Repa, J.J., Schoonjans, K., Kerr, T.A., Auwerx, J., and Mangelsdorf, D.J. 2000. Molecular basis for feedback regulation of bile acid synthesis by nuclear receptors. *Mol Cell* 6:507-515.
 109. Goodwin, B., Jones, S.A., Price, R.R., Watson, M.A., McKee, D.D., Moore, L.B., Galardi, C., Wilson, J.G., Lewis, M.C., Roth, M.E., et al. 2000. A regulatory cascade of the nuclear receptors FXR, SHP-1, and LRH-1 represses bile acid biosynthesis. *Mol Cell* 6:517-526.
 110. Seol, W., Choi, H.S., and Moore, D.D. 1996. An orphan nuclear hormone receptor that lacks a DNA binding domain and heterodimerizes with other receptors. *Science* 272:1336-1339.
 111. Russell, D.W. 2003. The enzymes, regulation, and genetics of bile acid synthesis. *Annu Rev Biochem* 72:137-174.
 112. Gadaleta, R.M., Cariello, M., Sabba, C., and Moschetta, A. 2015. Tissue-specific actions of FXR in metabolism and cancer. *Biochim Biophys Acta* 1851:30-39.
 113. Kast, H.R., Nguyen, C.M., Sinal, C.J., Jones, S.A., Laffitte, B.A., Reue, K., Gonzalez, F.J., Willson, T.M., and Edwards, P.A. 2001. Farnesoid X-activated receptor induces apolipoprotein C-II transcription: a molecular mechanism linking plasma triglyceride levels to bile acids. *Mol Endocrinol* 15:1720-1728.
 114. Claudel, T., Inoue, Y., Barbier, O., Duran-Sandoval, D., Kosykh, V., Fruchart, J., Fruchart, J.C., Gonzalez, F.J., and Staels, B. 2003. Farnesoid X receptor agonists suppress hepatic apolipoprotein CIII expression. *Gastroenterology* 125:544-555.
 115. Pineda Torra, I., Claudel, T., Duval, C., Kosykh, V., Fruchart, J.C., and Staels, B. 2003. Bile acids induce the expression of the human peroxisome proliferator-activated receptor alpha gene via activation of the farnesoid X receptor. *Mol Endocrinol* 17:259-272.
 116. Watanabe, M., Houten, S.M., Wang, L., Moschetta, A., Mangelsdorf, D.J., Heyman, R.A., Moore, D.D., and Auwerx, J. 2004. Bile acids lower triglyceride levels via a pathway involving FXR, SHP, and SREBP-1c. *J Clin Invest* 113:1408-1418.

117. Hartman, H.B., Gardell, S.J., Petucci, C.J., Wang, S., Krueger, J.A., and Evans, M.J. 2009. Activation of farnesoid X receptor prevents atherosclerotic lesion formation in LDLR^{-/-} and apoE^{-/-} mice. *J Lipid Res* 50:1090-1100.
118. Mencarelli, A., Renga, B., Distrutti, E., and Fiorucci, S. 2009. Antiatherosclerotic effect of farnesoid X receptor. *Am J Physiol Heart Circ Physiol* 296:H272-281.
119. Ma, K., Saha, P.K., Chan, L., and Moore, D.D. 2006. Farnesoid X receptor is essential for normal glucose homeostasis. *J Clin Invest* 116:1102-1109.
120. Zhang, Y., Lee, F.Y., Barrera, G., Lee, H., Vales, C., Gonzalez, F.J., Willson, T.M., and Edwards, P.A. 2006. Activation of the nuclear receptor FXR improves hyperglycemia and hyperlipidemia in diabetic mice. *Proc Natl Acad Sci U S A* 103:1006-1011.
121. Weigel, D., Jurgens, G., Kuttner, F., Seifert, E., and Jackle, H. 1989. The homeotic gene fork head encodes a nuclear protein and is expressed in the terminal regions of the *Drosophila* embryo. *Cell* 57:645-658.
122. Pani, L., Overdier, D.G., Porcella, A., Qian, X., Lai, E., and Costa, R.H. 1992. Hepatocyte nuclear factor 3 beta contains two transcriptional activation domains, one of which is novel and conserved with the *Drosophila* fork head protein. *Mol Cell Biol* 12:3723-3732.
123. Rada-Iglesias, A., Wallerman, O., Koch, C., Ameer, A., Enroth, S., Clelland, G., Wester, K., Wilcox, S., Dovey, O.M., Ellis, P.D., et al. 2005. Binding sites for metabolic disease related transcription factors inferred at base pair resolution by chromatin immunoprecipitation and genomic microarrays. *Hum Mol Genet* 14:3435-3447.
124. Cirillo, L.A., McPherson, C.E., Bossard, P., Stevens, K., Cherian, S., Shim, E.Y., Clark, K.L., Burley, S.K., and Zaret, K.S. 1998. Binding of the winged-helix transcription factor HNF3 to a linker histone site on the nucleosome. *EMBO J* 17:244-254.
125. Cirillo, L.A., Lin, F.R., Cuesta, I., Friedman, D., Jarnik, M., and Zaret, K.S. 2002. Opening of compacted chromatin by early developmental transcription factors HNF3 (FoxA) and GATA-4. *Mol Cell* 9:279-289.
126. Friedman, J.R., and Kaestner, K.H. 2006. The Foxa family of transcription factors in development and metabolism. *Cell Mol Life Sci* 63:2317-2328.
127. Kaestner, K.H. 2010. The FoxA factors in organogenesis and differentiation. *Curr Opin Genet Dev* 20:527-532.
128. Monaghan, A.P., Kaestner, K.H., Grau, E., and Schutz, G. 1993. Postimplantation expression patterns indicate a role for the mouse forkhead/HNF-3 alpha, beta and gamma genes in determination of the definitive endoderm, chordamesoderm and neuroectoderm. *Development* 119:567-578.

129. Sasaki, H., and Hogan, B.L. 1993. Differential expression of multiple fork head related genes during gastrulation and axial pattern formation in the mouse embryo. *Development* 118:47-59.
130. Ang, S.L., and Rossant, J. 1994. HNF-3 beta is essential for node and notochord formation in mouse development. *Cell* 78:561-574.
131. Weinstein, D.C., Ruiz i Altaba, A., Chen, W.S., Hoodless, P., Prezioso, V.R., Jessell, T.M., and Darnell, J.E., Jr. 1994. The winged-helix transcription factor HNF-3 beta is required for notochord development in the mouse embryo. *Cell* 78:575-588.
132. Lee, C.S., Friedman, J.R., Fulmer, J.T., and Kaestner, K.H. 2005. The initiation of liver development is dependent on Foxa transcription factors. *Nature* 435:944-947.
133. Hoffman, B.G., Robertson, G., Zavaglia, B., Beach, M., Cullum, R., Lee, S., Soukhatcheva, G., Li, L., Wederell, E.D., Thiessen, N., et al. 2010. Locus co-occupancy, nucleosome positioning, and H3K4me1 regulate the functionality of FOXA2-, HNF4A-, and PDX1-bound loci in islets and liver. *Genome Res* 20:1037-1051.
134. Sekiya, S., and Suzuki, A. 2011. Direct conversion of mouse fibroblasts to hepatocyte-like cells by defined factors. *Nature* 475:390-393.
135. Zhang, L., Rubins, N.E., Ahima, R.S., Greenbaum, L.E., and Kaestner, K.H. 2005. Foxa2 integrates the transcriptional response of the hepatocyte to fasting. *Cell Metab* 2:141-148.
136. Silva, J.P., von Meyenn, F., Howell, J., Thorens, B., Wolfrum, C., and Stoffel, M. 2009. Regulation of adaptive behaviour during fasting by hypothalamic Foxa2. *Nature* 462:646-650.
137. Barson, J.R., Morganstern, I., and Leibowitz, S.F. 2013. Complementary roles of orexin and melanin-concentrating hormone in feeding behavior. *Int J Endocrinol* 2013:983964.
138. Lee, C.S., Sund, N.J., Behr, R., Herrera, P.L., and Kaestner, K.H. 2005. Foxa2 is required for the differentiation of pancreatic alpha-cells. *Dev Biol* 278:484-495.
139. Heddad Masson, M., Poisson, C., Guerardel, A., Mamin, A., Philippe, J., and Gosmain, Y. 2014. Foxa1 and Foxa2 regulate alpha-cell differentiation, glucagon biosynthesis, and secretion. *Endocrinology* 155:3781-3792.
140. Sund, N.J., Vatamaniuk, M.Z., Casey, M., Ang, S.L., Magnuson, M.A., Stoffers, D.A., Matschinsky, F.M., and Kaestner, K.H. 2001. Tissue-specific deletion of Foxa2 in pancreatic beta cells results in hyperinsulinemic hypoglycemia. *Genes Dev* 15:1706-1715.
141. Lantz, K.A., Vatamaniuk, M.Z., Brestelli, J.E., Friedman, J.R., Matschinsky, F.M., and

- Kaestner, K.H. 2004. Foxa2 regulates multiple pathways of insulin secretion. *J Clin Invest* 114:512-520.
142. Wolfrum, C., Asilmaz, E., Luca, E., Friedman, J.M., and Stoffel, M. 2004. Foxa2 regulates lipid metabolism and ketogenesis in the liver during fasting and in diabetes. *Nature* 432:1027-1032.
143. Wolfrum, C., and Stoffel, M. 2006. Coactivation of Foxa2 through Pgc-1beta promotes liver fatty acid oxidation and triglyceride/VLDL secretion. *Cell Metab* 3:99-110.
144. Wan, M., Leavens, K.F., Saleh, D., Easton, R.M., Guertin, D.A., Peterson, T.R., Kaestner, K.H., Sabatini, D.M., and Birnbaum, M.J. 2011. Postprandial hepatic lipid metabolism requires signaling through Akt2 independent of the transcription factors FoxA2, FoxO1, and SREBP1c. *Cell Metab* 14:516-527.
145. Wolfrum, C., Besser, D., Luca, E., and Stoffel, M. 2003. Insulin regulates the activity of forkhead transcription factor Hnf-3beta/Foxa-2 by Akt-mediated phosphorylation and nuclear/cytosolic localization. *Proc Natl Acad Sci U S A* 100:11624-11629.
146. von Meyenn, F., Porstmann, T., Gasser, E., Selevsek, N., Schmidt, A., Aebersold, R., and Stoffel, M. 2013. Glucagon-induced acetylation of Foxa2 regulates hepatic lipid metabolism. *Cell Metab* 17:436-447.
147. van Gent, R., Di Sanza, C., van den Broek, N.J., Fleskens, V., Veenstra, A., Stout, G.J., and Brenkman, A.B. 2014. SIRT1 mediates FOXA2 breakdown by deacetylation in a nutrient-dependent manner. *PLoS One* 9:e98438.
148. Hammond, G.L., Wu, T.S., and Simard, M. 2012. Evolving utility of sex hormone-binding globulin measurements in clinical medicine. *Curr Opin Endocrinol Diabetes Obes* 19:183-189.
149. Goodarzi, M.O., Dumesic, D.A., Chazenbalk, G., and Azziz, R. 2011. Polycystic ovary syndrome: etiology, pathogenesis and diagnosis. *Nat Rev Endocrinol* 7:219-231.
150. Pascal, N., Amouzou, E.K., Sanni, A., Namour, F., Abdelmouttaleb, I., Vidailhet, M., and Gueant, J.L. 2002. Serum concentrations of sex hormone binding globulin are elevated in kwashiorkor and anorexia nervosa but not in marasmus. *Am J Clin Nutr* 76:239-244.
151. Xita, N., and Tsatsoulis, A. 2010. Genetic variants of sex hormone-binding globulin and their biological consequences. *Mol Cell Endocrinol* 316:60-65.
152. Thompson, D.J., Healey, C.S., Baynes, C., Kalmyrzaev, B., Ahmed, S., Dowsett, M., Folkard, E., Luben, R.N., Cox, D., Ballinger, D., et al. 2008. Identification of common variants in the SHBG gene affecting sex hormone-binding globulin levels and breast cancer risk in postmenopausal women. *Cancer Epidemiol Biomarkers Prev* 17:3490-

- 3498.
153. Cousin, P., Calemard-Michel, L., Lejeune, H., Raverot, G., Yessaad, N., Emptoz-Bonneton, A., Morel, Y., and Pugeat, M. 2004. Influence of SHBG gene pentanucleotide TAAAA repeat and D327N polymorphism on serum sex hormone-binding globulin concentration in hirsute women. *J Clin Endocrinol Metab* 89:917-924.
 154. Haiman, C.A., Riley, S.E., Freedman, M.L., Setiawan, V.W., Conti, D.V., and Le Marchand, L. 2005. Common genetic variation in the sex steroid hormone-binding globulin (SHBG) gene and circulating shbg levels among postmenopausal women: the Multiethnic Cohort. *J Clin Endocrinol Metab* 90:2198-2204.
 155. Becchis, M., Frairia, R., Ferrera, P., Fazzari, A., Ondeì, S., Alfarano, A., Coluccia, C., Biglia, N., Sismondi, P., and Fortunati, N. 1999. The additionally glycosylated variant of human sex hormone-binding globulin (SHBG) is linked to estrogen-dependence of breast cancer. *Breast Cancer Res Treat* 54:101-107.
 156. Gann, P.H., Hennekens, C.H., Ma, J., Longcope, C., and Stampfer, M.J. 1996. Prospective study of sex hormone levels and risk of prostate cancer. *J Natl Cancer Inst* 88:1118-1126.
 157. Mordukhovich, I., Reiter, P.L., Backes, D.M., Family, L., McCullough, L.E., O'Brien, K.M., Razzaghi, H., and Olshan, A.F. 2011. A review of African American-white differences in risk factors for cancer: prostate cancer. *Cancer Causes Control* 22:341-357.
 158. Grada, A., and Weinbrecht, K. 2013. Next-generation sequencing: methodology and application. *J Invest Dermatol* 133:e11.
 159. Gaj, T., Gersbach, C.A., and Barbas, C.F., 3rd. 2013. ZFN, TALEN, and CRISPR/Cas-based methods for genome engineering. *Trends Biotechnol* 31:397-405.
 160. Stone, J., Folkerd, E., Doody, D., Schroen, C., Treloar, S.A., Giles, G.G., Pike, M.C., English, D.R., Southey, M.C., Hopper, J.L., et al. 2009. Familial correlations in postmenopausal serum concentrations of sex steroid hormones and other mitogens: a twins and sisters study. *J Clin Endocrinol Metab* 94:4793-4800.
 161. Ding, E.L., Song, Y., Manson, J.E., Hunter, D.J., Lee, C.C., Rifai, N., Buring, J.E., Gaziano, J.M., and Liu, S. 2009. Sex hormone-binding globulin and risk of type 2 diabetes in women and men. *N Engl J Med* 361:1152-1163.
 162. Wang, Q., Kangas, A.J., Soininen, P., Tiainen, M., Tynkkynen, T., Puukka, K., Ruokonen, A., Viikari, J., Kahonen, M., Lehtimäki, T., et al. 2015. Sex hormone-binding globulin associations with circulating lipids and metabolites and the risk for type 2 diabetes: observational and causal effect estimates. *Int J Epidemiol* 44:623-637.

163. Hammond, G.L. 2002. Access of reproductive steroids to target tissues. *Obstet Gynecol Clin North Am* 29:411-423.
164. Yang, C.K., Kim, J.H., and Stallcup, M.R. 2006. Role of the N-terminal activation domain of the coiled-coil coactivator in mediating transcriptional activation by beta-catenin. *Mol Endocrinol* 20:3251-3262.
165. Sanchez, W.Y., de Veer, S.J., Swedberg, J.E., Hong, E.J., Reid, J.C., Walsh, T.P., Hooper, J.D., Hammond, G.L., Clements, J.A., and Harris, J.M. 2012. Selective cleavage of human sex hormone-binding globulin by kallikrein-related peptidases and effects on androgen action in LNCaP prostate cancer cells. *Endocrinology* 153:3179-3189.
166. Costantino, L., Catalano, M.G., Frairia, R., Carmazzi, C.M., Barbero, M., Coluccia, C., Donadio, M., Genta, F., Drogo, M., Boccuzzi, G., et al. 2009. Molecular mechanisms of the D327N SHBG protective role on breast cancer development after estrogen exposure. *Breast Cancer Res Treat* 114:449-456.
167. Key, T., Appleby, P., Barnes, I., and Reeves, G. 2002. Endogenous sex hormones and breast cancer in postmenopausal women: reanalysis of nine prospective studies. *J Natl Cancer Inst* 94:606-616.
168. Vohl, M.C., Dionne, F.T., Deriaz, O., Chagnon, M., and Bouchard, C. 1994. Detection of a MspI restriction fragment length polymorphism for the human sex hormone-binding globulin (SHBG) gene. *Hum Genet* 93:84.
169. Ohlsson, C., Wallaschofski, H., Lunetta, K.L., Stolk, L., Perry, J.R., Koster, A., Petersen, A.K., Eriksson, J., Lehtimaki, T., Huhtaniemi, I.T., et al. 2011. Genetic determinants of serum testosterone concentrations in men. *PLoS Genet* 7:e1002313.
170. Lewis, J.G., Longley, N.J., and Elder, P.A. 1999. Monoclonal antibodies to human sex hormone-binding globulin (SHBG): characterization and use in a simple enzyme-linked immunosorbent assay (ELISA) of SHBG in plasma. *Steroids* 64:259-265.
171. Hammond, G.L., and Robinson, P.A. 1984. Characterization of a monoclonal antibody to human sex hormone binding globulin. *FEBS Lett* 168:307-312.
172. Hammond, G.L., Langley, M.S., and Robinson, P.A. 1985. A liquid-phase immunoradiometric assay (IRMA) for human sex hormone binding globulin (SHBG). *J Steroid Biochem* 23:451-460.
173. Niemi, S., Maentausta, O., Bolton, N.J., and Hammond, G.L. 1988. Time-resolved immunofluorometric assay of sex-hormone binding globulin. *Clin Chem* 34:63-66.
174. Hammond, G.L., and Lahteenmaki, P.L. 1983. A versatile method for the determination of serum cortisol binding globulin and sex hormone binding globulin binding

- capacities. *Clin Chim Acta* 132:101-110.
175. Sumer-Bayraktar, Z., Nguyen-Khuong, T., Jayo, R., Chen, D.D., Ali, S., Packer, N.H., and Thaysen-Andersen, M. 2012. Micro- and macroheterogeneity of N-glycosylation yields size and charge isoforms of human sex hormone binding globulin circulating in serum. *Proteomics* 12:3315-3327.
 176. Bocchinfuso, W.P., Warmels-Rodenhiser, S., and Hammond, G.L. 1992. Structure/function analyses of human sex hormone-binding globulin by site-directed mutagenesis. *FEBS Lett* 301:227-230.
 177. Avvakumov, G.V., Matveentseva, I.V., Akhrem, L.V., Strel'chyonok, O.A., and Akhrem, A.A. 1983. Study of the carbohydrate moiety of human serum sex hormone-binding globulin. *Biochim Biophys Acta* 760:104-110.
 178. Hogeveen, K.N., Talikka, M., and Hammond, G.L. 2001. Human sex hormone-binding globulin promoter activity is influenced by a (TAAA)_n repeat element within an Alu sequence. *J Biol Chem* 276:36383-36390.
 179. Spiro, R.G. 2002. Protein glycosylation: nature, distribution, enzymatic formation, and disease implications of glycopeptide bonds. *Glycobiology* 12:43R-56R.
 180. Nilsson, I.M., and von Heijne, G. 1993. Determination of the distance between the oligosaccharyltransferase active site and the endoplasmic reticulum membrane. *J Biol Chem* 268:5798-5801.
 181. Gupta, R., and Brunak, S. 2002. Prediction of glycosylation across the human proteome and the correlation to protein function. *Pac Symp Biocomput*:310-322.
 182. Sodergard, R., Backstrom, T., Shanbhag, V., and Carstensen, H. 1982. Calculation of free and bound fractions of testosterone and estradiol-17 beta to human plasma proteins at body temperature. *J Steroid Biochem* 16:801-810.
 183. Hoppe, E., Bouvard, B., Royer, M., Audran, M., and Legrand, E. 2010. Sex hormone-binding globulin in osteoporosis. *Joint Bone Spine* 77:306-312.
 184. Le, T.N., Nestler, J.E., Strauss, J.F., 3rd, and Wickham, E.P., 3rd. 2012. Sex hormone-binding globulin and type 2 diabetes mellitus. *Trends Endocrinol Metab* 23:32-40.
 185. Hammond, G.L., Avvakumov, G.V., and Muller, Y.A. 2003. Structure/function analyses of human sex hormone-binding globulin: effects of zinc on steroid-binding specificity. *J Steroid Biochem Mol Biol* 85:195-200.
 186. Rial, D.V., and Ceccarelli, E.A. 2002. Removal of DnaK contamination during fusion protein purifications. *Protein Expr Purif* 25:503-507.
 187. Grishkovskaya, I., Sklenar, G., Avvakumov, G.V., Dales, D., Behlke, J., Hammond, G.L., and Muller, Y.A. 1999. Crystallization of the N-terminal domain of human sex

- hormone-binding globulin, the major sex steroid carrier in blood. *Acta Crystallogr D Biol Crystallogr* 55:2053-2055.
188. Pugeat, M., Nader, N., Hogeveen, K., Raverot, G., Dechaud, H., and Grenot, C. 2010. Sex hormone-binding globulin gene expression in the liver: drugs and the metabolic syndrome. *Mol Cell Endocrinol* 316:53-59.
 189. Ferik, P., Teran, N., and Gersak, K. 2007. The (TAAAA)_n microsatellite polymorphism in the SHBG gene influences serum SHBG levels in women with polycystic ovary syndrome. *Hum Reprod* 22:1031-1036.
 190. Xita, N., Tsatsoulis, A., Chatzikiyriakidou, A., and Georgiou, I. 2003. Association of the (TAAAA)_n repeat polymorphism in the sex hormone-binding globulin (SHBG) gene with polycystic ovary syndrome and relation to SHBG serum levels. *J Clin Endocrinol Metab* 88:5976-5980.
 191. Xita, N., Tsatsoulis, A., Stavrou, I., and Georgiou, I. 2005. Association of SHBG gene polymorphism with menarche. *Mol Hum Reprod* 11:459-462.
 192. Alevizaki, M., Saltiki, K., Xita, N., Cimponeriu, A., Stamatelopoulos, K., Mantzou, E., Doukas, C., and Georgiou, I. 2008. The importance of the (TAAAA)_n alleles at the SHBG gene promoter for the severity of coronary artery disease in postmenopausal women. *Menopause* 15:461-468.
 193. Lazaros, L., Xita, N., Kaponis, A., Zikopoulos, K., Sofikitis, N., and Georgiou, I. 2008. Evidence for association of sex hormone-binding globulin and androgen receptor genes with semen quality. *Andrologia* 40:186-191.
 194. Eriksson, A.L., Lorentzon, M., Mellstrom, D., Vandenput, L., Swanson, C., Andersson, N., Hammond, G.L., Jakobsson, J., Rane, A., Orwoll, E.S., et al. 2006. SHBG gene promoter polymorphisms in men are associated with serum sex hormone-binding globulin, androgen and androgen metabolite levels, and hip bone mineral density. *J Clin Endocrinol Metab* 91:5029-5037.
 195. Caturla, M., Van Reeth, T., Dreze, P., Szpirer, J., and Szpirer, C. 1997. The thyroid hormone down-regulates the mouse alpha-foetoprotein promoter. *Mol Cell Endocrinol* 135:139-145.
 196. Schmittgen, T.D., and Livak, K.J. 2008. Analyzing real-time PCR data by the comparative C(T) method. *Nat Protoc* 3:1101-1108.
 197. Dwivedi, S.K., Singh, N., Kumari, R., Mishra, J.S., Tripathi, S., Banerjee, P., Shah, P., Kukshal, V., Tyagi, A.M., Gaikwad, A.N., et al. 2011. Bile acid receptor agonist GW4064 regulates PPAR_γ coactivator-1_α expression through estrogen receptor-related receptor alpha. *Mol Endocrinol* 25:922-932.

198. Singh, N., Yadav, M., Singh, A.K., Kumar, H., Dwivedi, S.K., Mishra, J.S., Gurjar, A., Manhas, A., Chandra, S., Yadav, P.N., et al. 2014. Synthetic FXR agonist GW4064 is a modulator of multiple G protein-coupled receptors. *Mol Endocrinol* 28:659-673.
199. Balasubramanian, N., Luo, Y., Sun, A.Q., and Suchy, F.J. 2013. SUMOylation of the farnesoid X receptor (FXR) regulates the expression of FXR target genes. *J Biol Chem* 288:13850-13862.
200. Wu, Y.L., Peng, X.E., Wang, D., Chen, W.N., and Lin, X. 2012. Human liver fatty acid binding protein (hFABP1) gene is regulated by liver-enriched transcription factors HNF3beta and C/EBPalpha. *Biochimie* 94:384-392.
201. Pugeat, M., Moulin, P., Cousin, P., Fimbel, S., Nicolas, M.H., Crave, J.C., and Lejeune, H. 1995. Interrelations between sex hormone-binding globulin (SHBG), plasma lipoproteins and cardiovascular risk. *J Steroid Biochem Mol Biol* 53:567-572.
202. Ran, F.A., Hsu, P.D., Wright, J., Agarwala, V., Scott, D.A., and Zhang, F. 2013. Genome engineering using the CRISPR-Cas9 system. *Nat Protoc* 8:2281-2308.
203. Caron, S., Huaman Samanez, C., Dehondt, H., Ploton, M., Briand, O., Lien, F., Dorchies, E., Dumont, J., Postic, C., Cariou, B., et al. 2013. Farnesoid X receptor inhibits the transcriptional activity of carbohydrate response element binding protein in human hepatocytes. *Mol Cell Biol* 33:2202-2211.
204. Pang, X.N., Yuan, Y., Sun, Y., Shen, J.P., Zha, X.Y., and Hu, Y. 2014. The relationship of sex hormone-binding globulin (SHBG) gene polymorphisms with serum SHBG level and metabolic syndrome in Chinese Han males. *Aging Clin Exp Res* 26:583-589.
205. Vos, M.J., Mijnhout, G.S., Rondeel, J.M., Baron, W., and Groeneveld, P.H. 2014. Sex hormone binding globulin deficiency due to a homozygous missense mutation. *J Clin Endocrinol Metab* 99:E1798-1802.